Causes and consequences of calcareous nannoplankton evolution in the Late Jurassic : implications for biogeochronology, biocalcification and ocean chemistry.

PhD Thesis

Cristina Emanuela Casellato
Matricola R06325

Tutor	**Anno Accademico**	*Coordinatore*
Prof.ssa E. Erba	**2007-2008**	**Prof. Stefano Poli**

Contents
page

Abstract

The Jurassic was a time of important changes in the ocean/continent configuration: important reorganization of oceanic and climatic conditions are underlined by a most remarkable widespread shift from mostly siliceous to mainly calcareous sedimentation. In the western Tethys Ocean the beginning of the Late Jurassic was a time of exceptionally low carbonate accumulation rates, while the uppermost Jurassic is characterized by high sedimentation rates and the deposition of calcareous nannofossil oozes. During the Late Jurassic calcareous nannoplankton experienced a progressive increase in diversity, abundance and degree of calcification, culminating in the Middle Tithonian – Lower Berriasian interval.

Upper Callovian – Lower Berriasian sections from the Southern Alps (Northern Italy) have been analyzed for calcareous nannofossil biostratigraphy in order to revise and improve the available biostratigraphic schemes and integrate nannofossil events with magnetostratigraphy. Few sections (Southern Alps) and the DSDP Site 534 A (Atlantic Ocean) were quantitatively investigated for calcareous nannofossil relative and absolute abundances and to derive nannofossil *paleo*-fluxes.

Biostratigraphic investigations resulted in a refined taxonomy and improved biostratigraphy: three new biozones and two new subzones are here proposed. Quantitative investigations and derived *paleo*-fluxes show a calcareous nannofossil increase in diversity, abundance and calcification, inducing a major change in pelagic sedimentation from predominantly siliceous (lower part of the Rosso ad Aptici) to mostly calcareous (Rosso ad Aptici – Maiolica transition and Maiolica). In particular, a spectacular speciation episodestarted in the Tithonian, including the first occurrence and early diversification of nannoliths and nannoconids. The increase in abundance of coccoliths and nannoliths affected the ocean carbonate system, especially because of the high rates of some nannolith calcification. These nannoplankton calcification events (NCEs) occurred during times of low spreading rates, low pCO_2, low Mg/Ca ratio, cool climatic conditions and relatively oligotrophic oceans. Available data suggest that calcareous phytoplankton was stimulated by environmental stability rather than perturbations. This is consistent with modern coccolithophorid distribution, showing highest diversity and abundance as well as calcification

in stable oligotrophic oceanic areas. A precise stratigraphic control allows the modeling of the Late Jurassic nannofossil speciation episode and the abundance increase of high-calcified genera (*Conusphaera, Polycostella, Faviconus, Nannoconus*), evaluating environmental causes and consequences of evolution. The obtained results suggest that the Late Jurassic nannoplankton evolution was mostly controlled by the following factors: A) a decrease in pCO_2 due to decreased spreading rates and/or increased weathering rates ($^{87}Sr/^{86}Sr$); B) a decrease in oceanic Mg/Ca ratio values promoting low Mg-$CaCO_3$ and $CaCO_3$ biomineralization; C) cool climatic conditions (Price, 1999).

The Tithonian time interval provides examples of accelerated intra- and inter-generic evolutionary rates (originations) under stable environmental conditions, in absence of ecosystem preturbations. It provides an excellent opportunity to characterize nannoplankton evolutionary behaviour, and on the basis on the achieved stratigraphic and time framework, evolutionary trends of calcareous nannoplankton were quantified: example of Philetic Gradualism, Punctuated Equilibrium and Punctuated Gradualisms as well were identified. Evolutionary modes also suggest that at specific level both nannoliths and coccoliths gradually evolve in a time interval of more that 1 Ma, while at generic level a rapid speciation is most common.

1. INTRODUCTION

This PhD project has been focused on calcareous nannofossil of the latest Callovian – earliest Berriasian time interval in the western Tethys Ocean. The Jurassic was a time of important changes in the ocean/continent configuration. Hydrothermal activity associated to the fragmentation of Pangea was accelerated during this time interval, as mirrored by the decrease of strontium isotope ratio, reaching the lowest values of the Mesozoic (Sheridan, 1983; Jones *et al.*, 1994; Mc Arthur *et al.*, 2001). The separation of Eurasia and Gondwana triggered the opening of the Hispanic corridor, a seaway connecting the western Tethys and Pacific oceans. The oceanic circulation was superficial at that time. The gradual widening and deepening of the Hispanic Corridor (Haq *et al.*, 1988), allowed significant water mass exchanges between western Tethys and Pacific during the Late Jurassic (Winterer, 1991; Hotinski & Toggweiler, 2003). It has been shown that modification of the oceanic connection between oceanic basins have a strong influence on ocean circulation and global climate. The opening of the Hispanic Corridor triggered an improvement of latitudinal heat exchange due to a large-scale change in ocean currents pattern (Hotinski & Toggweiler, 2003).

The study of Late Jurassic sediments provides evidence for an important reorganization of oceanic and climatic condition. Most remarkable is the widespread shift from mostly siliceous to mainly calcareous sediments. The beginning of Late Jurassic was a time of exceptionally low carbonate accumulation rates, while the uppermost Jurassic is characterized by high sedimentation rates and the widespread deposition of calcareous nannofossil oozes. Around the Middle-Late Jurassic transition, the Tethys Ocean was almost free of carbonate sediments on a global scale (Dromart *et al.*, 2003a, 2003b): the pelagic sedimentation was dominated by radiolarian ooze and hardgrounds formed along shallow shelf environments and on submarine highs (Baumgartner, 1987; Dromart *et al.,* 2003a, 2003b). A drastic change in sediment production occurred during the Middle Oxfordian with the explosion of calcareous nannofossil (Cecca *et al.*, 2005), reaching lithogenic abundances during the Tithonian (Roth, 1983; Erba & Quadrio, 1987; Bornemann *et al.*, 2003).

During the Late Jurassic to earliest Cretaceous interval, eustatic sea-level reached a maximum in the early Tithonian (Haq *et al.*, 1987), probably as a consequence of increased

sea-floor spreading and rifting of the Pangea continent (Sheridan, 1983, 1997). Most of the Tithonian was characterized by a sea-level high followed by a drop at the Jurassic/Cretaceous boundary (Haq *et al.*, 1987; Hallam, 1988). Long sea-level fall was probably initiated by a major decrease in spreading rate, causing numerous semi-restricted epicontinental seas, which might have favoured the evolution of endemic taxa. Provincialism in the Tithonian to Berriasian time interval has been documented for many marine floral and faunal groups on a global scale (belemnite, ammonite). Similar patterns are also reflected by calcareous nannofossil, exhibiting distinctive latitudinal differences (Mutterlose & Kessels, 2000; Steet & Bown, 2000).

The paleoclimatic conditions of the latest Jurassic and earliest Cretaceous are still poorly constrained. According to Price (1999), the latest Jurassic was characterized by an episode of cold and subfreezing polar conditions, with possible polar ice sheets approximately about one-third of the size of those at present day. The hypothesis of cooler temperatures and presence of polar ice sheets is supported by the oxygen isotope record from the high latitudes (Podlaha *et al.*, 1998) and by global circulation model (GCM) for the Late Jurassic (Moore *et al.*, 1992a; Moore *et al.*, 1992b). The GCM allows the presence of ephemeral ice. Based on palynomorphs, dry climate conditions are thought to have prevailed in western Europe and in the Atlantic region in the latest Jurassic (Hallam, 1985; Wignall & Ruffell, 1990; Abbink *et al.*, 2001). In the earliest Cretaceous climatic conditions changed to more humid and relatively warmer.

Main objectives and general outline of this study

The purposes of this study are:

- high-resolution bio-magneto stratigraphy of sections, mainly from the Southern Alps, in order to achieve a revised stratigraphic framework for the Upper Jurassic – lowermost Cretaceous interval.

- quantification the calcareous nannofossil contribution to the biogenic calcite sedimentation in the Tithonian – Berriasian time interval, characterized by a major change in pelagic sedimentation from predominantly siliceous to mostly calcareous.

- Characterization of the calcareous nannofossil Tithonian speciation episode: it provides an example of accelerated intra- and inter-generic evolutionary rates during a time period of environmental stability, without perturbations, thus providing an excellent opportunity

2

to study calcareous nannofossil evolutionary behaviour. This study aims at reconstruction of both tempo and mode of nannoplankton evolution during the Tithonian speciation episode.

In Chapter 2 the state of the Late Jurassic calcareous nannofossil biostratigraphy, and nannofloral potential as paleoceanographic and/or paleoclimatic proxies are summarized.

Chapter 3 describes the sample preparation techniques and the abundance (semi-quantitative and quantitative) analysis adopted for calcareous nannofossil investigations. Particularly, the *modus operandi* used for calcareous nannofossil *paleo*-fluxes computing is presented.

In Chapter 4 the descriptions of western Tethys and Central Atlantic oceans paleogeographic settings are reported. Then follows a detailed description of the location, paleogeography and lithology of each investigated section.

The thesis results are presented in Chapter 5: the high-resolution bio-magnetostratigraphy of the uppermost Callovian – Lower Berriasian interval; the description of calcareous nannofossil relative and absolute abundances fluctuations and derived *paleo*-fluxes. Then a brief definition of the nannofacies observed in the Tithonian interval is following. Finally calcareous nannofossil data regarding the Tithonian speciation episode are summarized.

Chapter 6 is the discussion of calcareous nannofossil data: a revised calcareous nannofossil biostratigraphic scheme is proposed for the Upper Jurassic; biogenic calcite fluxes are interpreted and their implications and applications are presented. Nannofossil Calcification Events (NCEs) are described and interpreted, and their impact on the sedimentation of western Tethys ocean is discussed. Possible paleoceanographic and paleoclimatic controlling factors of NCEs are taken into account and evaluated. Finally, calcareous nannofossil evolutionary tempo & mode are discussed.

The conclusions are compiled in Chapter 7.

A taxonomic index and some notes on selected calcareous nannofossil taxa are reported in Chapter 8, while calcareous nannofossil plates constitute Chapter 9.

A CD is provided with the printout. It contains: detailed lithologic profile of every studied section; calcareous nannofossil range charts of every investigated section; the achieved semi-

quantitative data sets of Torre de Busi, Monte Pernice and Foza A sections, and the absolute abundances and derived *paleo*-fluxes data sets of Torre de Busi, Monte Pernice sections, and DSDP Site 534a. A copy of all figures included in thesis is also provided. A copy of all the abstracts presented at international meetings during the PhD is included.

2. LATE JURASSIC CALCAREOUS NANNOFOSSIL OVERVIEW

2.1. Calcareous Nannofossil biostratigraphy

The term *calcareous nannofossil* is usually used to include all calcareous fossils smaller than 30 µm and comprises a wide and diverse range of organisms, ascidian spicules, calcispheres (calcareous dinoflagellates) or juvenile foraminifera, but the main proportion is represented by calcitic remains of haptophyte algae. Calcareous nannofossils are thus mainly constituted by disc-like calcite plates, a clear analogues of coccoliths produced by coccolithophorids (living haptophytes), and by a significant number of variously-shaped nannoliths, whose biological affinities are less certain due to the lack of a living analogue, presumably also of algal origin. Calcisphere are not considered as nannoliths since they have been produced by dinoflagellates (Lohmann, 1909; Perch-Nielsen, 1987; Bown & Young, 1998).

Calcareous nannofossils were widespread in ancient oceans, similarly to modern calcareous nannoplankton, distributed from coastal areas to open ocean settings: this is one of the reason they are a powerful stratigraphic tool. The uppermost Jurassic – Lower Cretaceous calcareous nannofossil biostratigraphic scheme was first proposed by Thierstein (1971, 1973). In recent years it has been applied, improved or modified by different authors (Erba & Quadrio, 1987; Bralower *et al.*, 1989; De Kaenel *et al.*, 1996; Bown, 1998; Mattioli & Erba, 1999). A brief summary is presented in Figure 2.1.1. No Thetyan zonation has been yet formalized for the Late Bathonian – Late Kimmeridgian time interval. This study aims to explore and propose a revised calcareous nannofossil biostratigraphic scheme for the Middle to Late Jurassic. Biostratigraphic events will be calibrated with magnetostratigraphic data in order to obtain an integrated stratigraphy applicable to the Tethyan Realm.

The biostratigraphic scheme proposed by Bralower *et al.* (1989) has been preferred for my biostratigraphic investigations for two reasons: it was integrated to the available magnetic polarity chron sequence, thus resulting more appropriate to our aim, and was previously applied to few Italian (Tethyan) land sections, providing some basic guidelines to regional biostratigraphy. The biozonation of Bralower *et al.* (1989) is described below.

Fig. 2.1.1 – Comparative chart of calcareous nannofossi zonations available for the Tethyan Realm: Roth *et al,* (1986), Bralower *et al.* (1989), De Kaenel *et al.* (1996).

Vagalapilla stradneri **Zone, NJ-19**

Definition: interval from the first occurrence of *Vagalapilla stradneri* (Rood, Hay and
Bernard, 1971; Thierstein, 1973) to the first occurrence of *Conusphaera mexicana*
(Trejo, 1969) subsp, *minor* Bralower and Thierstein, 1989.

Range: Upper Oxfordian to lowermost Tithonian.

Subzones: - *Zeugrhabdotus embergeri* Subzone, NJ-19B

Definition: interval from the first occurrence of *Zeugrhabdotus embergeri*
(Noël, 1959; Bralower, Monechi & Thierstein, 1989) to the first
occurrence of *Conusphaera mexicana* (Trejo, 1969) subsp. *minor*
(Bralower and Thierstein, 1989).

Range: Kimmeridgian-Tithonian boundary interval.

Conusphaera mexicana **Zone (NJ-20)**

Definition: interval from the first occurrence of *Conusphaera mexicana* (Trejo, 1969)
subsp, *minor* Bralower and Thierstein, 1989 to the first occurrence of *Microstaurus
chiastius* (Worsley, 1971).

Range: Lower and Middle Tithonian.

Subzones: - *Hexapodorhabdus cuvillieri* Subzone, NJ-20A

Definition: interval from the first occurrence of *Conusphaera mexicana*
(Trejo, 1969) subsp. *minor* Bralower and Thierstein, 1989 to the
first occurrence of *Polycostella beckmannii* (Thierstein, 1971).

Range: Lower Tithonian.

- *Polycostella beckmannii* Subzone, NJ-20B

Definition: interval from the first occurrence of *Polycostella beckmannii*
(Thierstein, 1971) to the first occurrence of *Microstaurus chiastius*
(Worsley, 1971) Bralower, Monechi and Thierstein, 1989.

Range: middle Tithonian.

Microstaurus chiastius **Zone, NJK**

Definition: interval from the first occurrence of *Microstaurus chiastius* (Worsley, 1971)
Bralower, Monechi and Thierstein, 1989 to the first occurrence of *Nannoconus*

steinmannii (Kamptner, 1931) subsp. *steinmannii*.

Range: Upper Tithonian, across the Jurassic/Cretaceous boundary, to lowermost Berriasian.

Subzones: - *Hexalithus noeliae* Subzone, NJK-A

Definition: interval from the first occurrence of *Hexalithus noeliae* (Noël, 1956) Loeblich and Tappan, 1964 to the first occurrence of *Umbria granulosa* subsp. *granulosa* Bralower and Thierstein in Bralower, Monechi and Thierstein, 1989.

Range: Upper Tithonian.

- *Umbria granulosa* subsp. *granulosa* Subzone, NJK-B

Definition: interval from the first occurrence of *Umbria granulosa* subsp. *granulosa* Bralower and Thierstein in Bralower, Monechi and Thierstein, 1989 to the first occurrence of *Rotellapillus laffittei* (Noël, 1956) Noël, 1973.

Range: Upper Tithonian.

- *Rotellapillus laffittei* Subzone, NJK-C

Definition: interval from the first occurrence of *Rotellapillus laffittei* (Noël, 1956) Noël, 1973 to the first occurrence of *Nannoconus steinmannii* (Kamptner, 1931) subsp, *minor* Dares and Achéritéguy, 1980.

Range: Upper Tithonian through the Jurassic/Cretaceous boundary.

- *Nannoconus steinmannii* subsp. *minor* Subzone, NJK-D

Definition: interval from the first occurrence of *Nannoconus steinmannii* (Kamptner, 1931) subsp, *minor* Dares and Achéritéguy, 1980 to the first occurrence of *Nannoconus steinmannii* (Kamptner, 1931) subsp. *steinmannii*.

Range: across the Jurassic/Cretaceous boundary to lowermost Berriasian.

Nannoconus steinmannii subsp. steinmannii Zone, NK-1

Definition: interval from the first occurrence of *Nannoconus steinmannii* (Kamptner, 1931) subsp. *steinmannii* to the first occurrence of *Cretarhabdus angustiforatus* (Black, 1971)

Bukry, 1973.

Range: middle Berriasian.

Cretarhabdus angustiforatus **Zone, NK-2**

Definition: interval from the first occurrence of *Cretarhabdus angustiforatus* (Black, 1971) Bukry, 1973 to the first occurrence of *Calcicalathina oblongata* (Worsley, 1971) Thierstein, 1971.

Range: middle Berriasian to Lower Valanginian.

Subzones: - *Assipetra infracretacea* Subzone, NK-2A

Definition: interval from the first occurrence of *Cretarhabdus angustiforatus* (Black, 1971) Bukry, 1973 to the first occurrence of *Percivalia fenestrata* (Worsley 1971) Wise, 1983.

Range: middle and Upper Berriasian.

- *Percivalia fenestrata* Subzone, NK-2B

Definition: interval from the first occurrence of *Percivalia fenestrata* (Worsley 1971) Wise, 1983 to the first occurrence of *Calcicalathina oblongata* (Worsley, 1971) Thierstein, 1971.

Range: This zone spans the Berriasian/Valanginian boundary.

2.2. The Tithonian – Berriasian time interval at low latitudes

The Callovian – Berriasian pelagic successions recorded a major change in pelagic sedimentation from predominantly siliceous to mostly calcareous through time (Fig. 2.2.1).

This transitional change, which affected the low latitude pelagic sedimentation of both Tethys and Atlantic oceans, has been linked to a shift of carbonate deposition from the shallow seas and shelf areas to the open-ocean, due to a major increase in calcareous nannofossil carbonate production (*Kuenen Event*, Roth, 1986), then lately interpreted as consequence of carbonate compensation depth (CCD) fluctuations (Winterer & Bosellini, 1981; Roth, 1989), or a tectonic plate drifting (Muttoni *et al.*, 2005; Channell *et al.*, 2007), or of a change in oceanic circulation (Hotinski & Toggweiler, 2003; Rais *et al.*, 2007) (See Chapters 2 and 6 for details).

Fig. 2.2.1 – Private quarry near Kaberlaba (Asiago Plateau, Southern Alps, North Italy).
The picture shows the change in pelagic sedimentation from predominantly siliceous (red nodular
limestones) to mostly calcareous (white limestones) through time.

Calcareous nannofossils, which are considered to be widespread in the ancient oceans as nowadays marine calcareous nannoplankton, started to bio-calcify approximately 220 Ma: the appearance of calcified nannofossils strongly affected marine ecosystem changing significantly the pelagic sedimentation. Particularly, the uppermost Jurassic is characterized by a speciation episode among nannofossils: several new genera and species first occurred and rapidly evolved reaching lithogenic abundances and are considered since then one of the most effective producers of calcite in the oceanic system. Calcareous nannofossil evolutionary history is grossly coeval with major events such as climate and sea level changes, large igneous episodes and variations in ocean structure and composition, suggesting that calcareous nannofossil are intimately linked to environmental and climatic modifications (Erba, 2006). Here after are

reported several factors that may influence, and in some cases are influenced by calcareous nannofossil patterns, such as fluctuations in diversity, abundance or calcification degree:

- The *bio*-calcification chemical reaction directly influences CO_2 oceanic/atmospheric concentrations as for every $CaCO_3$ molecule synthesized a CO_2 molecule is released in the oceanic/atmospheric system, consequently calcareous phytoplankton can directly influence both the short and long time C-cycle. On the other hand oceanic/atmospheric CO_2 concentration could directly control calcareous nannofossil *bio*-mineralization processes, as pCO_2 increases provoke a calcification loss, particularly among planktonic *bio*-calcifiers. The geological record suggests that large pCO_2 increases provoked biogenic calcite *paleo*-flux reductions, while low pCO_2 concentration stimulated an increase of calcareous nannofossil calcification degree and diversity.

- Eustatic sea level fluctuations can also influence calcareous nannofossil diversity: marine transgressions or high-standing phases let calcareous nannoplankton to conquer numerous new ecological niches thus stimulating a diversity increase; on the contrary marine regressions or low-standing phases could provoke diversity turnovers until extinction episodes.

- Oceanic chemical composition has changed through the Phanerozoic: wide fluctuations of Ca^{+2} and Mg^{+2} ions concentration, and thus of Mg/Ca ratio, have been used to subdivide the Phaneozoic in two types of time intervals characterized respectively by aragonitic or calcitic oceanic composition. Calcareous nannofossil evolution apparently follows Ca^{2+} and Mg/Ca ratio fluctuations.

- Calcareous nannofossil abundance and diversity mainly reflect trophic regime of superficial marine waters. Coccolitophorids live in stable meso- to oligo-trophic environments: stable environmental conditions and scarce nutrients can promote diversification and abundance increases, while high fertility (nutrients and/or metals like Fe or Zn) and unstable environmental conditions may cause abundance losses or intoxications.

For all these reasons, calcareous nannofossil quantitative analysis could represents a useful tool to investigate linkages between the documented changes in pelagic sedimentation from predominantly siliceous to mostly calcareous and any related paleoceanographic condition across the Tithonian – Berriasian time interval. One aim of this project is to quantify the

calcareous nannofossil biogenic calcite contributions to the sedimentation on two sections from the Lombardian Basin (Torre de Busi section), from Trento Plateau - Lombardian Basin boundary (Monte Pernice section), and on DSDP site 534A from the Atlantic Ocean.

2.3. Evolution theories and uppermost Jurassic calcareous nannofossil

The Tithonian is characterized by a major calcareous nannofossil speciation episode: several successful genera and species of both coccoliths and nannoliths first appear and rapidly evolve, reaching a high diversity, abundances, dimensions and calcification degree. The history of calcareous nannofossils indicates that such times of accelerated rates of radiations or extinctions correlate with global changes in the geosphere, hydrosphere and atmosphere suggesting that evolutionary patterns are intimately linked to environmental modifications (Erba, 2006) (see for detail paragraph 2.2). Nevertheless, the Tithonian interval provides examples of accelerated intra- and inter-generic evolutionary rates (a speciation event) during a time period of environmental stability, in absence of coeval environmental change evidence (Fig. 2.3.1).

The modern paleobiology is trying to understand the mechanisms that force the evolution of life, but is still elusive how biotic or abiotic factors trigger speciation or/and extinction. Two different evolutionary hypotheses emphasize this discrepancy between biotic or abiotic factors as the evolution drivers: the Red Queen Hypothesis (Van Valen, 1973) and the Stationary Model (Stenseth & Maynard Smith, 1984). In the first one, evolution is seen as a response to biotic interactions operating even in absence of enviromental changes ("It takes all the running you can do, to keep in the same place", by L.Carroll from *Alice's adventures in Wonderland*). The second one postulates that evolution is largely driven just by abiotic changes, thus operates during enviromental changes and is slowed down under environmental quiescence. Indipendently from the discussion on the evolution driving factors, different evolution modes have been proposed since Darwin's Evolutionary Theory (Fig. 2.3.2): Phyletic Gradualism (Darwin, 1859), Punctuated Equilibrium (Gould & Eldredge, 1977) and Punctuated Gradualism (Malmgren et al., 1984). *Phyletic gradualism* holds that new species arise from slow, steady transformation of populations providing gradational fossil series linking separate phylogenetic species. *Punctuated gradualism* implies long-lasting evolutionary stasis interrupted by rapid, but gradual phyletic transformation without lineage

Fig. 2.3.1 – Tihonian calcareous nannofossil speciation episode: severa events (mainly FO) are reposted against magneto chron sequence (data after Bralower *et al.*, 1989)

splitting. *Punctuated equilibrium* explains the appearance of new species by rapid speciation occurring in small peripheral isolated populations, followed by migration to other areas where fossil sequence usually shows a series of sharp morphological breaks.

EVOLUTIONARY MODELS

| PHYLETIC GRADUALISM (Darwin 1859) | PUNCTUATED EQUILIBRIUM (Gould & Eldredge 1977) | PUNCTUATED GRADUALISM (Malmgren et al 1984) |
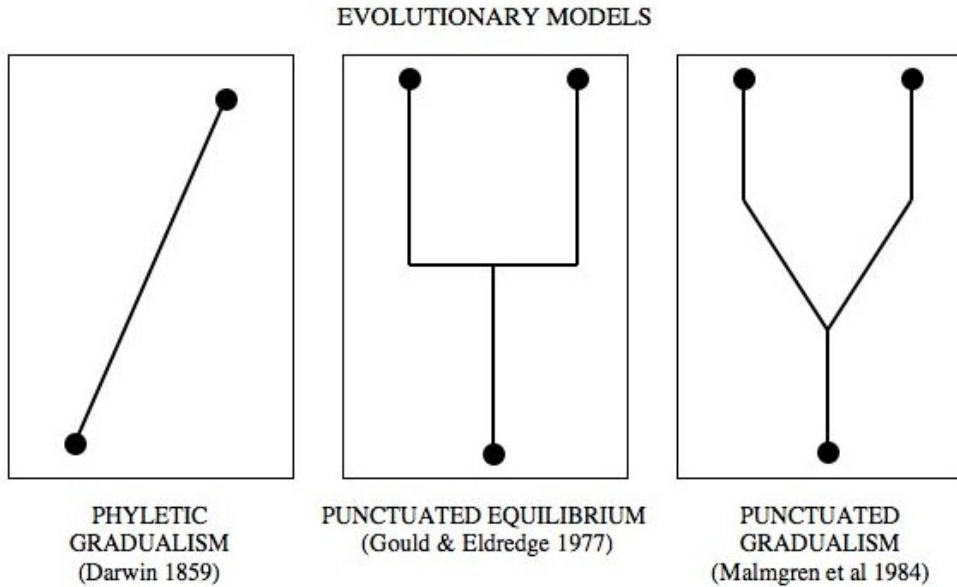
Fig. 2.3.2 – Sketches representing the three evolutionary models described in the text

The Tithonian calcareous nannofossil speciation event provides an excellent opportunity to investigate nannoplankton evolutionary behaviour during a period of inferred climatic and environmental stability. On the basis of the stratigraphic and time framework, this study aims to: quantify tempo and mode of evolutionary trends of calcareous nannoplankton in a time interval marked by origination rates higher than "normal"; separate evolutionary changes of coccoliths *versus* nannoliths.

3. GEOLOGY, PALEOGEOGRAPHY AND LITHOSTRATIGRAPHY OF INVESTIGATED SECTIONS

3.1 Geology and local paleogeography of North-Western Tethys Ocean (Southern Alps, Northern Italy)

The studied area is situated in the Southern Alps (Orobic Alps and Asiago Plateau), Northeast Italy. The Southern Alps formed mostly in the Cretaceous and Tertiary during the Alpine Orogeny. In the Mesozoic they were a part of the southern Tethyan passive margin and belonged to an Africa promontory or to the Adria plate, bordered to the North and West by the Liguria-Piemonte segment of the Tethys Ocean (Alpine Tethys), and to the East by the Neo-Tethys Ocean (Baumgartner *et al.*, 2001; Stampfli *et al.*, 2001).

In the Lower Mesozoic this continental margin experienced two major phases of extentional tectonic. A first rifting phase (Middle Triassic) which led to a progressive disintegration of wide Upper Triassic - Lowermost Jurassic carbonate platforms creating numerous shallow basins lately filled by sediments. A second more incisive rifting phase fragmented the margin in a *Horst and Graben* structure, and lasted until the beginning of the Alpine Orogeny (Bernoulli & Jenkyns, 1974; Winterer & Bosellini, 1981).

The Tethyan Upper Jurassic – Lower Cretaceous sedimentary sequences are well known since fourty years (Bernoulli, 1964; Pasquarè, 1965; Bernoulli *et al.*, 1979; Bosellini *et al.*, 1980; Winterer & Bosellini, 1981) and recently a number of studies have improved the stratigraphy of the Upper Jurassic sections (Erba & Quadrio, 1987; Baumgartner *et al.*, 2001; Bersezio *et al.*, 2002; Martire *et al.*, 2006). The Jurassic sedimentary evolution of Southern Tethyan margin is well documented and exposed in the Italian Southern Alps.

The Jurassic extensional phase led to the formation of four different paleogeographic domains (Fig 3.1.1): the deep pelagic Lombardian Basin; the pelagic submarine high of Trento Plateau; the relatively deep pelagic Belluno Basin; the shallow Friuli Platform. These domains are still arranged in their original pre-Alpine order, and allow a relatively clear paleogeographic reconstruction (Bernoulli *et al.*, 1979; Winterer & Bosellini, 1981; Baumgartner *et al.*, 2001). During the Middle - Late Jurassic reef limestones characterized the
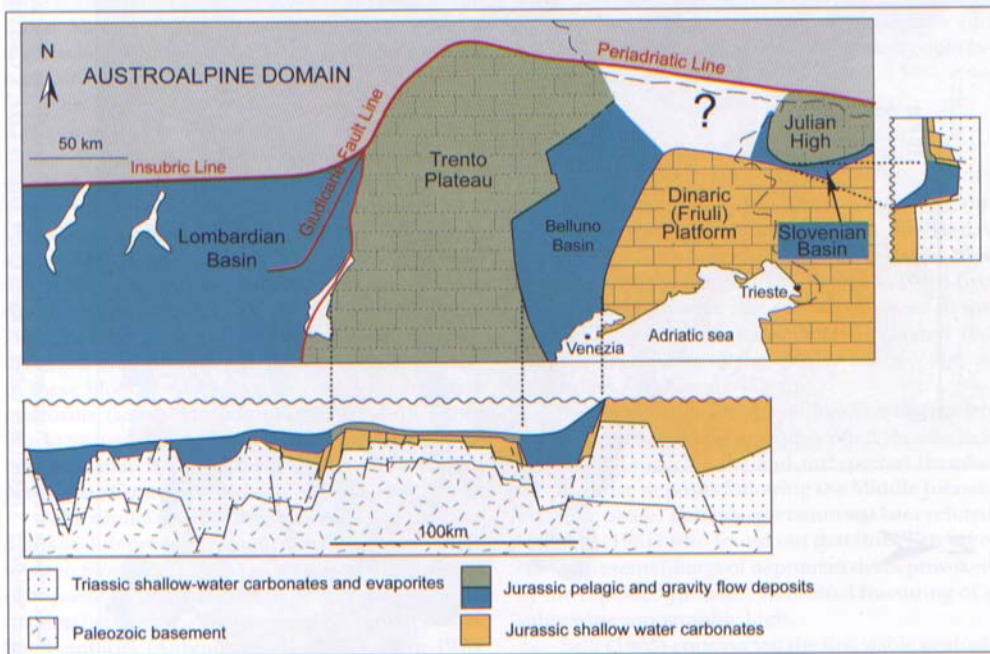
Fig. 3.1.1 – Present-day position of paleogeographic units and schematic paleogeographic cross sections, Uppermost Jurassic. (Compiled by Smuc, 2005 after Bosellini *et al*., 1981 and Martire, 1992)

Friuli Platform while limestones composed of resedimented shallow water debris with *in-situ* and resedimented pelagic material were deposited in the Belluno Basin, which was essentially a slope joining the Friuli Platform and the Trento Plateau (Bosellini et al., 1980; Winterer & Bosellini, 1981). The Middle Jurassic – Lowermost Cretaceous sequence (Fig 3.1.2) of the Trento Plateau comprised red condensed nodular pelagic limestones (Rosso Ammonitico Formation) followed by white-grey micritic pseudo-nodular pelagic limestones with chert (Maiolica or Biancone Formation), whereas coeval section of the adjacent Belluno Basin consists of red cherty marls and limestones (Calcare Selcifero di Fonzaso) followed transitionally by white-grey pelagic limestones (Biancone Formation). Several studies on regional sedimentology and lithostratigraphy (Baumgartner *et al.,* 2001; Martire, 2003; Martire *et al*., 2006 and references therein), on radiolarite (Baumgartner *et al.*, 1995) or ammonite associations (Clari *et al.*, 1984; Martire *et al.* 1991; Martire, 1996) let to attribute the Rosso Ammonitico Inferiore to the Upper Bajocian - Upper Callovian interval, the Rosso Ammonitico Medio and correlated Calcare Selcifero di Fonzaso to Upper Callovian – Middle

Oxfordian interval and the Rosso Ammonitico Superiore to Middle Oxfordian – Tithonian interval (Fig.3.1.2).

A similar and coeval Middle Jurassic – Lowermost Cretaceous succession deposited in the deeper Lombardian basin: violet, red to greenish siliceous marls and siliceous limestones (Radiolarite Formation) transitionally followed by red siliceous to calcareous limestones with red chert lists and nodules (Rosso ad Aptici Formation) which transitionally change into white calcareous limestones with grey chert nodules (Maiolica formation).

The sedimentary sequence of the Southern Alps is everywhere characterized by a progressive up-ward decrease of siliceous content, coeval with an increase of calcareous content. Different hypotheses are reported to explain this regional change: a) a carbonate compensation depth (CCD) fluctuation during the rifting phase (Winterer & Bosellini, 1981); b) a plate drifting initially toward and then away from a near equatorial upwelling zone of biosiliceous productivity (Muttoni *et al.*, 2005; Channell *et al.*, 2007); c) a change in ocean circulation due to the opening of a new seaway at a time of progressive collapse of Pangea (Rais *et al.*, 2007; Hotinski & Toggweiler, 2003).
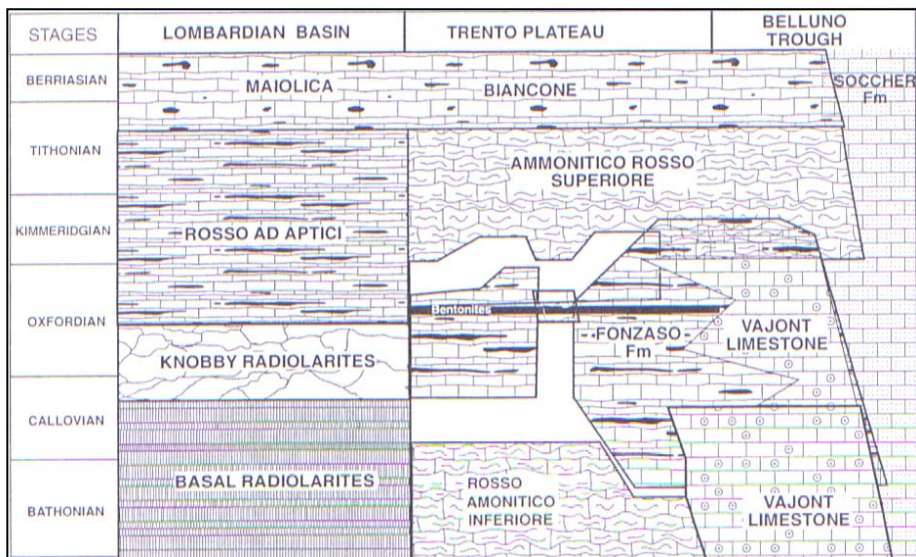
Fig. 3.1.2 – Chronostratigraphic synopsis of Jurassic formation of Southern Alps, based mainly on ammonites, radiolarian and calcareous nannofossil data Lombardian Basin, from Trento Plateau and Belluno Trough (after Baumgartner *et al.*, 2001).

3.2 Tethys Ocean sections

3.2.1. **Torre de Busi**

Location: The outcrop is located on the road SP 179 that goes from Torre de Busi village to
Sogno village and Colle di Sogno (Lombardy, North Italy) (Fig. 3.2.1).

Fig 3.2.1 – Geographic position of Torre de Busi section (1:250000).

Remarks: The investigated section spans the upper part the Radiolariti, the Rosso ad Aptici and
the lowermost part of the Maiolica. Samples were collected for calcareous nannofossil
biostratigraphic and quantitative investigations, and for geochemical analysis. Additional
sampling for paleomagnetic investigation was also performed (see Fig.4.1 for details). (A
detailed profile is given on the attached digital support).

Stratigraphic range: Upper Oxfordian – Lower Berriasian

Paleogeography: The section belongs to the Lombardian Basin.

Lithology: Violet-red listed chert (Radiolarite) gradually changing into red cherty marlstones and cherty limestones (Rosso ad Aptici) followed by grey, light brown to white limestones with chert nodules (Maiolica).

3.2.2. Monte Pernice

Location: The outcrop is located near Monte Pernice, on the secondary road going from Aquilini village to Uccellada Magnoli (Lombardy, North Italy) (Fig. 3.2.2).
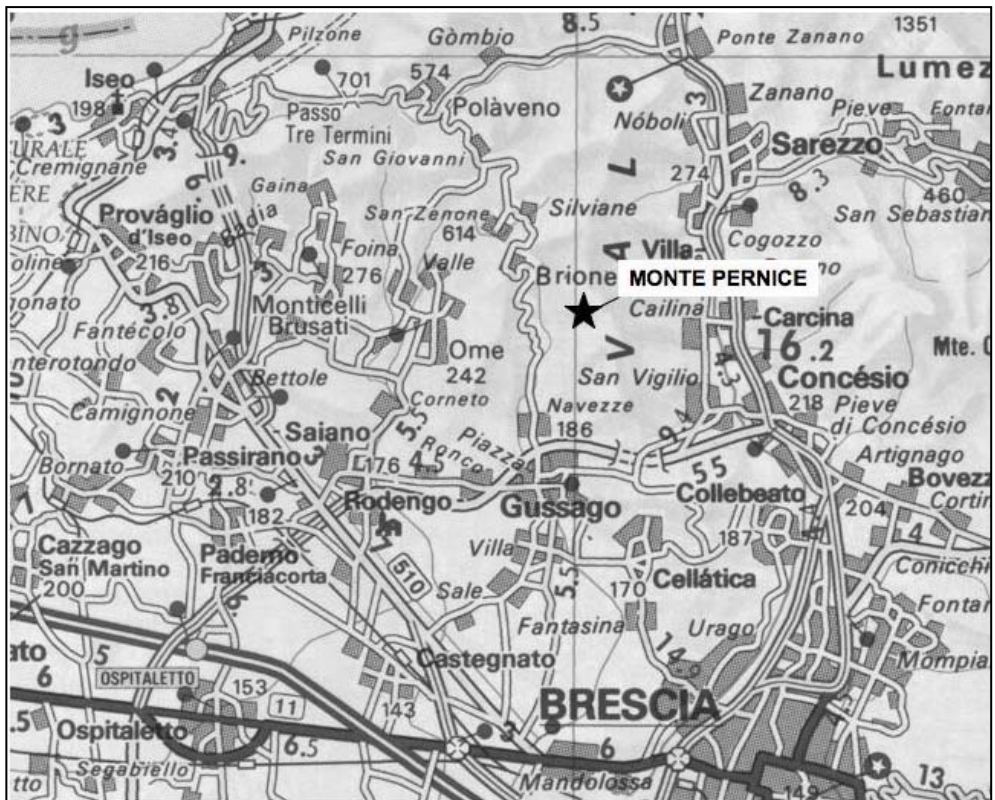
Fig. 3.2.2 – Geographic position of Monte Pernice section (1:250000).

Remarks: The investigated section spans the transitional interval between the Rosso ad Aptici and the lowermost Maiolica. Samples were collected for calcareous nannofossil quantitative investigations (see Fig. 4.1 for detail and also Erba & Quadrio, 1987).

Stratigraphic range: Lower Tithonian – lowermost Berriasian

Paleogeography: The section belongs to the easternmost part of the Sebino Through, close to the Lombardian Basin / Trento Plateau boundary.

Lithology: transitional interval between red cherty marlstones and red limestones with red chert nodules (Rosso ad Aptici) and grey, light brown to white limestones with chert nodules (Maiolica).

3.2.3. **Colme di Vignola**

Location: The outcrop is located along the secondary road going from Brentonico village to Monte Vignola (Asiago Plateau, Veneto, North East Italy) (Fig. 3.2.3).
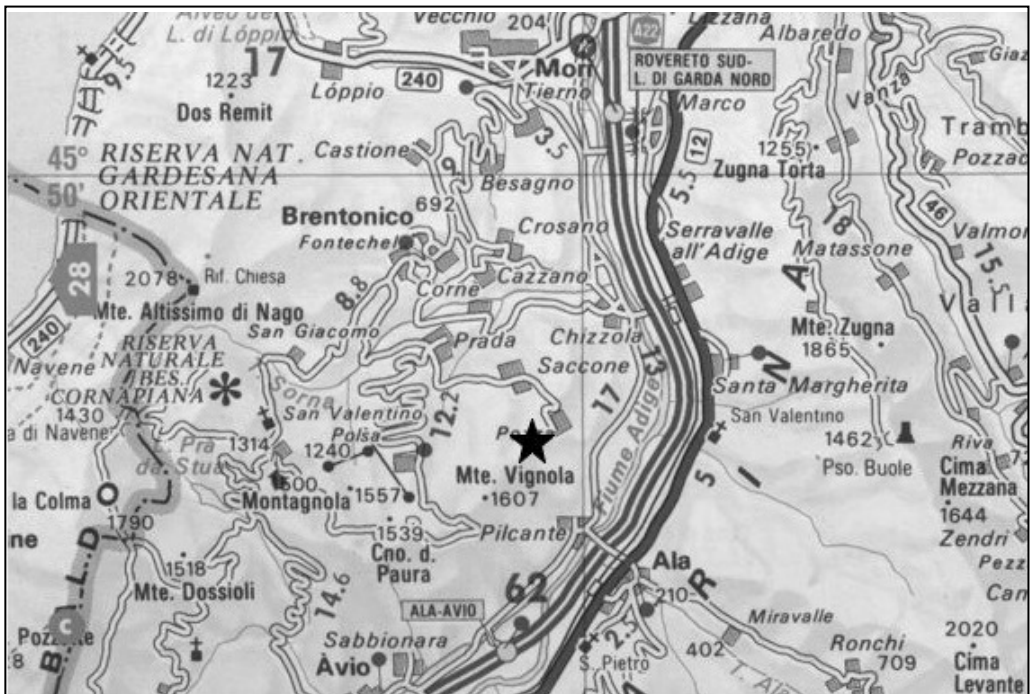
Fig. 3.2.3 – Geographic position of Colme di Vignola (1:250000).

Remarks: The investigated section spans the Calcare Selcifero di Fonzaso, the Rosso Ammonitico Superiore and the lowermost part of the Biancone. Samples were collected for paleomagnetic and biostratigraphic investigations (see Fig. 4.1 for details). (A detailed profile is given on the attached digital support).

Stratigraphic range: uppermost Kimmeridgian – Lower Berriasian

Paleogeography: The section belongs to the Trento Plateau.

Lithology: Red nodular cherty marlstones (Calcare Selcifero di Fonzaso) followed by reddish-pinkish nodular limestones with chert nodules (Rosso Ammonitico Superiore) and then followed by whitish pseudo-nodular limestones with red chert nodules of the lowermost part of the Biancone.

3.2.4. **Foza A, B**

Location: The outcrop is located along the road SP 76 going from Gallio village to Foza village (Asiago Plateau, Veneto, North East Italy). The two sections outcrop on the two different sides of a road curve: Foza B outcrops first, then Foza A after the corner (Fig. 3.2.4).

Remarks: The investigated sections span the upper part of Rosso Ammonitico Inferiore and the lowermost part of Biancone. Samples were collected for paleomagnetic and biostratigraphic investigations (see Fig. 4.1 for details). (A detailed profile is given on the attached digital support).

Stratigraphic range: Lower Kimmeridgian – Upper Berriasian

Paleogeography: The sections belong to the Trento Plateau.

Lithology: Red nodular condensed limestones and cherty marls (Rosso Ammonitico Inferiore) followed by red nodular cherty marlstones (Calcare Selcifero di Fonzaso / Rosso Ammonitico Medio), then by reddish-pinkish nodular condensed limestones with chert nodules (Rosso Ammonitico Superiore) and finally by whitish pseudo-nodular limestones with red chert nodules of the lowermost part of the Biancone.

3.2.5. **Frisoni**

Location: The outcrop is located along the road SP 76 that goes from Foza village to Frisoni village before the Valgadena bridge (Asiago Plateau, Veneto, North East Italy) (Fig. 3.2.4).

Remarks: The investigated sections span the upper part of the Rosso Ammonitico Superiore and the lowermost part of the Biancone. Samples were collected for paleomagnetic and biostratigraphic investigations (see Fig. 4.1 for details). (A detailed profile is given on the attached digital support).

   Stratigraphic range: uppermost Kimmeridgian – Lower Berriasian

Paleogeography: The sections belong to the Trento Plateau.

Lithology: Reddish nodular condensed limestones with shaly interbeds (Rosso Ammonitico Superiore) followed by pinkish to white pseudo-nodular limestones with red chert nodules (lowermost Biancone).

3.2.6. **Bombatierle quarry**

Location: The section is located in an active quarry, where Rosso Ammonitico is excavated as ornamental stones. The quarry is located in the surrounding of Asiago village, near Monte Kaberlaba (Asiago Plaetau, Veneto, North East Italy) (Fig. 3.2.4).

Remarks: The investigated sections spans the upper part of the Rosso Ammonitico Inferiore to the lowermost part of the Biancone. Samples were collected for paleomagnetic and biostratigraphic investigations (see Fig.4.1 for details). (A detailed profile is given on the attached digital support).

   Stratigraphic range: Upper Callovian – Middle/Upper Tithonian

Paleogeography: The section belongs to the Trento Plateau.

Lithology: Red nodular condensed limestones and grey to pinkish less nodular limestones characterized by *hardgrounds* and *burrowings* (Rosso Ammonitico Inferiore); red-brown cherty marls (Calcare Selcifero di Fonzaso or Rosso Ammonitico Medio) characterized by a distinct bentonite layer; red-brown listed Radiolarite followed by red nodular condensed cherty limestones with red chert nodules (Rosso Ammonitico Superiore); pinkish to white nodular to pseudo-nodular limestones with chert nodules (Biancone).

3.2.7. **Sciapala quarry**

Location: The section is located in an abandoned quarry, where Rosso Ammonitico was excavated as ornamental stones. The quarry is located in the surroundings of Asiago village, near Cima Echar (Asiago Plaetau, Veneto, North-East Italy) (Fig. 3.2.4).
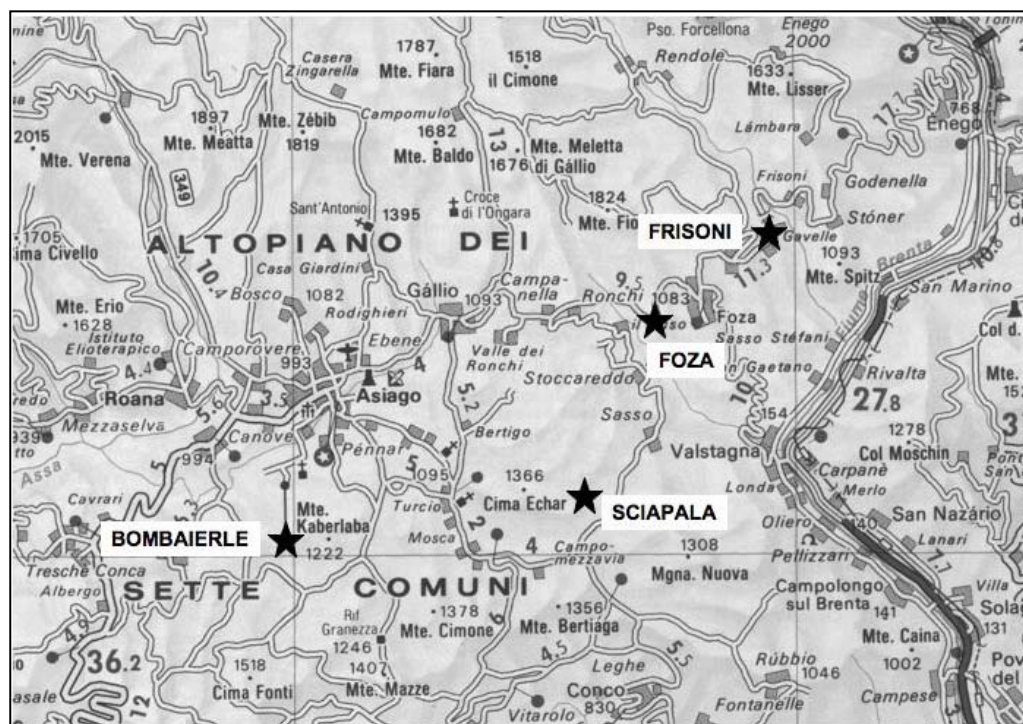
Fig. 3.2.4 – Geographic position of Foza A, B and Frisoni sections, Bombatierle and Sciapala quarries (1:250000).

Remarks: The investigated sections spans the upper part of the Rosso Ammonitico Inferiore to the lowermost part of the Biancone. Samples were collected for paleomagnetic and biostratigraphic investigations (see Fig. 4.1 for details). (A detailed profile is given on the attached digital support).

 Stratigraphic range: Middle Oxfordian – Upper Tithonian

Paleogeography: The section belongs to the Trento Plateau.

Lithology: Red nodular condensed limestones and grey to pinkish less nodular limestones characterized by *hardgrounds* and *burrowings* (Rosso Ammonitico Inferiore); red nodular condensed to pinkish pseudo-nodular cherty limestones with red chert nodules (Rosso Ammonitico Superiore); pinkish to white nodular to pseudo-nodular limestones with chert nodules (Biancone).

3.3 Geology and paleogeography of the central Atlantic Ocean (DSDP site 534A, Blake-Bahama Basin, Atlantic Ocean)

The opening of the Central Atlantic Ocean started in the Middle Jurassic between North America and North-Western Africa, with the oldest sediments of Callovian age (Sheridan, 1983). During the Late Jurassic time interval the Central Atlantic was a NE-SW oriented basin with a maximum length of approximately 6000 km extending from the equator to 30°N. It was of minor oceanographic importance due to its relatively small size and restricted geography in comparison to the Tethys Ocean or modern Atlantic Ocean. The central Atlantic Ocean was episodically connected with the Pacific Ocean (to the West), with the Arctic-Boreal Sea (to the North) while a permanent seaway connected Central Atlantic to the Alpine-Tethys (East side).
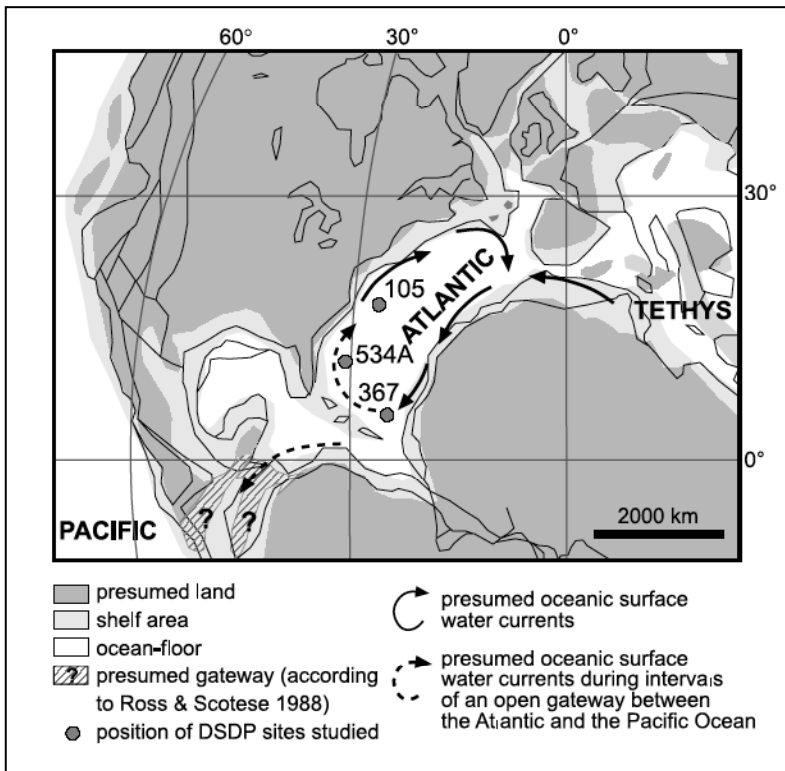

Fig. 3.3.1 – Palaeogeographic setting of Central Atlantic (after Bornemann *et al.*, 2003). The hatched area in Central America indicates the possible gateway between the Atlantic and Pacific Ocean according to the plate-tectonic reconstructions of Ross and Scotese (1988). Black lines and arrows show the hypothesized surface water circulation.

During Late Jurassic to Early Cretaceous time a clockwise surface water circulation system is suggested in the Central Atlantic (Bornemann *et al.*, 2003), sustained by a circum-equatorial current system linked to a low-latitude circumglobal passage (Berggren & Hollister, 1977; Winterer, 1991; Adatte *et al.*, 1996; Hotinski & Toggweiler, 2003). Plate-tectonic reconstructions suggest a permanent connection via the Strait of Panama gateway established in the latest Tithonian, CM19 Magnetochron, Calpionellid Zone B (Ross and Scotese, 1988).

The Middle Jurassic to lowermost Cretaceous sedimentary sequence, recovered at DSDP sites 105, 367 and 534, is characterized by interbedded light grey limestones, green-grey claystones and greyish-red calcareous claystones with rare ammonites (Cat Gap Formation, Lower Tithonian); nannofossil-radiolarian micritic limestones, nannofossil chalks, marls, claystones and siltstones are following (Blake-Bahama Formation, Upper Tithonian – Lower Berriasian).

The carbonate content generally increases upwards, while the siliceous content decreases during the Callovian – Tithonian interval. This situation has been explained by a lowering of the CCD (Roth, 1983) but other explanations are not excluded due to changing in ocean-circulation or plate motions (see paragraph 3.1).

3.4 Atlantic Ocean DSDP site 534 A

Location: DSDP Site 534 A is located east of Florida near the center of Blake-Bahama Basin at
  28°26.6'N, 75°22.9'W at a water depth of 4976 meter (Roth, 1983) (see Fig. 3.4.1).
Remarks: The studied interval is 130 m thick. It spans the Cat Gap Formation and the Blake-
  Bahama Formation. Samples were collected for calcareous nannofossil quantitative
  investigations (see Fig. 4.1 for details).
Investigation: Calcareous nannofossil absolute abundances have been achieved on the basis of
  the calcareous nannofossil biostratigraphy published by Bralower and others (1989).
  Stratigraphic range: Kimmeridgian – Upper Tithonian
Paleogeography: The section belongs to Blake-Bahama Basin, Western Atlantic Ocean.
Lithology: The Cat Gap formation consists of interbedded light grey limestones and green-grey
  claystones (cores 76-543A-111 to 76-543A-103) followed by greysh to red calcareous
  claystones with rare ammonites (cores 76-543A-103 to 76-543A-92). The Blake-Bahama
  Formation consists of cemented limestones with minor claystone partings (core 543-A 91 to

85) followed by laminated nannofossil chalk, bioturbated chalk, claystone and siltstone (cores 76-543A-84 to 76-543A-75).
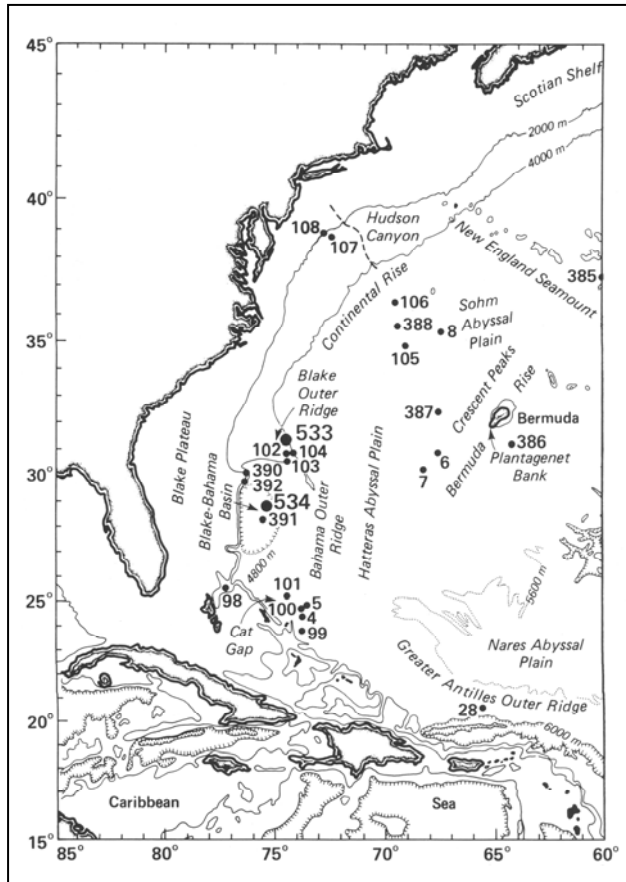
Fig. 3.4.1 – Geographic setting of Central Atlantic (after Gradstein & Sheridan, 2003) and DSDP site 534 A.

4. MATERIALS & METHODS

Different kinds of investigation have been carried out during this PhD project. A first phase has been focused on the integrated stratigraphy (lithostratigraphy, calcareous nannofossil and calpionellid biostratigraphy, magnetostratigraphy, sable isotope chemostratigraphy and carbonate content analysis) of several new and/or historical sections. A second phase has been focused on paleoceanographic reconstructions derived from calcareous nannofossil (and where available from calpionellid) absolute abundances (Fig. 4.1). Based on semiquantitative and quantitative analysis, evolutionary trends of some coccolith and nannolith groups have been reconstructed. Where magnetic investigation has been performed, every sample was prepared from un-heated magneto-core end-pieces, and analyzed with a polarizing light microscope at 1250x magnification.

4.1. Sample preparations techniques

4.1.1. Smear slide

Calcareous nannofossil biostratigraphic investigation has been performed on smear slide prepared following the procedure described by Bown (1998). A total of 514 samples of different lithologies have been chosen: marlstones for Radiolarite marly interbeds and from Calcare Selcifero di Fonzaso; marlstones and limestones form Rosso Ammonitico inter-nodular micrite; limestones from Maiolica. A small amount of rock material has been powdered adding few drops of bi-distillate water. The obtained suspension has been mounted onto a microscope slide, covered with a slide cover and fixed with Norland Optical Adhesive, without centrifuging, ultrasonic cleaning or settling the sediment in order to retain the original composition.

4.1.2. Ultra-thin section

A total 135 thin section has been prepared following a standard preparation technique. Thin sections were prepared in order to investigate calcareous nannofossil and calpionellid absolute abundances: while calpionellids are countable on a normal thin section (25 µm thick),

SECTION	LITTERATURE	CALCAREOUS NANNOFOSSIL - this thesis		ANALYSIS		OTHERS		
		Bio-stratigraphy	Paleocea-nography	total smear slides prepared and analized and their sampling rate	*ultra*-thin sections	Calpionellid biostratigraphy	Chemo-stratigraphy	Magneto-stratigraphy
BOMBATIERLE quarry Asiago Plateau, Italy	*Channell et al., in prep.*	X		a total of 53 total; one sample every 40-50 cm *circa*				X
COLMA DI VIGNOLE Trento Plateau, Italy	*Channell et al., in prep.*	X		a total of 45; one sample every 40-50 cm *circa*				X
DSDP site 534 A Blake Bahama Basin, Atlantic Oceans	*Ogg, 1983; Roth, 1983; Bralower et al., 1989; Bornemann et al., 2003; Tremolada et al., 2006*	X	X		a total of 18; one sample every core (from core 76-534A-102 to 76-534A-90) - *preliminar data*	X		
FOZA A Asiago Plateau, Italy	*Bralower et al., 1989; Weissert & Channell, 1989; Channell et al., in prep.*	X		a total of 99; one sample every 30-40 cm *circa*				X
FOZA B Asiago Plateau, Italy	*Bralower et al., 1989; Weissert & Channell, 1989; Channell et al., in prep.*	X		a total of 22; one sample every 80-100 cm *circa*				X
FRISONI Trento Plateau, Italy	*Weissert & Channell, 1989; Channell et al., in prep.*	X		a total of 42; one sample every 40 cm *circa*			δ¹³C	X
MONTE PERNICE Lombardian basin, Italy	*Erba & Quadrio, 1987*	X	X	a total of 16; one sample every 100-120 cm *circa*	a total of 16; one sample every 100-120 cm *circa*	X		
SCIAPALA quarry Asiago Plateau, Italy	*Channell et al., in prep.*	X		a total of 56; one sample every 20-50 cm *circa*				X
TORRE DE BUSI Lombardian basin, Italy	*Rais, PhD thesis; Channell et al., in prep.*	X	X	a total of 181; one sample every 20-40 cm *circa*	a total of 101; one sample every 40 cm *circa*	X	δ¹³C	X

Fig. 4.1 – Summary of performed investigations and applied methodologies.
Calpionellid biostratigraphic investigation performed by G.Andreini.

calcareous nannofossils need a thinner thin section (7-8 µm thick) to be visible, for that reason every thin section has been thinned using different kind of emery. A total of 117 thin sections from marly limestones of Rosso ad Aptici and Maiolica limestones (Torre de Busi and Monte

Pernice sections, see paragraphs 3.2.1 and 3.2.2) have been thinned using an emery powder mixed with water.

18 thin sections from soft marly shale of Cat Gap Formation and calcareous shale of Blake-Bahama Formation (DSDP Site 534 A, see paragraph 3.4) have been thinned using an emery paper, as the ones made from soft marlstones were water-soluble.

4.2. Preservation and abundance analysis

4.2.1. Preservation

The preservation was characterized adopting the codes described by Roth (1983) (Fig. 4.2).

ETCHING	DESCRIPTION
E1	slight etching: many coccolith show serrate outlines; delicate structures have been somewhat affected by dissolution but are generally preserved.
E2	moderate etching: the more delicate species have been preferentially dissolved; delicate central structures have been destroyed in many specimens; irregular outlines of shields are common.
E3	strong dissolution: salmpe contains mainly dissolution-resistant species, more delicate forms are very rare; nannofossil fragments are abundant.
OVERGROWTH	DESCRIPTION
O1	slight overgrowth: irregular secondary growth of crystallites and slight thickening of central area structures.
O2	moderate overgrowth: delicate central structures are frequently overgrowth to a degree that makes them difficult to be recognized; irregular growth of crystallites in common.
O3	strong overgrowth: delicate species are often so much covered with secondary calcite that identification is nearly impossible.
notes	frequently slight to moderate etching and slight to moderate overgrowth has been observed in the same sample, which might be indicative of secondary overgrowth on larger forms at the expense of the delicate/tiny ones.

Fig. 4.2 - Scheme used to quantify the preservation of calcareous nannofossil (after Roth, 1983)

A preservation estimate of the analyzed *ultra*-thin section was qualitatively carried out as reported in Figure 4.6.

	ESTIMATE OF ROCK PRESERVATION
G	Good: less than 5 field of view per mm^2 is affected by secondary calcite veins or micrite recristallization
M	Moderate: few until several field of view per mm^2 are affected by micrite recristallization, coccolith or nannoliths overgrowth and secondaru calcite viens
B	Bad: less than 1 every 10 field of view is well preserved: micrite is often obliterated by diagenesis, recristallization or/and secondary calite veins or patches

Fig. 4.6 - Qualitative scheme used to quantified rock preservation

4.2.2. Biostratigraphy (semiquantitative abundances)

Calcareous nannofossil biostratigraphy and relative abundance were achieved on smear slides. Biostratigraphy was based on at least 200 microscope fields of view per sample, in order to observe and describe the assemblage, and, when necessary, additional 200 fields of view were investigated to identify rare and/or marker taxa. The nannofloral abundance was coded as reported in Figure 4.3.

	ESTIMATE OF NANNOFOSSIL ABUNDANCES
A	Abundant: more than 10 specimens per field of view
C	Common: 1-10 specimens per field of view
F	Few: 1 speciment every 1 - 1o field of view
R	Rare: 1 speciment every 11 - 1oo field of view
B	Barren: no specimen has been found

Fig. 4.3 - Qualitative scheme used to quantified single taxon abundance

4.2.3. Relative abundances

Relative abundances were quantified counting at least 300 specimens in each sample. Total abundance is the number of specimens per field of view; relative abundances species were calculated as percentage of the total nannoflora assemblage.

4.2.4. Absolute abundances and derived biogenic calcite *paleo*-fluxes

One of the main goals of this study was the reconstruction of nannofossil biogenic calcite *paleo*-fluxes across the investigated interval (see Chapter 5 for details). Several steps are required to achieve *paleo*-fluxes as the amount of biogenic calcite [$CaCO_3$ µgr] per unit area [mm^2] per unit of time [yr]: 1) absolute abundance of single taxon (number of specimens per mm^2); 2) volume of single taxon [$µm^3$] to calculate its calcite mass [µgr]; 3) sedimentation rate [m/Ma; µm/yr]; 4) *Paleo*-fluxes [$CaCO_3$ µgr / mm^2/yr]. Every step is described in detail below.

1) <u>Absolute abundances</u> - Calcareous nannofossil absolute abundances have been obtained counting all specimens recognized in 1 mm^2 of *ultra*-thin sections (7 µm thick) (1 mm^2 = 50 fields of view at 1250x magnification).

2) <u>Taxon volume and mass weigh</u> – Volumes and weights of individual taxa were partially derived from available data (Tremolada & Young, 2002; Bornemann *et al.*, 2003) and partially estimated in this study approximating nannofossil forms to simple geometric solids. Then volumes were calculated based on holotype dimensions (data mainly from Bralower *et al.*, 1989). The dimensions and derived average volumes and masses are summarized in Fig. 4.4.

Gen. *Watznaueria* – Each *Watznaueria* species shows huge size fluctuations. Since the genus *Watznaueria* is one of the most abundant across the studied interval, was divided into six dimensional groups on the basis of coccolith greatest axis (Fig.4.4), then available factor shape (Ks, Tremolada & Young, 2002) was applied to each group.

Gen. *Cyclagelosphaera* – As the genus *Cyclagelosphaera*, it was divided in three dimensional groups on the basis of coccolith diameter (Fig. 4.4), then available Ks was applied.

COUNTED SPECIES (and dimensional group)	Ks FACTOR	LENGHT range (µm)	WIDTH range (µm)	mean VOLUME (µm³)	mean MASS (ǫgr)
Braarudosphaera regularis	…	3,0 - 5,0	…	38 **	103 **
Micrantholithus ssp.	1,41 - 0,85**	3,0 - 6,0	…	97,5	262,275
Conusphaera mexicana minor	…	3,0 - 4,0	...	8,3 *	22,4 *
C. mexicana maxicana	…	5,0 - 10,0	…	55,3 *	149,3 *
Pseudolithraphidites ssp.	…	8,5 - 11,5	0,7 - 1,0	5,67	15,2523
Lithraphidites ssp.	…	26	2,5	42,48	114,2712
Faviconus multicolumnatus I	…	6,0 - 12,0	4,0 - 6,0	231	623.7
F. multicolumnatus II	…	12,0 - 15,0	6,0 - 9,0	604,3	1625,6
Hexalitus noeliae	…	4,0 - 6,0	...	23	59,8
Hexalitus sp. I	…	<5,0	…	23,4	62,946
Hexalitus sp. II	…	>5,0	…	186,8	502,492
Nannoconus compressus	…	5,0 - 7,5 *	…	119,2 *	321,8 *
N.infans	…	2,0 - 6,5 *	…	38,3 *	103,4 *
N.wintereri	…	4,0 - 8,0	4,0 - 8,0	70,6	189,9
N.globulus minor	…	3,0 - 6,0	4,0 - 8,5	55,6	149,6
N. globulus globulus	…	6,0 - 12,0	8,5 - 14,0	368,7	991,8
N.steinmanni minor	…	8,0 - 10,0	7,0 - 9,0	183,7 *	496 *
N.steinmanni steinmanni	…	10,0 - 20,0	7,0 - 13,0	509,7	1371,1
N.kamptneri minor	…	6,0 - 10,0*	4,0 - 6,0*	169,1*	456,6*
N.kamptneri kamptneri	…	15,0 - 22,0	6,0 - 12,0	438	1258,9
Polycostella beckmannii	…	3,0 - 6,0	…	24,2 *	65,3 *
Watznaueria barnesiae I	0,122 *	3,0 - 5,0	…	7,8	20,982
W.barnesiae II A	0,122 *	5,0 - 7,0	…	26,4	71,016
W.barnesiae II B	0,122 *	7,0 - 9,0	…	62,5	168,125
W. manivitae III	0,129 *	9,0 - 12,0	…	210,8	567,052
W. manivitae IV	0,129 *	12,0 - 15,0	…	353,98	952,2062
W. manivitae V	0,129 *	> 15,0	…	528,38	1421,342
W. britannica I	0,011*	3,0 -13 ,0	…	13,87	37,3103
W.britannica II A	0,011*	5,0 - 7,0	…	23,97	64,4793
W.britannica II B	0,011*	7,0 - 9,0	…	56,8	152,792
W.britannica III	0,011*	9,0 - 12,0	…	128,5	345,665
W. fossacincta I	0,111 *	3,0 - 5,0	…	10,1	27,169
W.fossacincta II	0,111 *	5,0 - 7,0	…	18,5	49,765
W.communis I	0,122 *	3,0 - 5,0	…	7,8	20,982
W.communis II A	0,122 *	5,0 - 7,0	…	26,4	71,016
W.communis II B	0,122 *	7,0 - 9,0	…	62,5	168,125
W.communis III	0,129 *	9,0 - 12,0	…	210,8	567,052
Cyclagelosphaera margereli (I)	0,0565*	3,0 - 8,0	...	15,20	40.9
C.tubulata (I)	0,0505	5,0 - 7,0	…	10.9	29.3
C. argoensis (II)	0,0565-0.116	8,0 - 9,0	…	52.9	142.3
C. deflandrei (III)	0.116*	9,0 - 13,0	...	154.3	415.1
C.ryadensis (III)	0.116	13,0 - 15,0	…	381.3	1025,7
Diazomatolithus lehemanii	0,048-0.053 *	3,0 - 5,0	…	3 *	8,1 *
Zeogrhabdotus embergeri	0,094-0,095 *	7,0 - 10,0 *	…	58,8*	200,3*
Z.cooperi	0,094-0,095 *	7,0 - 10,0 *	…	58,8*	200,3*
Z.erectus	0,044*	3,2 - 5,7*	…	4,1*	15,5*
Umbria granulosa minor	0,053*	4,0 - 6,0	…	6,6	17,754
U. granulosa granulosa	0,053*	4,0 - 10,0	…	18,2	48,958
Rhagodiscus asper	0,058*	4,0 - 8,0	…	6,7*	18,1*
Cretarhabdus ssp.	0,072*	6,0 - 9,0	…	31,43*	84,9*
Cruciellipsis cuvillieri	0,066-0,081 *	7,0 - 10,0 *	…	49,9 *	133,1 *

Fig. 4.4 – Taxa counted on *ulta*-thin sections, related Ks factors, dimensions and derived mean volume and mean masses. *: data from Bornemann *et al.* (2003); **: data from Tremolada & Young (2002).

Gen. *Hexalithus* – *H.noeliae* (see Chapter 8 for details) volume was calculated as a six irregular rhombuses volume sum, computing its holotype dimensions. *Hexalithus* sp.1 volume was calculated as a six irregular tetrahedron volume sum, computing observed dimensions. Two dimensional groups were considered to best approximate volume fluctuations due to nannolith dimensional changes (Fig. 4.4).

Gen. *Faviconus* – Two dimensional groups were observed characterized by the same outline. *F.multicolumatus* volume was approximated to a cylinder and two semi-spherical caps sum. following the Bralower and others (1989) holotype dimension (group I) and the ones observed during this study (Fig. 4.4).

Gen. *Nannoconus* – Volume computing for nannoconids has been more complicated than other taxa since longitudinal cuttings, the only ones diagnostic at species level, are few in *ultra*-thin section and most of the nannoconids result cut in any oblique or axial section by the *ultra*-thin section surface. For that reason *Nannoconus* absolute abundances were achieved mainly as the number of nannoconid oblique or axial sections subdivided in four dimensionals groups on the basis of their minimum diameter (Fig. 4.5).
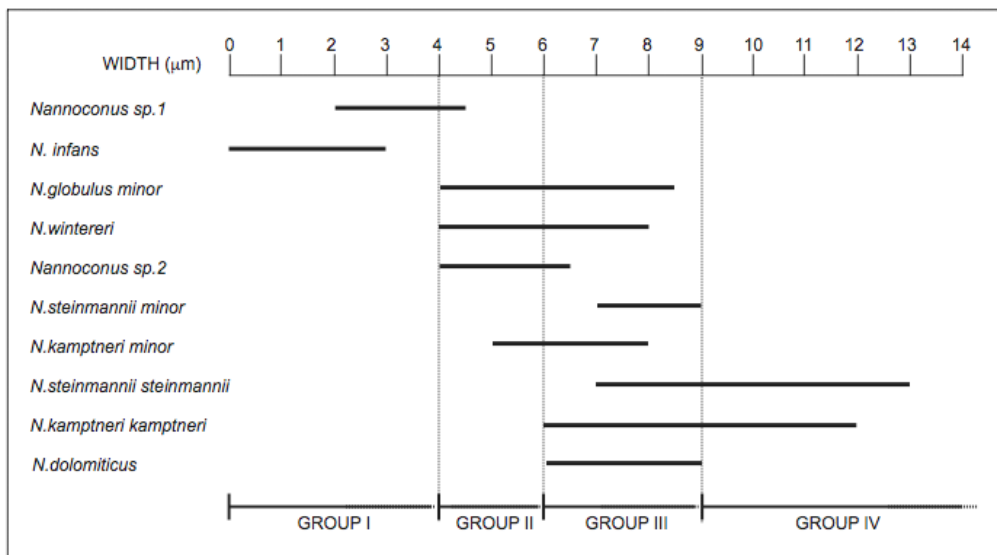
Fig. 4.5 – *Nannoconus* dimensional groups.

Every group may correspond both to the aptical part of a big conical nannoconid or to the basal part of a small conical one. In this way every diameter possibility between the aptical part to the basal one of both smallest and biggest conical shaped nannoconids is automatically taken into account; in the same way any dimension increase of certain *Nannoconus* sp. (as *N.steinmanni minor* vs *N.steinmannii steinmannii*) is also accounted.
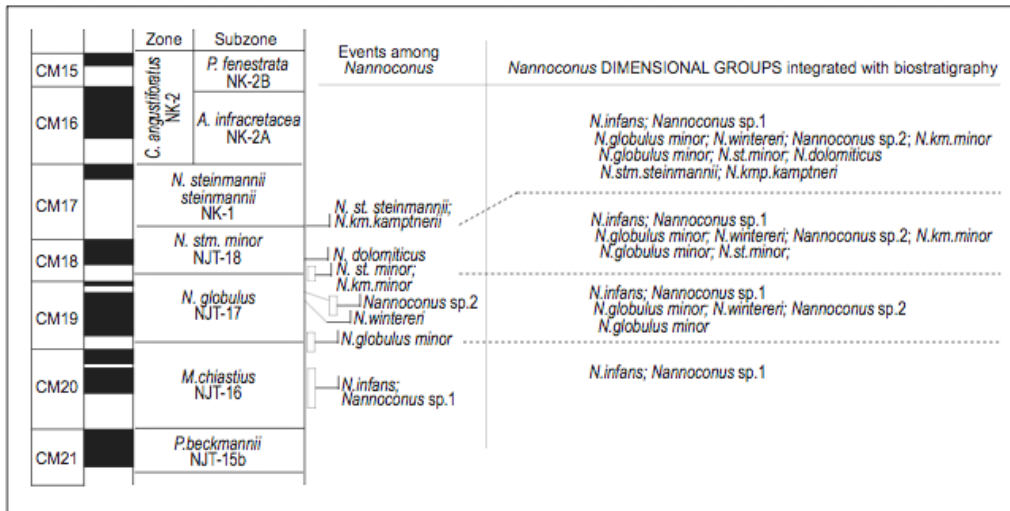
Fig. 4.6 – The stratigraphic distribution of the *Nannoconus* four dimensional groups.

To calculate nannoconid *paleo*-fluxes it has been necessary to couple a calcite mass estimation to each dimensional group, which has been assumed as the average mass of every *Nannoconus* sp. belonging to that dimensional group. The stratigraphic distribution of the four dimensional groups is given in Figure 4.6.

3) <u>Sedimentation rate</u> – it was calculated for each magnetochron thickness: its relative time duration was extrapolated directly from the Time Scale of Channell and others (1995). For the Monte Pernice section magnetostratigraphy is not available: in this case biostratigraphy was taken into account (Fig. 4.7).

4) *Paleo*-fluxes - Nannofossil paleofluxes have been calculated for the micrite-constituting nannofossils, taking into account absolute abundances of the most common taxa, volume/mass

of individual taxon, unit area [mm^2], and unit time [1 yr]. The latter was derived from sedimentation rates (see point 3). Depending on sedimentation rates, the thickness of thin sections (= 7 µm) represents different time duration. Then all absolute abundances have been normalized to one year. *Paleo*-fluxes were achieved as biogenic CaCO$_3$ µgr / mm^2 / yr.

CHRON	DURATION (My)	TORRE DE' BUSI			DSDP site 534A		
		base of each magnetochron (meter level)	thickness (m)	sedimentation rate (m/My)	base of each magnetochron (meter level)	thickness (m)	sedimentation rate (m/My)
CM16N	1,36				1269,01	5,8	4,264706
CM16R	0,65				1276,59	7,58	11,66154
CM17N	0,39				1283,22	6,63	17
CM17R	1,61				1313,24	30,02	18,64596
CM18N	0,71	5,5	...		1323,02	9,78	13,77465
CM18R	0,41	9,66	4,16	10,14634	1328,38	5,36	13,07317
CM19N	1,44	23,33	13,67	9,493056	1356,35	27,97	19,42361
CM19R	0,29	25,33	2	6,896552	1363,21	6,86	23,65517
CM20N	1,34	36,83	11,5	8,58209	1373,07	9,86	7,358209
CM20R	0,82	39,83	3	3,658537	1377,89	4,82	5,878049
CM21N	1,04	43,5	3,67	3,528846			
CM21R	0,5	44,85	1,35	2,7			
CM22N	1,73		...				
CM22R	0,7				1420,67	42,78	9,464602
CM22AN	0,23						
CM22AR	0,32						
CM23N	0,89				1428,16	7,49	8,41573
CM23R	0,47						

Calcareous Nannofossil Subzones	MONTE PERNICE		
	Calcareous Nannofossil Subzones duration	Calcareous nannofossil Subzones thickness (m)	sedimentation rate (m/My)
NJK-D	1,178	5,8	4,923599
NJK-C	1,107	4	3,613369
NJK-B	0,714	3,9	5,462185
NJK-A	2,107	2,1	0,996678
NJ-20	0,857	6,2	7,234539

Fig. 4.7 – Sedimentation rate calculated for Torre de Busi section and DSDP site 534A on available magnetochrons; for Monte Pernice section biostratigraphy was taken into account.

5. RESULTS

5.1. High-resolution bio-magnetostratigraphy of the Oxfordian-Berriasian interval

In this study a detailed lithostratigraphy and calcareous nannofossil biostratigraphy were integrated with calpionellid biostratigraphy (Andreini, *in prep.*) and magnetostratigraphy (Channell *et al.*, *in prep.*) to establish a high-resolution integrated stratigraphic framework for the Upper Jurassic – lowermost Cretaceous of the Southern Alps. In Figure 5.1 the nannofossil biostratigraphy of individual sections is plotted against magnetostratigraphy and calpionellid biostratigraphy, where available.

As discussed in Chapter 2 the calcareous nannofossil biozonation of Bralower *et al.* (1989) was adopted. Calcareous nannofossils are common since the lower Tithonian and become common to abundant from the uppermost lower Tithonian. Most events, Zones and Subzones have been recognized, reported from the base to the top of the studied interval:

- Main events:
    - First occurrence (FO) of *Faviconus multicolumnatus, M.quadratus, C.deflandrei, C.mexicana minor, C.mexicana mexicana, P.beckmannii, M.chiastius, H.noeliae, N.globulus minor, N.wintereri, N.steinmannii minor, N.kamptneri minor, N.steinmannii steinmannii, N.kamptneri kamptneri, C.angustiforatus.*
    - Last occurrence (LO) of *C.wiedmannii, L.sigillatus.*
- Secondary events:
    - First occurrence (FO) of *P.senaria, Hexalithus* sp.1, *Nannoconus* sp.1, *N.infans, U.granulosa, R.asper, C.surirellus, C.cuvillieri, C.octofenestratus.*
    - Last occurrence (LO) of *L.crucicentralis, A.helvetica, U.granulosa.*

- Zones: C.*mexicana* (NJ-20); *M.chiastius* (NJK); *N.steinmannii steinmannii* (NK-1); *C.angustiforatus* (NK-2)*.
- Subzones: *H.cuvillieri* (NJ-20A); *P.beckmannii* (NJ-20B); *H.noeliae* (NJK-A); *N.steinmannii minor* (NJK-D).
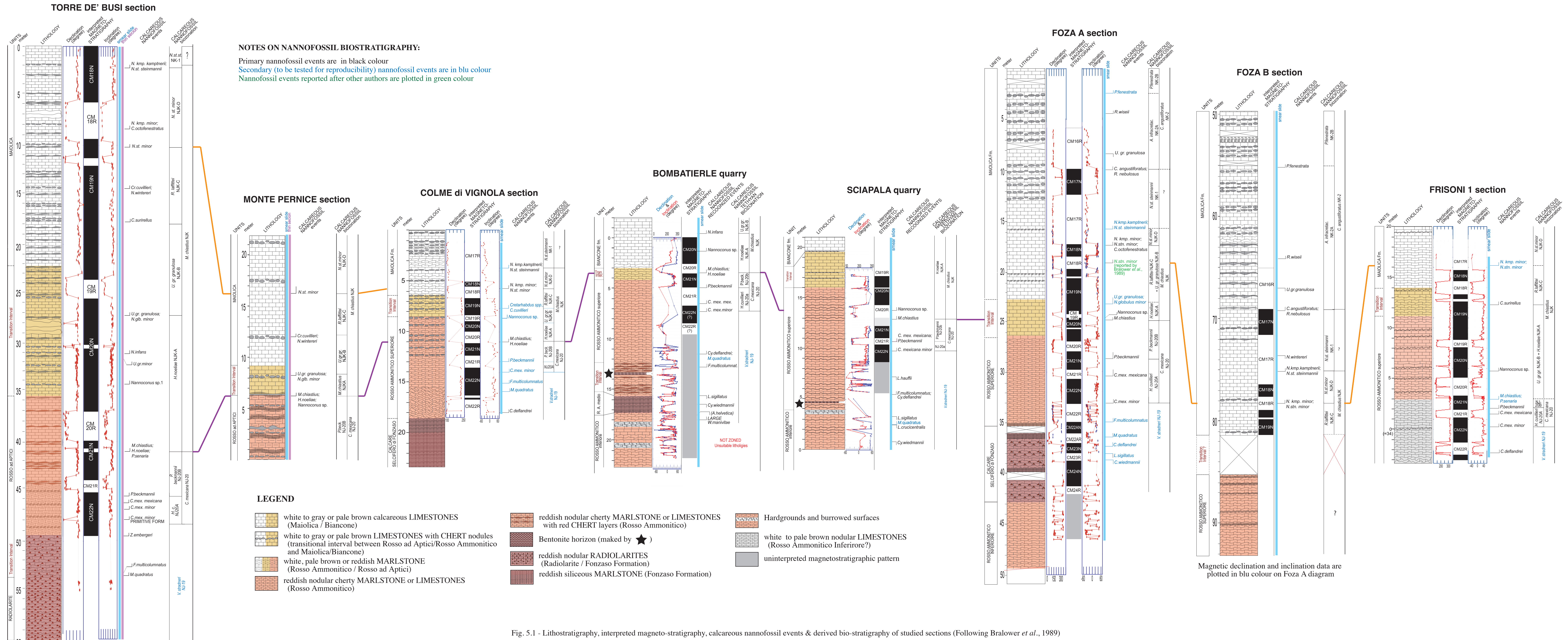
Fig. 5.1 - Lithostratigraphy, interpreted magneto-stratigraphy, calcareous nannofossil events & derived bio-stratigraphy of studied sections (Following Bralower *et al.*, 1989)

NOTES ON NANNOFOSSIL BIOSTRATIGRAPHY:

Primary nannofossil events are in black colour
Secondary (to be tested for reproducibility) nannofossil events are in blu colour
Nannofossil events reported after other authors are plotted in green colour

LEGEND

white to gray or pale brown calcareous LIMESTONES (Maiolica / Biancone)

white to gray or pale brown LIMESTONES with CHERT nodules (transitional interval between Rosso ad Aptici/Rosso Ammonitico and Maiolica/Biancone)

white, pale brown or reddish MARLSTONE (Rosso Ammonitico / Rosso ad Aptici)

reddish nodular cherty MARLSTONE or LIMESTONES (Rosso Ammonitico)

reddish nodular cherty MARLSTONE or LIMESTONES with red CHERT layers (Rosso Ammonitico)

Bentonite horizon (maked by ★)

reddish nodular RADIOLARITES (Radiolarite / Fonzaso Formation)

reddish siliceous MARLSTONE (Fonzaso Formation)

Hardgrounds and burrowed surfaces

white to pale brown nodular LIMESTONES (Rosso Ammonitico Inferirore?)

uninterpreted magnetostratigraphic pattern

Magnetic declination and inclination data are plotted in blu colour on Foza A diagram

With the respect to the biostratigraphic scheme adopted, some differences have been noted, mainly due to the high-resolution sampling rate (Fig. 4.1) or, on the other hand, to the poor preservation of condensed lithologies studied (Chapter 3). Differences in nannofossil biostratigraphy are described below from the base to the top of the studied interval:

- The LO of *C.wiedmannii* and *L.sigillatus* represent secondary events due to rareness in all studied samples.

- The FO of *V.stradneri* was never identified, and, consequently, the base of *V.stradneri* Zone was not recognized.

- The FO *U.granulosa* subsp. *granulosa* does not represent a replicable event in the majority of the studied sections, probably due to diagenesis, which affect the most delicate form: as a consequence *U.granulosa* subsp. *granulosa* Subzone (NJK-B) was difficult to recognize, and often was approximated with the FO of *N.globulus minor*.

- The FO of *R.laffittei* was never identified in the studied sections mainly as it is extremely rare in Tethyan land sections (Bralower *et al.*, 1989). As a consequence the base of the *R. laffittei* Subzone (NJK-C) was identified on the FO of *C.surirellus.*

Some events, when integrated with the magnetostratigraphy, occur at different levels than reported in literature and/or occur at different levels in the studied sections (Fig. 5.1).

- The FOs of *C.mexicana mexicana* and *P.beckmannii* were identified whitin the CM21, while at Torre de Busi they occur during CM22n. This discrepancy is possibly due to sample preparation, since while rock samples are powdered, several nannoliths are destroyed. Indeed, the older FOs of *C.mexicana mexicana* and *P.beckmannii* at Torre de Busi derive from *ultra*-thin section investigations, preserving the original micrite. Moreover, *C.mexicana mexicana* and *P.beckmannii* are rare at the beginning of their stratigraphic range and most probably the FOs whitin CM21 correspond to the first common occurrences, while the FOs in CM22n are presumably the "real" FOs.

- The FO of *M.chiastius* (and *H.noeliae*) is correlatable with the base of CM20r in all sections, while in Torre de Busi it correlates with the upper part of CM19n. In both cases this event is older than reported by Bralower *et al.* (1989).

- The FOs of *Nannoconus* sp.1 and *N.infans*, representing the nannoconid primitive forms, span from the CM20r (Sciapala quarry) to the upper part of CM20n (Foza A). *N.infans* occurs at levels older than reported by Bralower *et al.* (1989) (CM19n).

- The FO of *C.angustiforatus* correlates with the uppermost part of CM17n at Foza, so slightly before the FO reported in the literature.

5.2. Calcareous nannofossil relative abundances in the Tithonian-Berriasian interval

Calcareous nannofossil relative abundances have been investigated at Torre de Busi, Monte Pernice and Foza A sections (see Figure 5.2.1, 5.2.2, 5.2.3, respectively). The nannofossil preservation is lithology dependent. In siliceous samples they have a high etching degree, while in the marly ones nannofossils are characterized by low etching and overgrowth degrees. The most calcareous samples reveal generally a good nannofossil preservation: the most delicate and tiny coccoliths are usually slightly to strongly etched, viceversa the most calcified nannoliths or the dissolution resistant coccoliths often present a moderate to high overgrowth.

Quantitative analyses reveal that only few taxa (*Watznaueria* spp., *Cyclagelosphaera* spp., *Conusphaera* spp., *Polycostella* spp. and *Nannoconus* spp.) contribute to the 50-70% of the total nannoflora (see Figure 5.2.1, 5.2.2, 5.2.3 for each taxa relative abundances curves). In particular, the genera *Watznaueria* and *Cyclagelosphaera* are the most abundant taxa along the entire studied interval: the highest abundance of these genera occurs through the *M.chiastius* Zone in Torre de Busi and Monte Pernice sections, while it is lower, from the upper part of *V.stradneri* Zone to the upper most part of *H.cuvillieri* Subzone in Foza section. As far as the genus *Waznaueria* is concerned, fluctuations in both size and abundance of different *Watznaueria* species were recognized through the *V.stradneri* Zone: the lower part of this zone is often characterized by an increase of *W.britannica* and *W.britannica* large forms; while from the middle part of this Zone (approximatively from the first occurrence of *M.quadratus*) to the first occurrence of *C.mexicana minor* an increase in both size and abundance of *W.manivitiae*, *W.communis* and their respective large forms were observed. As far as the genus *Cyclagelosphaera* is concerned no evident abundance fluctuations were observed: *C.margerelii*, the most abundant species, is present in all investigated samples and represents the 2% up to 20% of the total assemblage.

40
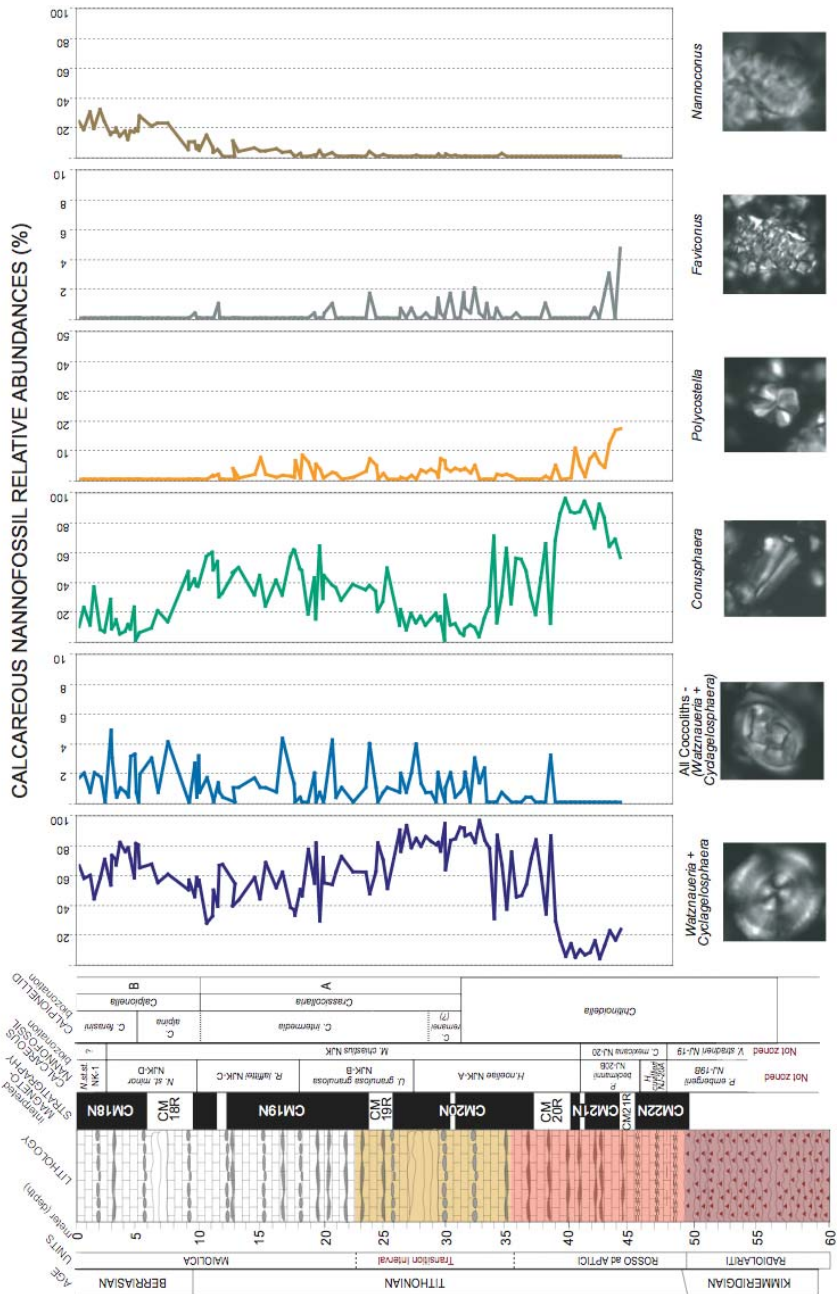
Fig. 5.2.1 – Calcareous nannofossil relative abundances of Torre de Busi section.
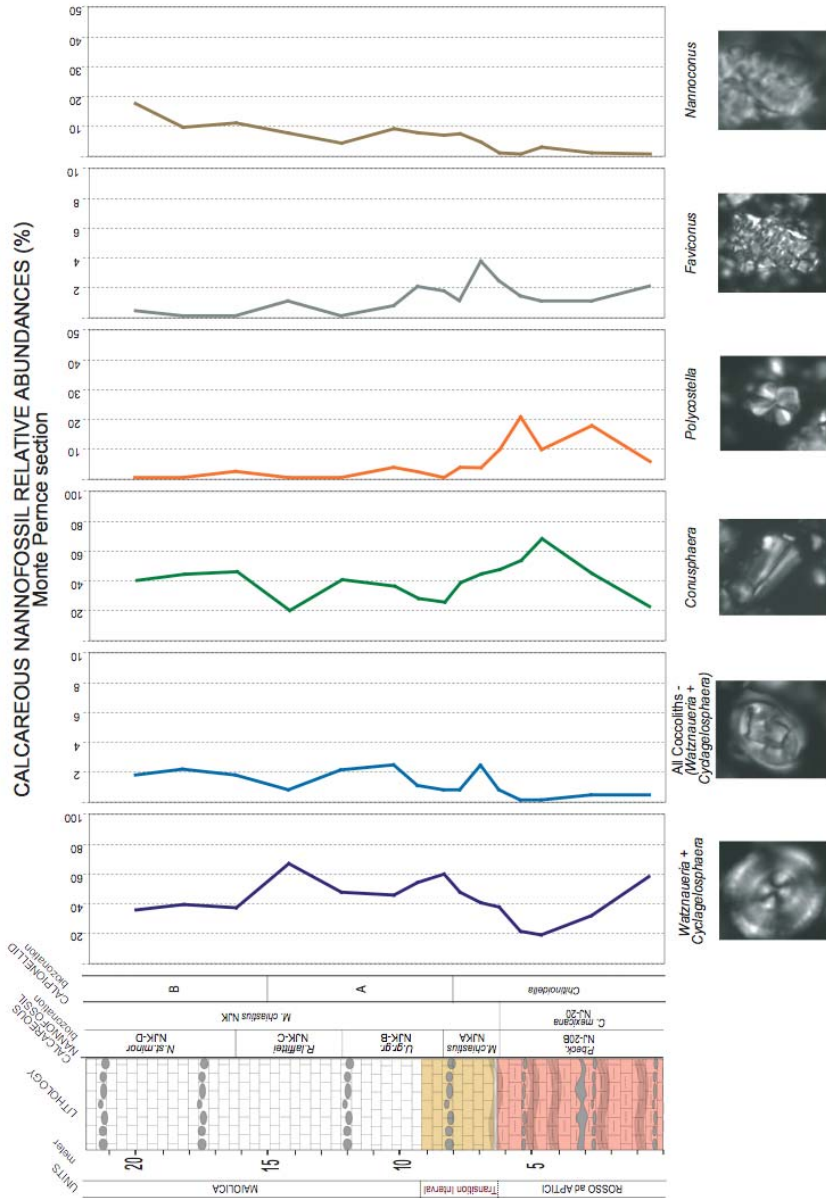
Fig. 5.2.2 – Calcareous nannofossil relative abundances of Monte Pernice section.
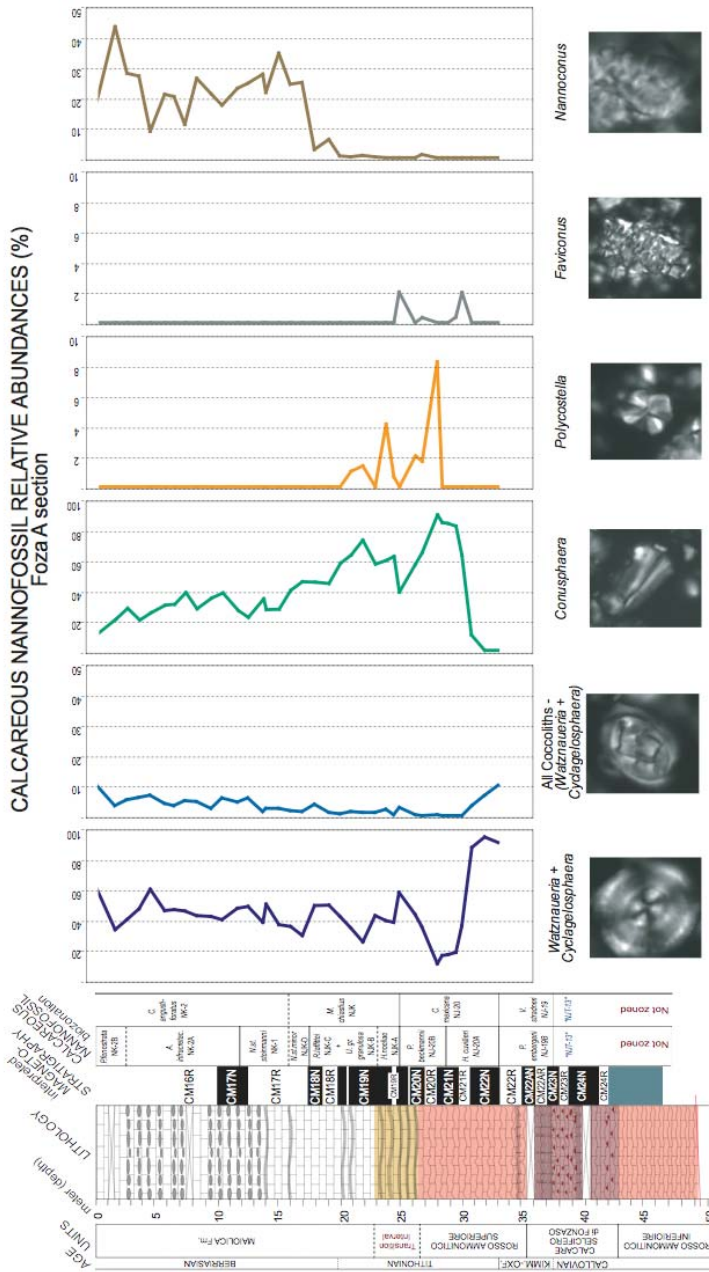
Fig. 5.2.3 – Calcareous nannofossil relative abundances of Foza A section.

The most significant fluctuations in the investigated interval are those of the nannoliths *Faviconus* spp., *Conusphaera* spp., *Polycostella* spp. and *Nannoconus* spp. The first occurrence of *Faviconus multicolumnatus* lies in the *V.stradneri* Zone, around CM22r in Colme di Vignola and Foza A sections, while it is somewhat older in Torre de Busi section, Bombatierle and Sciapala quarries. *Faviconus multicolumnatus* abundance is around 1% and reaches a maximum of 5% (Torre de Busi section) in the *C.mexicana* Zone to the lower part of *M.chiastius* Zone.

The genus *Conusphaera* is one of the most abundant taxa from the *C.mexicana* Zone: the first occurrence of *Conusphaera mexicana minor* lies in the mid part in CM22n of every section but of Foza A, where it lies at the base of CM22n; the first occurrence of *Conusphaera mexicana mexicana* lies in the lower part of CM21r or somewhat before in Torre de Busi section. *Conusphaera* spp. average abundance is around 20% through out the studied interval, but is characterized by notable fluctuations: in the interval between its first occurrence and the *U.granulosa granulosa* Subzone it reaches its highest values from 70% to 90% of the total assemblages, then slightly decreases around an average of 40% in *N.steinmanni minor* Subzone, then progressively reaches an average of 20% of the total assemblages.

Polycostella beckmannii is also one of the most abundant nannoliths and shows a similar distribution pattern like the genus *Conusphaera*. The first occurrence of *P.beckmannii* lies between the mid part of CM21r and the mid part of CM21n. Sooner after this level it reaches its highest abundance, around 10% to 20% until *U.granulosa granulosa* Subzone, then declines around an average of 5% maximum of the total assemblages and in *N.steinmanni minor* Subzone becomes very rare.

The genus *Nannoconus,* also one of the most abundant nannolith of the studied interval, shows a specular distribution pattern like the genus *Conusphaera* and *Polycostella*. The first occurrence of small and primitive *Nannoconus* sp. lies between in CM20n of all section but at Colme di Vignola where it lies in the middle part of CM19n. Soon after this level the genus *Nannoconus* rapidly evolves increasing in number of species, dimension, calcification degree and abundance. The abundance of *Nannoconus* spp. is characterized by an increasing trend through the *M.chiastius* Zone to the top of the studied interval: it reaches values below 10% in the *R.laffittei* Subzone, then starts to increase reaching 20% around the base of the *N.steinmanni minor* Subzone, then slightly increases to a maximum of 40% of the total

assemblages.

Other coccolith taxa such as *Crepidolithus* spp., *Biscutum* spp., *Diazomatolithus lehmanii*, *Microstaurus* spp., *Zeugrhabdotus* spp., *Miravetesina favula*, *Cruciellipsis cuvillieri*, *Rhagodiscus* spp., *Umbria* spp., *Cretarhabdus* spp. and *Percivalia fenestrata* combined together account for less than 5%; while other nannolith taxa like *Schizosphaerella* sp., *Hexalithus* spp., *Pseudolithraphidites* sp., *Lithraphidites carniolensis*, *Assipetra infracretacea* and *Micrantholithus* spp. combined account for less than 2% of the total assemblage.

5.3. Biogenic calcite paleo-fluxes in the Tithonian-Berriasian interval

The Tithonian-Berriasian interval is characterized by a major calcareous nannofossil speciation episode and the appearance of calpionellids: several nannoliths (particularly the nannoconid group) and coccolith genera and species first appear and rapidly evolve, showing an increase in diversity, abundance and calcification degree. Calcareous nannofossil absolute abundances have been performed on Torre de Busi and Monte Pernice sections and on DSDP Site 534 site to reconstruct nannofossil biogenic calcite *paleo*-fluxes (Figures 5.3.1, 5.3.2, 5.3.3, 5.3.4).

Absolute abundances confirm that only few calcareous nannofossil taxa (*Watznaueria* spp., *Cyclagelosphaera* spp., *Faviconus* spp., *Conusphaera* spp., *Polycostella* spp. and *Nannoconus* spp; Figures 5.3.1, 5.3.3, 5.3.4) display significant values, and also that only two calpionellid taxa contribute to calcite *paleo*-fluxes (*Crassicollaria* spp. and *Calpionella* spp.; Figures 5.3.2 and 5.3.3). Quantitative calpionellid and nannofossil analyses point out major changes during the Tithonian – Berriasian interval: nannolith taxa (*F.multicolumnatus*, *C.mexicana*, *P.beckmannii*) increase in abundance, size and calcification degree in discrete steps in the Lower Tithonian (Rosso ad Aptici and Rosso ad Aptici – Maiolica transition interval; DSDP Site 534 from core 100 to core 94); immediately after their acme level the first calcified calpionellids (*Tintinnopsella*) occur. Then nannoconids appear and rapidly develop reaching high abundances and lithogenetic amounts in the Upper Tithonian to Lower Berriasian (Rosso ad Aptici – Maiolica transition and Maiolica; DSDP Site 534 core 95 to core 90). Nannoconids and calcified calpionellids (*Crassicollaria, Calpionella, Remaniella*) increase across the Tithonian/Berriasian boundary interval reaching lithogenetic abundances: the rise in high-calcified nannoconids roughly corresponds with the Acme of *C. alpina* spherical forms.
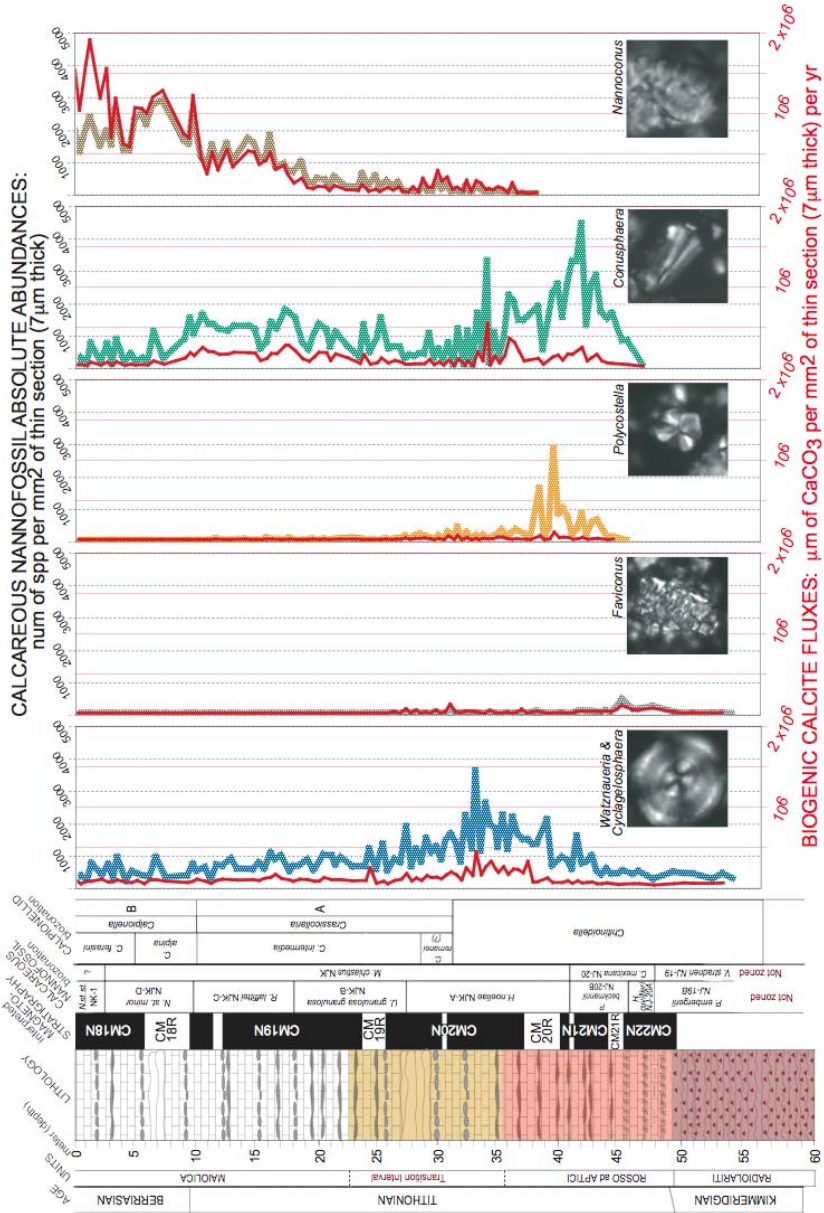
Fig. 5.3.1 – Calcareous nannofossil absolute abundances (coloured lines) and derived *paleo*-fluxes (red line) of Torre de Busi section.
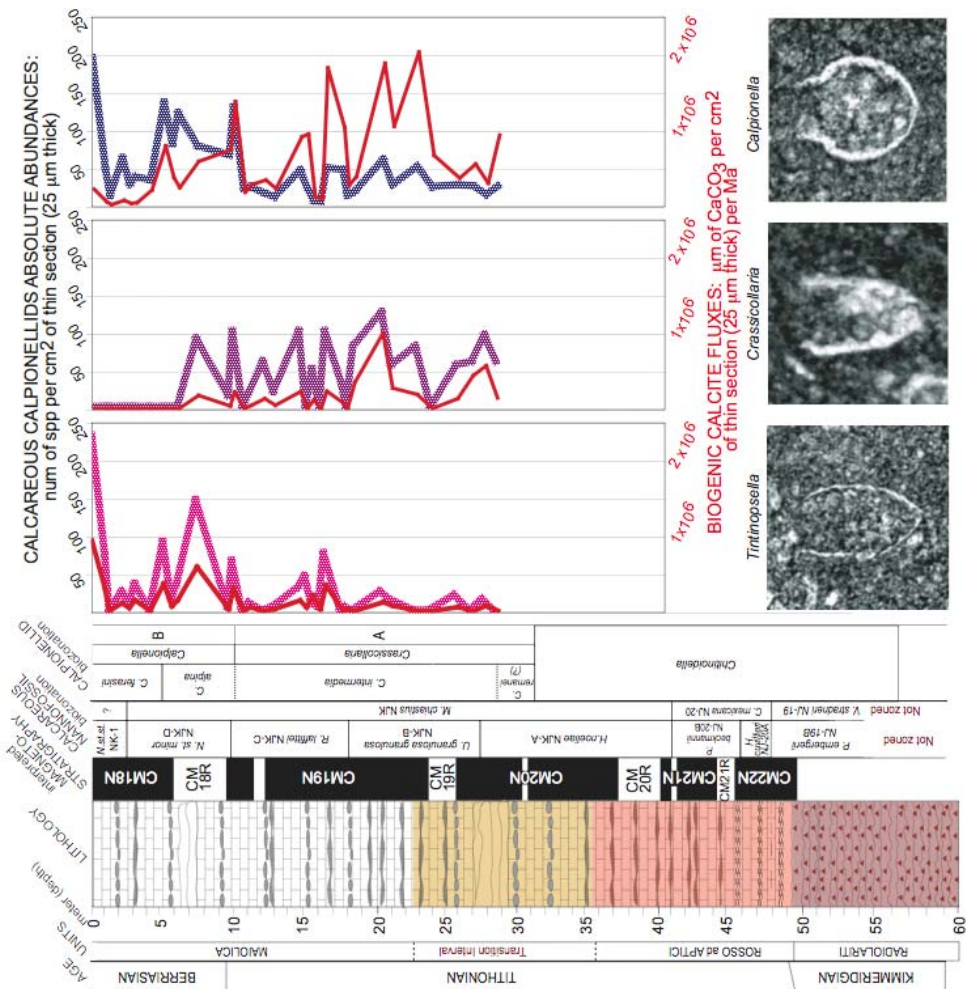
Fig. 5.3.2 – Calpionellid absolute abundances (coloured lines) and derived *paleo*-fluxes (red line) of Torre de Busi section.

The genera *Watznaueria* and *Cyclagelosphaera* are confirmed to be one of the most abundant taxa through the entire studied interval. The highest absolute abundances of these genera occur from the middle of *P.beckmannii* Subzone to the middle part of *R.laffittei* Subzone where they reach an average of 1500 specimens per unit of area corresponding to an average *paleo*-flux of 0,09 to 0.1·10⁶ CaCO₃ µgr / mm² / yr at Torre de Busi section and DSDP 534A. From the middle part of the *R.laffittei* Subzone to the top of the studied interval they fluctuate around 500 specimens per 1 mm² corresponding to an average *paleo*-flux of 0.05·10⁶

$CaCO_3$ µgr / mm^2 / yr. Nevertheless genera *Watznaueria* and *Cyclagelosphaera* derived *paleo*-fluxes contribute less than other nannolith taxa to biogenic calcite production as they are less calcified.

The most significant fluctuations in the investigated interval, confirmed by absolute abundances, are those of nannoliths *Faviconous* spp., *Conusphaera* spp., *Polycostella* spp. and *Nannoconus* spp..

Faviconus multicolumnatus reaches its maximum absolute abundance from the uppermost part of *V.stradneri* Zone and *H.noeliae* Subzone, then decreases and becomes rare. The acme interval is characterized by an average of 45 specimens per 1 mm^2 corresponding to an average *paleo*-flux of $0.02 \cdot 10^6$ $CaCO_3$ µgr / mm^2 / yr. *Faviconus* reaches an absolute maximum of 450 specimens at Torre de Busi section, and *circa* 250 elements at DSDP Site 534A both falling in the middle part of *C.mexicana* Zone, the derived *paleo*-flux contribute to biogenic calcite production for an amount of *circa* $0.35 \cdot 10^6$ $CaCO_3$ µgr / mm^2 / yr.

The genus *Conusphaera* is revealed by absolute abundances to be the most abundant taxa from the base of the *C.mexicana* Zone to the top of the *H.noeliae* Subzone. From the *C.mexicana* Zone to the base of the *U.gr.granulosa* Subzone *Conusphaera* sp. is characterized by an average absolute abundance around 1300 specimens per 1 mm^2, corresponding to an average *paleo*-flux of 0.09 to $0.1 \cdot 10^6$ $CaCO_3$ µgr / mm^2 / yr. In the same interval it reaches a maximum of 4500 at Torre de Busi section and 3100 *circa* at DSDP Site 534, corresponding to *paleo*-fluxes of $0.25 \cdot 10^6$ $CaCO_3$ µgr / mm^2 / yr. From the *U.gr.granulosa* Subzone to the top of the studied interval *Conusphaera* spp. slightly decreases to an average of 750 specimens per 1 mm^2, corresponding to an average *paleo*-flux of $0.05 \cdot 10^6$ $CaCO_3$ µgr / mm^2 / yr: this decrease is due to *C.mexicana minor* which is more abundant than *C.mexicana mexicana* but smaller in size and lighter in weight, thus contributing less to calcite *paleo*-fluxes.

P.beckmannii also shows high absolute abundance with a similar pattern like the genus *Conusphaera*. *P.beckmannii* reaches its highest abundance from *P.beckmannii* Subzone to the top of the *H.noeliae* Subzone with an average of 330 specimens per 1 mm^2 at Torre de Busi section, corresponding to an average *paleo*-flux of $0.02 \cdot 10^6$ $CaCO_3$ µgr / mm^2 / yr; at DSDP site 534A it reaches an average of 600 specimens per 1 mm^2 corresponding to an average *paleo*-flux of $0.03 \cdot 10^6$ $CaCO_3$ µgr / mm^2 / yr. Then *Polycostella* sp. declines to an average of 30 specimens per 1 mm^2 at the base of the *N.steinmanni minor* Subzone, corresponding to an

average *paleo*-flux of $0.002 \cdot 10^6$ CaCO$_3$ µgr / mm^2 / yr, and then becomes very rare.

Absolute abundances of the genus *Nannoconus* reveal that it is the most abundant nannolith, characterized by an exponential increasing trend from the base of the *M.chiastius* Zone to the top of the studied interval. It is possible to subdivide its trend in three intervals: 1) from the base of the *H.noeliae* Subzone to the top of the *U.gr.granulosa* Subzone: *Nannoconus* sp. reaches an average of 300 specimens per 1 mm^2 at Torre de Busi and Monte Pernice sections, corresponding to an average *paleo*-flux of $0.05 \cdot 10^6$ CaCO$_3$ µgr / mm^2 / yr, while at DSDP Site 534 it reaches an average of 550 specimens per 1 mm^2 and an average *paleo*-flux of $0.1 \cdot 10^6$ CaCO$_3$ µgr / mm^2 / yr; 2) *Nannoconus* sp. starts to increase up to the base of the *N.steinmannii minor* Subzone reaching an average of 1100 specimens per 1 mm^2 at Torre de Busi sections and DSDP Site 534, corresponding to an average *paleo*-flux of $0.4 \cdot 10^6$ CaCO$_3$ µgr / mm^2 / yr; 3) from the FO of *N.steinmanni minor* nannoconid absolute abundances exponentially increase to an average of 2500-3000 specimens per 1 mm^2, corresponding to a maximum average *paleo*-flux of $1.1 \cdot 10^6$ – $1.3 \cdot 10^6$ CaCO$_3$ µgr / mm^2 / yr.

As far as Calpionellids is concernes the genera *Crassicollaria* and *Calpionella* are confirmed to be one of the most abundant taxa in the studied interval. The genus *Crassicollaria* shows fluctuation in absolute abundances around an average of 50 specimens per 1 cm^2 from A Zone to the base of B Zone, corresponding to average *paleo*-flux of $0.1 \cdot 10^6$ CaCO$_3$ µgr / cm^2 / yr ($0.001 \cdot 10^6$ CaCO$_3$ µgr / mm^2 / yr). The genus *Calpionella* shows an increase from the base of A Zone to the top of the studied interval. It is possible to recognize two intervals: 1) the calpionellid A Zone is characterized by 30 specimens per 1 cm^2 corresponding to an average *paleo*-flux of $1.5 \cdot 10^6$ CaCO$_3$ µgr / cm^2 / yr ($0.015 \cdot 10^6$ CaCO$_3$ µgr / mm^2 / yr); 2) the upper part of the studied interval is characterized by 70 specimens per 1 cm^2 corresponding to an average *paleo*-flux of $0.27 \cdot 10^6$ CaCO$_3$ µgr / cm^2 / yr ($0.0027 \cdot 10^6$ CaCO$_3$ µgr / mm^2 / yr). These *paleo*-fluxes discrepancies are due to *Calpionella alpina* large form and *Calpionella alpina* spherical form: the first one is less abundant but being larger in size and heavier in mass it contributes more to *paleo*-fluxes. On the contrary *Calpionella alpina* spherical form is more abundant, but contribute less to biogenic calcite *paleo*-fluxes.
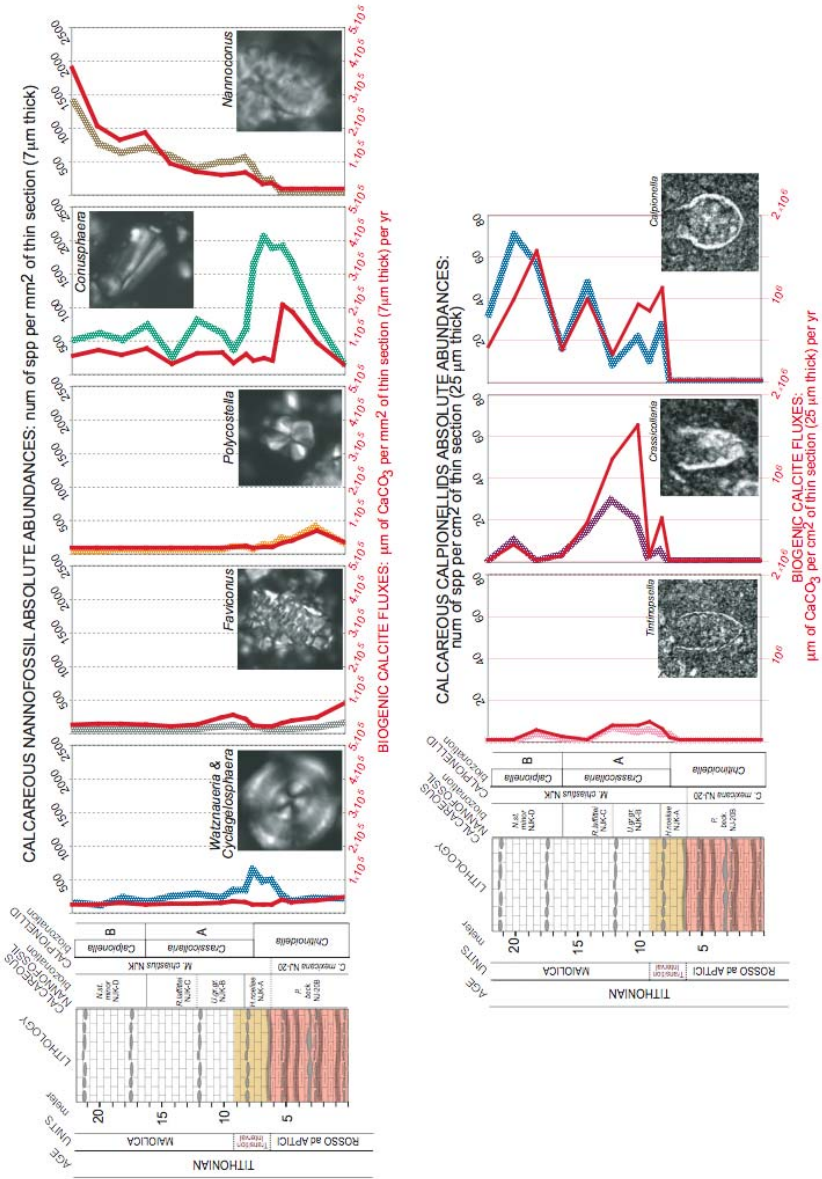
Fig. 5.3.3 – Calcareous nannofossil (above) and calpionellid (below) absolute abundances (coloured lines) and derived *paleo*-fluxes (red line) of Monte Pernice section.
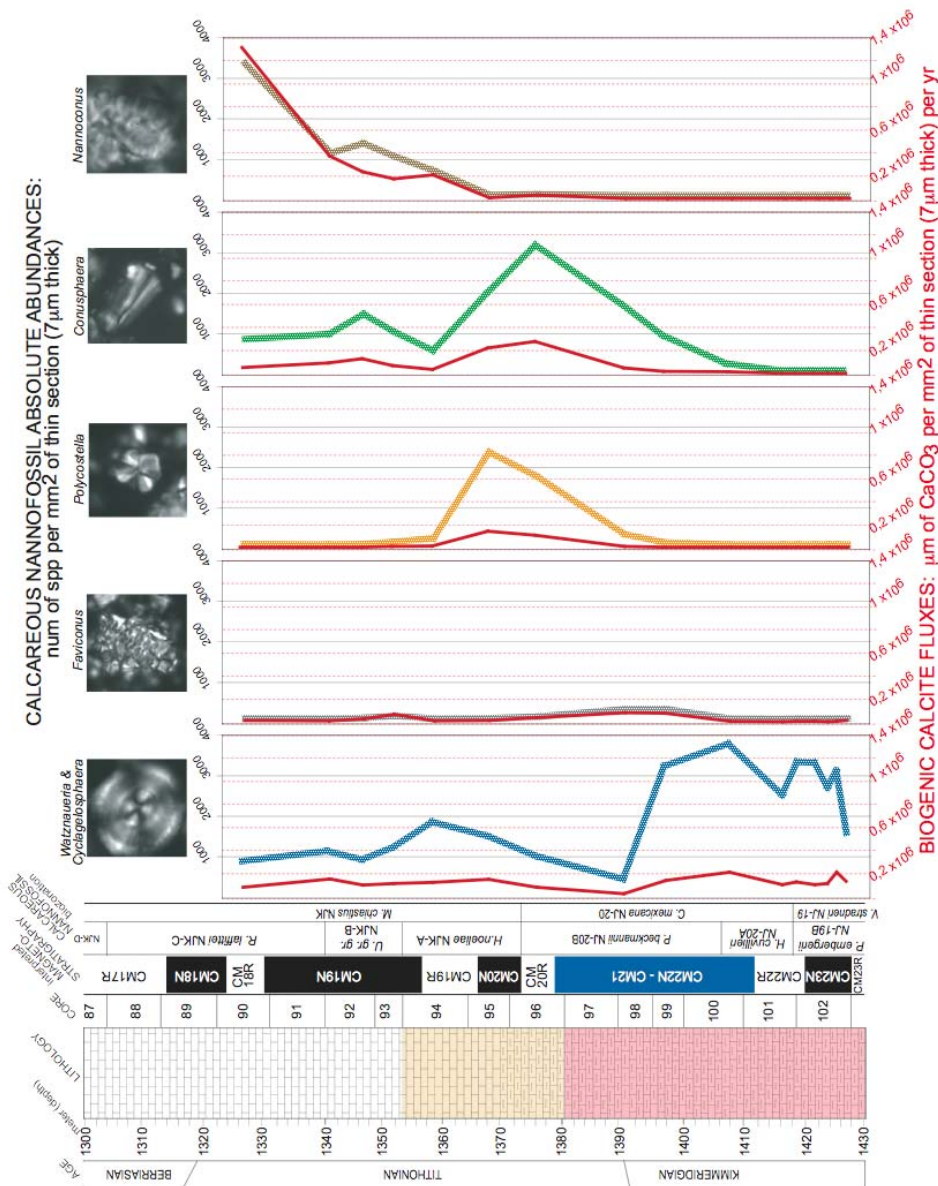
Fig. 5.2.4 – Calcareous nannofossil absolute abundances (coloured lines) and derived *paleo*-fluxes (red line) of DSDP Site 534A.

5.4. Nannofacies in the Tithonian – early Berriasian interval

The Callovian – Berriasian pelagic successions recorded a major change in sedimentation from predominantly siliceous to mostly calcareous. The investigation of nannofossil assemblages in *ultra*-thin section (Torre de Busi, Monte Pernice, DSDP Site 534A) revealed substantially different proportions of some taxa. As a result, the micrite can be classified as produced by one-two nannofossil groups, regarded as rock forming. Seven different types of *nanno*-facies (observed at 1250x magnification) were distinguished from bottom to top (Fig. 5.4.1).
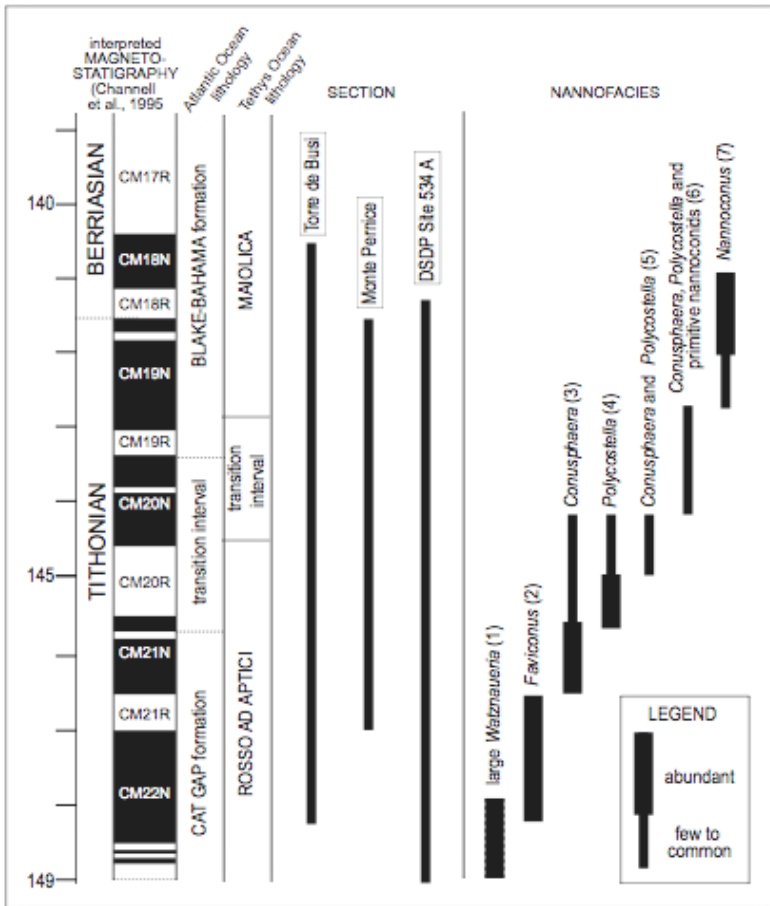

Fig. 5.4.1 – Stratigraphic distribution of nannofacies.

1. Large *Watznaueria* nannofacies. Marly micrite characterized by a large amount of *W.manivitiae* (large forms) and by few *C.deflandrei* (Fig. 5.4.2-1). The micrite is reddish due to limonitic oxides (lower Rosso ad Aptici and/or Cat Gap formations).

2. *Faviconus* nannofacies. Micrite characterized by a huge amount of *F.multicolumnatus* fragments and spheres or aggregates, *W.manivitiae* (large forms), and by few calcareous dinoflagellate calcispheres. *Faviconus* aggregates are particularly abundant and can reach a maximum of 8-10 specimens, lenght greater than 15µm and width greater than 5µm (Fig. 5.4.2-2) (lower – middle Rosso ad Aptici and/or Cat Gap formations, CM22n-CM21r).

3. *Conusphaera* nannofacies. Micrite consisting of huge amounts of *C.mexicana mexicana,* few *C.mexicana mexicana* spheres and calcareous dinoflagellate calcispheres. *C.mexicana mexicana* spheres are made by a variable number of specimens (up to 20-25 specimens), reaching a diameter greater than 30µm (Fig. 5.4.2-3) (upper Rosso ad Aptici and/or Cat Gap formations, CM21n).

4. *Polycostella* nannofacies. Micrite characterized by a huge amount of *P.beckmannii* specimens and spheres or aggregates. At DSDP Site 534 sphere/aggregates can reach different dimensions and, proportionally, number of specimens. This nannofacies is also characterized by abundant *C.mexicana mexicana* (Fig. 5.4.2-4) (upper Rosso ad Aptici and/or Cat Gap fm.– Blake-Bahama fm. transition, uppermost CM21n – upper CM20r).

5. *Conusphaera* and *Polycostella* nannofacies. The micrite is characterized by few to common *Conusphaera* sp. and *P.beckmannii* (uppermost Rosso ad Aptici and/or Cat Gap formations, uppermost CM20r – lower CM20n).

6. *Conusphaera, Polycostella* and small nannoconids nannofacies. The micrite is characterized by few to common *Conusphaera* sp., *P.beckmannii* and primitive small nannoconids, which are generally smaller than 6µm (Fig. 5.4.2-4) (Rosso ad Aptici – Maiolica transition and/or upper Cat Gap formations, lower CM20n – lower CM19n).

7. *Nannoconus* nannofacies. The micrite is made of nannoconids (*Nannoconite*), which are usually greater than 6µm (Fig. 5.4.2-6) (Maiolica and Blake-Bahama formations, lower CM19n – top of the studied interval).
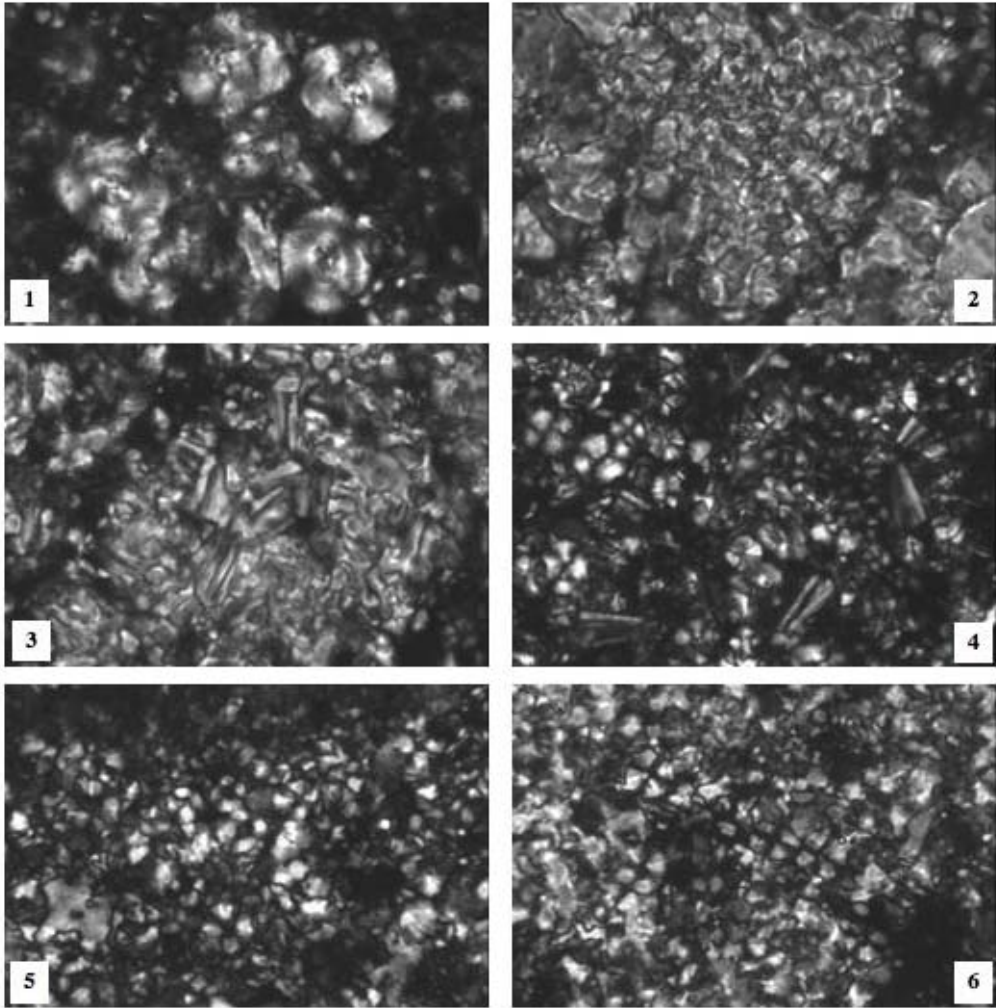
Fig. 5.4.2 – Nannofacies examples: 1. large *Watznaueria* and *Cyclagelosphaera* micrite; 2. *Faviconus multicolumnatus* micrite; 3. *Conusphaera mexicana mexicana* micrite; 4. *Polycostella beckmannii* micrite; 5. Small nannoconids micrite; 6. Nannoconids micrite (*Nannoconite*). Pictures are from Torre de Busi section and DSDP site 534A.

5.5. Calcareous nannofossil evolution modes in the latest Jurassic – earliest Cretaceous interval

The latest Kimmeridgian - early Berriasian interval provides an example of accelerated intra- and intergeneric evolutionary rates, namely a speciation episode, occurred during a time period of environmental stability or characterized by the absence of evidence of coeval

54

environmental changes. In particular, the Tithonian - Berrisian interval is characterized by a distinct speciation episode (Fig. 2.3.1; Fig.5.5.1): several new nannolith and coccolith genera and species first occur and rapidly evolve, reaching high diversity, abundances, dimensions and calcification degree. This speciation episode provides an excellent opportunity to study tempo and mode of calcareous nannofossil evolution in absence of environmental change, which is believed to drive species evolution (see Chapter 2, paragraph 2.2).

This speciation episode is characterized by the first occurrence of several new nannolith genera (*Conusphaera*, *Polycostella*, *Pseudolithraphidites* and *Lithraphidites*, *Nannoconus*, *Assipetra*), few new coccoliths genera (*Umbria*, *Rhagodiscus*, *Cruciellipsis*) and several coccoliths and nannolith new species (*M.chiastius*, *H.noeliae*, *C.surirellus*, *C.octofenestratus*, *C.angustiforatus*). A sequence of events is illustrated in figure 5.5.1. Most new species rapidly evolved generating related new species or subspecies, often in a time interval shorter than two million of years.

Three cases have been analyzed in detail:

1. Generally the majority of ancestral species survives and both the ancestral and the descendant species are found together in the same association. Usually ancestral and descendant species are very similar and differ only for the whole nannolith/coccolith dimension or for the coccoliths central area dimension. *C.mexicana minor* and *C.mexicana mexicana* provide an example among nannoliths, while *Z.erectus* and *Z.embergeri* is an example of coccoliths (Fig. 5.5.2).

2. Sometimes the ancestral species disappears just after or at the same time of the descendant species appearance, like *U.granulosa minor* and *U.granulosa granulosa*.

3. Occasionally, the descendant species are preceded by peculiar morphotypes characterized by transitional features between the ancestral and the descendant ones, as was observed for *Nannoconus* sp. 2 and *N.steinmannii* minor, or for R.*asper* and *R.nebulosus*.
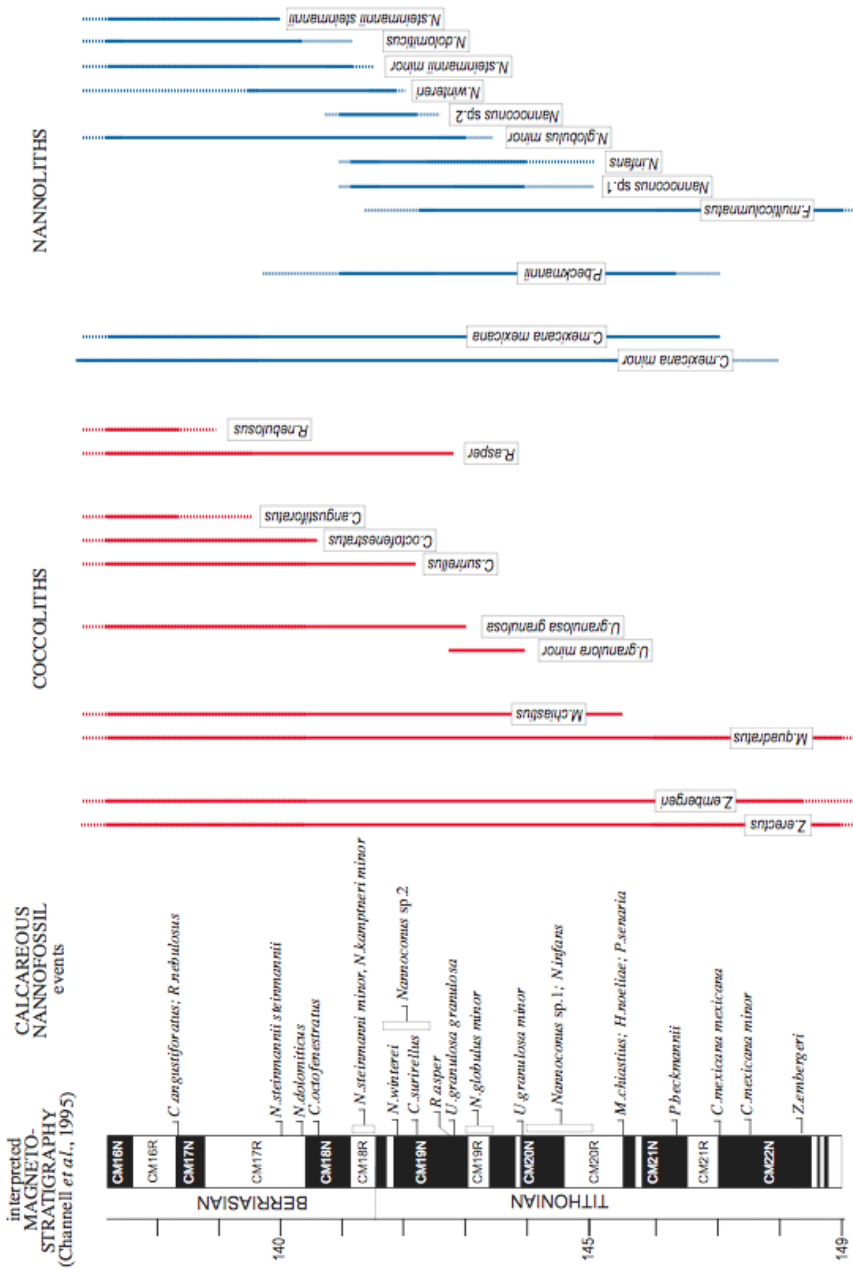
Fig 5.5.1 – Tithonian – early Berriasian speciation episode and ranges of the most abundant or peculiar species, (data from this study and Bralower *et al.*, 1989)

56
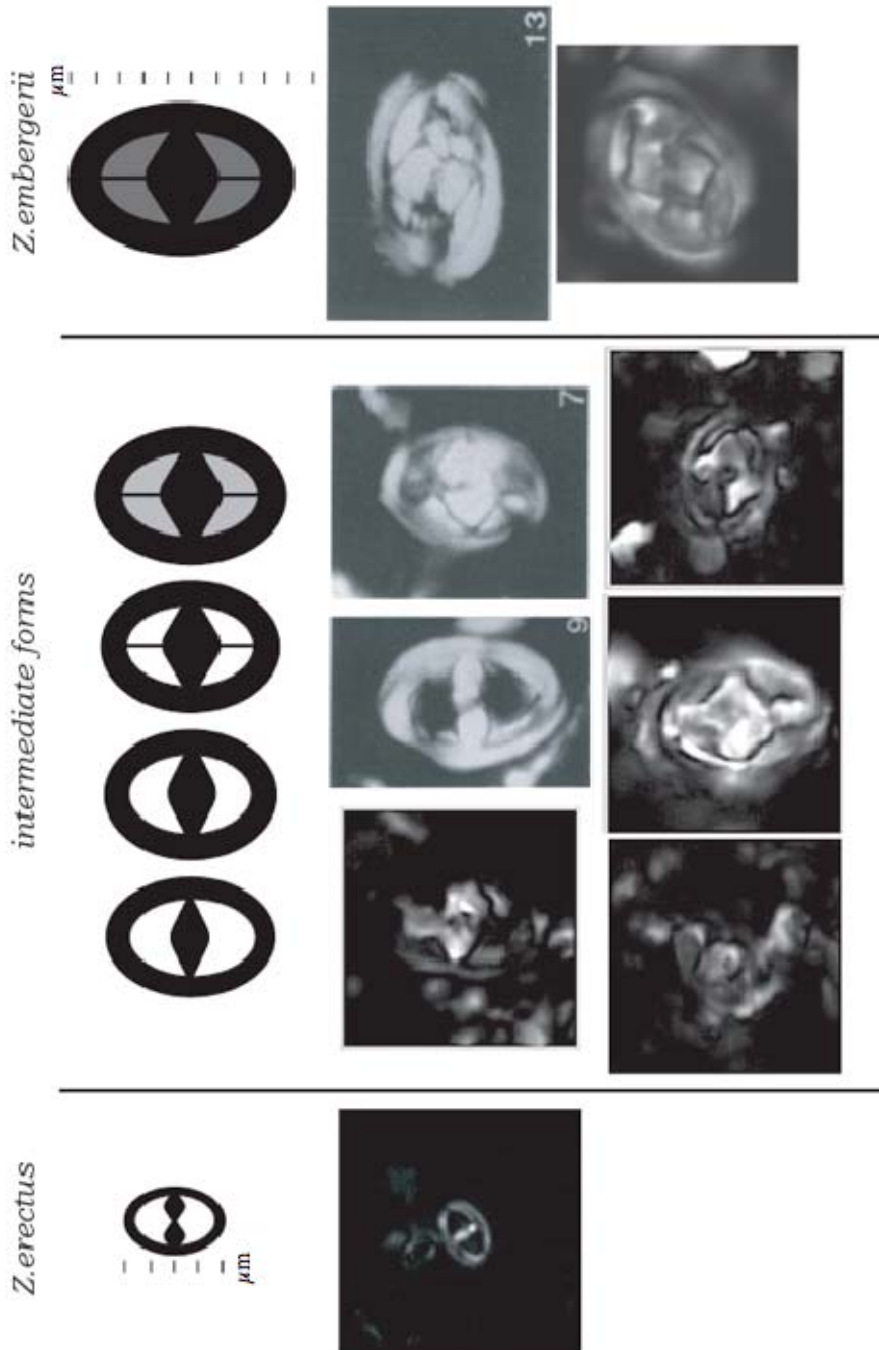
Fig. 5.5.2 – *Z.erectus* and *Z.embergeri* transitional forms.

5. Results

6. DISCUSSIONS

6.1. Callovian – Tithonian revised biostratigraphy.

In this study high-resolution calcareous nannofossil biostratigraphy has been achieved for the Upper Jurassic – lowermost Cretaceous (Fig 5.1). The nannofossil biozonation after Bralower *et al.* (1989) was adopted (see paragraph 2.1), however, as that scheme does not formalize any zone or subzone for the Late Bathonian – Late Kimmeridgian time interval, other studies (De Kaenel *et al.*, 1996, Bown & Cooper, 1998, Mattioli & Erba, 1999) were chosen as guidelines. The revised calcareous nannofossil biostratigraphic scheme here proposed for the Middle to Late Jurassic time interval is based on primary and secondary events used to emend previous zone and/or propose new biozone/subzones. All events are calibrated with magnetostratigraphy (Channell *et al.*, in prep.) from CM24 to CM16 (Fig. 6.1). Despite the uppermost Callovian – Kimmeridgian interval is represented by nodular siliceous marlstones or limestones (Calcare Selcifero di Fonzaso, or Rosso Ammonitico from Trento Plateau, and Radiolarite - Rosso ad Aptici transition from Lombardian Basin) often severely affected by diagenesis, nannofossil biostratigraphy was obtained. In the Upper Callovian - Oxfordian interval nannofossil bioevents are calibrated against ammonite biostratigraphy. A chronologic datum is given by a bentonite layer, outcropping at Sciapala and Bombatierle quarries, which has been dated as latest Middle Oxfordian (Bernoulli & Peters, 1970, 1974).

A description of the calcareous nannofossil biostratigraphic scheme (Fig. 6.1) proposed in this study is coded following the Tethyan Jurassic biozones of Mattioli & Erba (1999) and therefore the lower zone in this study is NJT-12, following the *W.barnesiae* Zone (NJT-11) of Bathonian age.

Zone NJT-12

Definition: interval between the FO *C.wiedmannii* and the LO of *C.wiedmannii*.

Range: uppermost Bathonian – uppermost Callovian.

Reference Sections: Bombatierle quarry (upper part of NJT-12 Zone, since the FO of *C.wiedmannii* in not observed).

Remarks: the upper part of this zone is also characterized by the occurrence *W.manivitiae* large form (see Chapter 8 for detail) and by the LO *A.helvetica*.

59

Comments: This zone is correlatable to the NJ-12, NJ-13 zones and the lower part of NJ-14 Zone of Bown *et al.* (1988) and Bown & Cooper (1998).

NJT-13 Zone

Definition: interval between the LO of *C.wiedmannii* and the LO of *L.sigillatus*.

Range: uppermost Callovian – Middle Oxfordian.

Reference Sections: Bombatierle and Sciapala quarries.

Remarks: this interval is also characterized by the LO of *L.crucicientralis*.

Comments: This zone correlates with the base of *Vagalapilla stradneri* Zone (NJ-19) of Bralower *et al.* (1989). The *Vagalapilla stradneri* Zone (NJ-19) is only applicable to Northern Europe and the Western North Atlantic, whereas is cannot be identified in the Tethyan sections because *V.stradneri* does not appears until the Berriasian (Thierstein, 1973; Bralower *et al.*, 1989). This zone is also correlatable to the upper part of NJ-14 and the lower part of NJ-15a Zone of Bown *et al.,* (1988) and Bown & Cooper (1998).

NJT-14 Zone

Definition: interval between the LO of *L.sigillatus* and the FO of *C.mexicana* subsp. *minor*.

Range: Middle Oxfordian - Lower Tithonian (upper CM22n).

Reference Sections: Bombatierle and Sciapala quarries for Subzone NTJ-14a; Bombatierle and Sciapala quarries and Torre de Busi section for Subzone NTJ-14b.

Remarks: this interval is characterized by the appearance of *M.quadratus*, *F.multicolumnatus* and *C.deflandrei.* In the lower part of this zone a distinct increase in abundance and dimension of *W.communis* was observed, followed by a parallel slight increase in abundance and dimension of *W.britannica.* As this interval is poorly characterized due to unsuitable lithology, it is difficult to place precisely this event; further biostratigraphic and quantitative investigations on more calcareous sections are needed.

Comments: This zone correlates with the *Vagalapilla stradneri* Zone (NJ-19) of Bralower *et al.* (1989).

　　Subzones: - **Subzone NJT-14a**

60

Definition: interval between the LO of *L.sigillatus* and the FO of *F.multicolumnatus*.

Range: Middle Oxfordian – uppermost Oxfordian

Reference Sections: Bombatierle and Sciapala quarries for Subzone.

Remarks: this interval is characterized by the appearance of *M.quadratus*, but, this event is difficult to be placed and further investigations on more calcareous sections are needed.

- **Subzone NJT-14b**

Definition: interval between the FO of *F.multicolumnatus* and the FO of *C.mexicana* subsp. *minor*.

Range: uppermost Oxfordian (CM25n) – Lower Tithonian (upper CM22n).

Reference Sections: Bombatierle and Sciapala quarries and Torre de Busi section.

Remarks: this interval is also characterized by the LO of *T.beaminsterensis* (base of CM24) and by the FO of *C.deflandrei* (base of CM23n). The very upper part of this zone, spanning the Kimmeridgian/Tithonian boundary interval, is characterized by a dramatic increase in size and abundances of *F.multicolumnatus*, mainly from observations on *ultra*-thin sections.

Comment: The FO of *F.multicolumnatus* could be use to approximate the Oxfordian/Kimmeridgian boundary, but precisely studies are needed to further calibrate this event with other stratigraphic tools. The FO of *C.deflandrei* is reported as a secondary event as further studies are needed to better calibrate this event.

Zone NJT-15

Definition: interval between the FO *C.mexicana* subsp. *minor* and the FOs of *M.chiastius* and *H.noeliae*.

Range: Lower Tithonian (CM22n - base of CM20)

Comments: This zone is essentially the same as the *Conusphaera mexicana* Zone (NJ-20)

of Bralower *et al.* (1989). We have emended its name as the FOs of *M.chiastius* and *H.noeliae* where found significantly below that what reported by Bralower *et al.* (1989) (Fig. 6.1).

<u>Subzones</u>: - **Subzone NJT-15a**

<u>Definition</u>: interval from the FO of *C. mexicana* subsp. *minor* to the FO of *P.beckmannii*.

<u>Range</u>: Lower Tithonian (uppermost CM22n – upper CM21r).

<u>Remarks</u>: this interval is also characterized by the FO of *C.mexicana* subsp. *mexicana.*

<u>Comments</u>: This subzone has the same definition of the *Hexapodorhabdus cuvillieri* Subzone (NJ-20a) of Bralower *et al.* (1989), however its base is older, as *P.beckmannii* appears before than what reported by Bralower *et al.* (1989).

- **Subzone NJT-15b**

<u>Definition</u>: interval from the FO of *P.beckmannii* to the FO of *M.chiastius* and *H.noeliae*.

<u>Range</u>: Lower Tithonian (uppermost CM21r – top of CM21n).

<u>Comments</u>: This subzone has the same definition of the *Polycostella beckmannii* Subzone (NJ-20b) of Bralower *et al.* (1989), however its base is older, as the FOs of P.*bckmannii, M.chiastius* and *H.noeliae* where found significantly before that what reported by Bralower *et al.* (1989) (Fig. 6.1).

Zone NJT-16

<u>Definition</u>: interval from the FOs of *M.chiastius* and *H.noeliae* to the FO of *N.globulus minor*.

<u>Range</u>: upper Lower Tithonian (base of CM20r – CM19r) to lowermost Berriasian (CM17r).

<u>Remarks</u>: the lowermost part of this zone is also characterized by the FOs of *P.senaria* and *Hexalithus* sp.1 and by the appearance of the primitive nannoconids *N.infans* and *Nannoconus* sp.1 (see Chapter 8 for details).

Comments: This correlates with the *H.noeliae* Subzone (NJK-A) of Bralower *et al.* (1989), but it has a different definition, since the FO *U.granulosa* subsp. *granulosa* does not represent a replicable event in the majority of the studied sections and is considered here as a secondary event. For this reason the FO of *N.globulus minor* has been chosen as the main event to define the top of this zone.

Zone NJT-17

Definition: interval from the FO of *N.globulus* subsp. *minor* to the FO *N. steinmannii* subsp. *minor*.

Range: Upper Tithonian to lowermost Berriasian (CM19r – CM18r).

Remarks: this zone is also characterized by the FO of *N.wintereri* and secondarily by the FOs of *U.granulosa* subsp. *granulosa*, *R.asper*, *C.surirellus*, *C.cuvillieri*.

Comment: this zone correlates with the *U.granulosa* subsp. *granulosa* (NJK-B) and *R.laffittei* (NJK-C) subzones of Bralower *et al.* (1989). *R.laffittei* is virtually absent in the investigated sections, while *U.granulosa* subsp. *granulosa* is considered here as a secondary event due to poor preservation and an every gradual change from *U.granulosa* subsp. *minor*. For this reason *N.globulus minor* has been chosen as the main event to define the base of this zone, as it is easily recognizable and occurs in all studied sections.

Zone NJT-18

Definition: interval from the FO of *N.steinmannii* subsp. *minor* to the FO of *N.s steinmannii* subsp. *steinmannii*.

Range: lowermost Berriasian (CM18r – CM17r).

Remarks: this zone is also characterized by the FO of *C.octofenestratus*

Comment: this zone corresponds to the *N.steinmannii* subsp. *minor* Subzone (NJK-D) of Bralower *et al.* (1989).

Fig. 6.1.1 – The calcareous nannofossil biostratigraphic scheme proposed in this study.

6.2. Calcareous nannofossil acme events in the Tithonian – Berriasian interval: implications and applications.

Calcareous nannofossil quantitative data achieved for the Torre de Busi and Monte Pernice sections (Tethys Ocean), and preliminary data from DSDP site 534 (Atlantic Ocean) (Chapter 5, paragraph 5.3), clearly indicate that a major change in the nannofossil associations occurred during the Tithonian – Berriasian interval, mainly due to a spectacular increase in nannolith taxa (Fig. 5.3.1, 5.3.3, 5.3.4). Coccoliths of the genera *Watznaueria* and *Cyclagelosphaera* also increase in abundance, but never reach lithogenetic proportions, while nannolith taxa of genera *Faviconus*, *Conusphaera*, *Polycostella* and *Nannoconus* increase significantly in abundance, as well as in size and degree of calcification gaining lithogenetic proportions during the Tithonian – Berriasian interval. Four "Acme intervals" (equated to intervals with maximum abundance) are recognized as follows (Fig.6.2.1):

- *F.multicolumnatus* acme: from the lower to middle Rosso ad Aptici and/or Cat Gap formation (CM22n – upper CM21r) (500 specimens per mm^2).
- *C.mexicana* acme: from the upper Rosso ad Aptici and/or Cat Gap formation (CM21n) (3000 to 4000 specimens per mm^2).
- *P.beckmannii* acme: upper Rosso ad Aptici and/or Cat Gap fm.– Blake-Bahama fm. transition (lower CM20r) (2000 specimens per mm^2).
- *Nannoconus* acme: exponential increase from the base of the Maiolica and/or Blake-Bahama formation until the top of the studied interval (lower CM19n – top of the studied interval). The acme is reached in the lower Maiolica and/or Blake-Bahama formation (CM18r) (3000 specimens per mm^2), concomitant with the acme of *C.alpina* spherical form.

As far as absolute abundances are concerned *Faviconus*, *Polycostella*, *Conusphaera,* and *Nannoconu*s nannoliths are the most abundant calcareous nannoplankton forms during the Tithonian - Berriasian interval. It is also evident from *paleo*-fluxes that these nannoliths were the major producers of pelagic micrite, as they were the most abundant forms, were bigger in volume and heavier in mass than all other nannoliths and coccoliths. In particular, the most effective calcite producer was the genus *Conusphaera* during the early Tithonian and the genus *Nannoconus* during the late Tithonian to the top of the studied interval. Interestingly, nannoconids result less abundant in number than *Conusphaera* sp., but as they are bigger in

volume and heavier in mass, contribute more to biogenic calcite production.
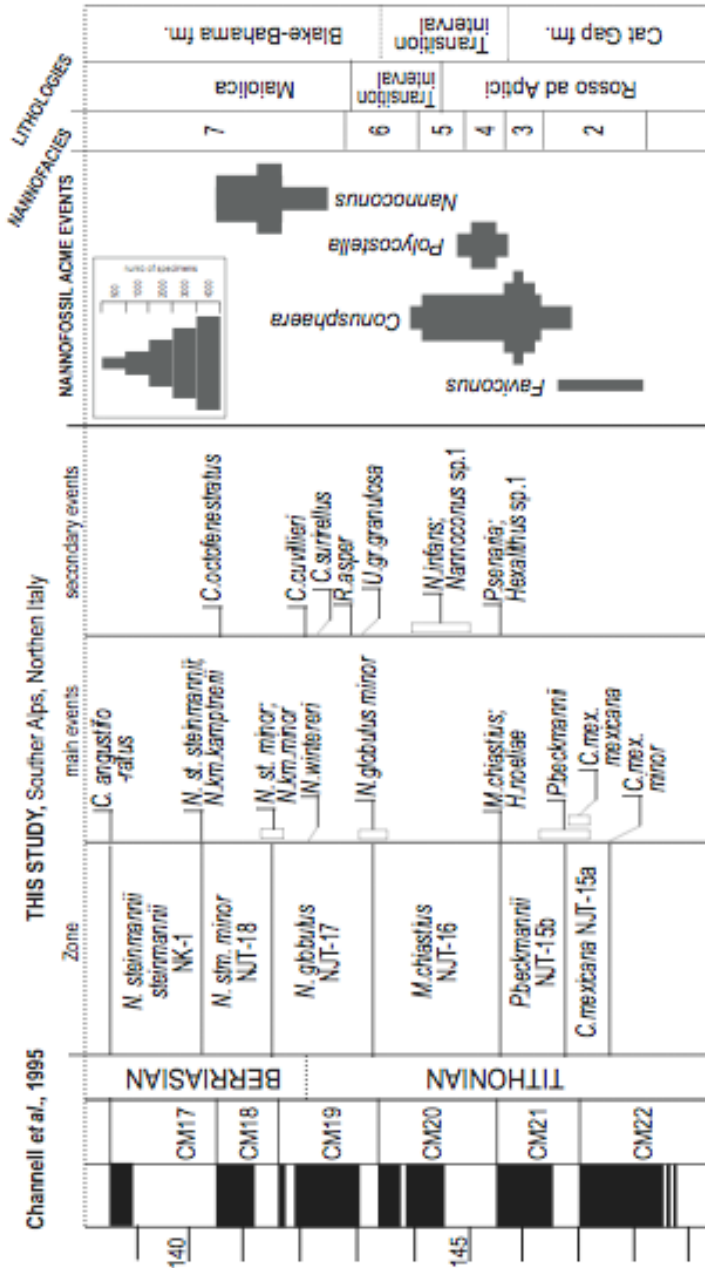
Fig. 6.2.1 – Calcareous nannofossil acme intervals.

Calcareous nannofossil and calpionellid contributions to the sedimentation at Torre de

Busi and Monte Pernice sections were compared to extract the impact of each fossil group on the lithology: calcareous nannofossil *paleo*-fluxes are obviously one hundred times greater that calpionellid *paleo*-fluxes. The cumulative calcareous nannofossil and calpionellid *paleo*-fluxes curve at Torre de Busi is reported in Figure 6.2.2, and clearly shows that biogenic calcite contribution to the sedimentation is controlled by nannofossils, particularly by nannoliths.
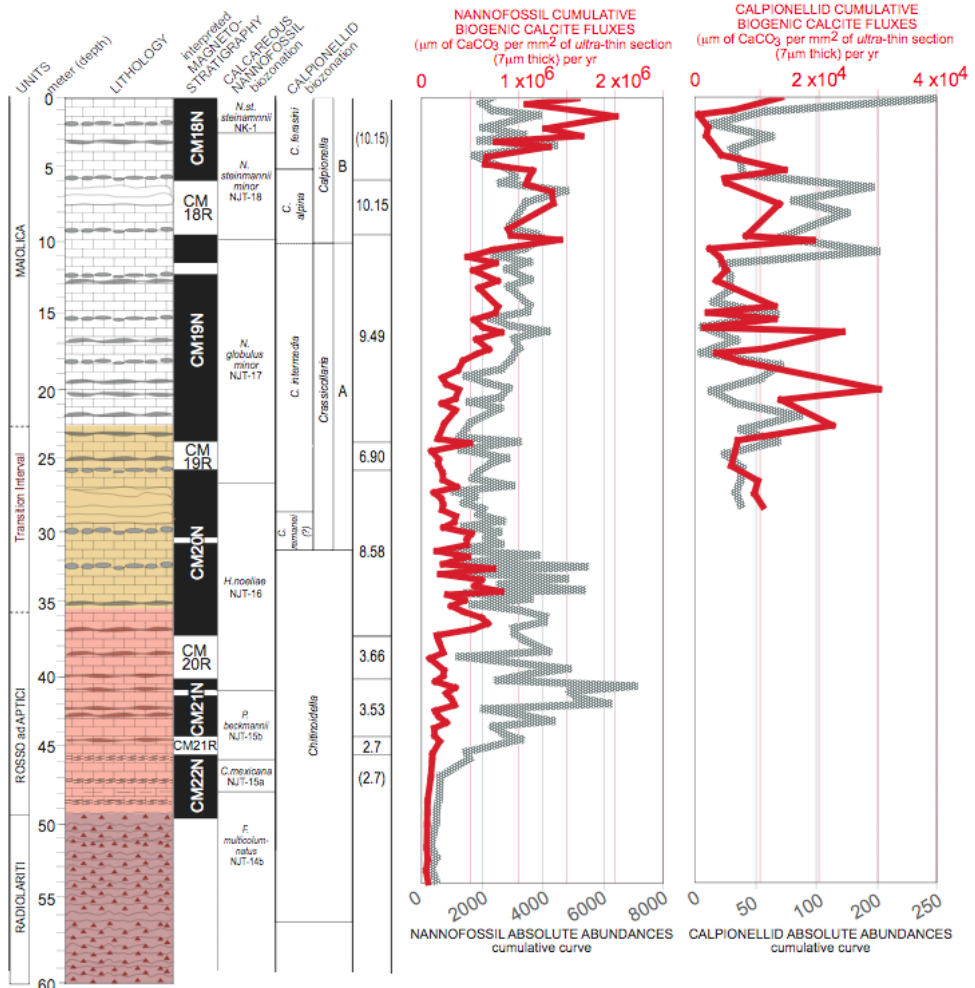

Fig. 6.2.2 – nannofossil cumulative *paleo*-fluxes and calpionellid cumulative *paleo*-fluxes comparison.

The described quantitative trends, interpreted and defined as nannofossil acme intervals

(Fig.6.2.1), have important implications for the amount of biogenic calcite production in the ocean and, consequently, for the pelagic sedimentation. A comparison between the nannofacies (Paragraphs 5.4) and the acme intervals (Fig. 6.2.1) reveals the linkage between the lithological changes from Rosso ad Aptici (Cat Gap formation) to Maiolica (Balke-Bahama formation) and the appearance, diversification and increase in absolute abundance of genera *Faviconus*, *Polycostella*, *Conusphaera,* and *Nannoconus* (see also Paragraph 6.3)*.* The described quantitative trends have also important applications: their calibration with magnetostratigraphy indicates that they could be very useful as additional biostratigraphic tools in the Tithonian – lower Berriarian interval, and eventually for determining the Jurassic/Cretaceous boundary, especially when ammonites are absent as in the Tethyan Maiolica. Nannofossil acme intervals provide new reliable stratigraphic events for the Tithonian - Berriasian interval: *Conusphaera* and *Polycostella* acme intervals might roughly approximate upper Lower Tithonian (CM21n – CM20r), while *Nannoconus* acme event roughly approximate the Jurassic/Cretaceous boundary interval (upper CM19n – lower CM18r).

6.3. Nannofossil calcification events (NCEs) in the Tithonian – Berriasian interval

6.3.1. Nannofossil Calcification Event (NCEs)

Nannofossil Calcification Events (NCEs) were first outlined by Bornemann *et al.* (2003) after the analysis of Tithonian – Berriasian sediments and nannofossil assemblages in the central Atlantic Ocean (DSDP Sites 105, 367, 534A). Their results concerning both biogenic nannofossil carbonate estimates and the measured bulk-rock carbonate, reveal a period characterized by an increasing in the nannofossil carbonate accumulation caused by mass occurrences of strongly calcified taxa (*C. mexicana*, *P. beckmannii*, *Nannoconus* spp., *W.manivitiae*), increasing in both abundance and size. This episode was named 'Nannofossil Calcification Event' (NCE) also because of the dramatic increase in size of those taxa (Bornemann, pers. comm., 2007). Bornemann *et al.* (2003) point out the presence of a second interval of enhanced carbonate production in the late Berriasian, related to the rise in absolute abundances of nannofossils and amplified by an overall increase of the sedimentation rate.

In this study calcareous nannofossil (and calpionellid) *paleo*-fluxes were achieved (see Chapter 5 and paragraph 6.2) on two sections from the Southern Alps, Tethys Ocean, and on
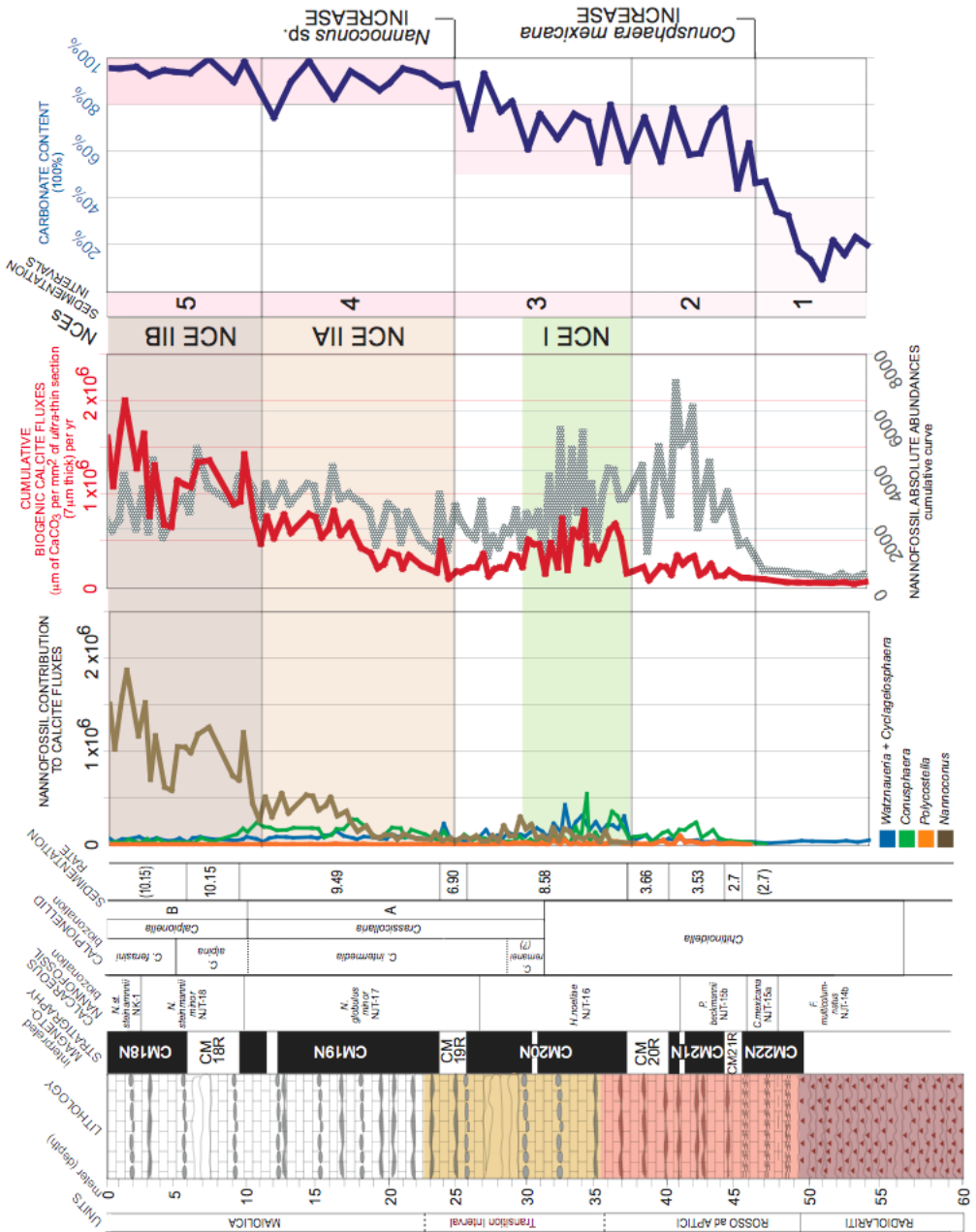
Fig. 6.3.1 – NCE I and NCE II (A and B) at Torre de Busi, plotted against lithology, magnetostratigraphy and carbonate content.

the same samples analyzed by Bornemann *et al.* (2003) on DSDP Site 534A from the Atlantic Ocean. The results presented in Chapter 5 allow to revise the NCEs definition and characterization. The calcareous nannofossil *paleo*-fluxes obtained in this study allow the identification of two different intervals characterized by a dramatic increase in nannofossil number, size and consequently in biogenic calcite. Therefore, two Nannofossils Calcification Events (NCE I and NCE II) were identified (Fig. 6.3.1). The first event, NCE I, corresponds to the NCE previously identified by Bornemann *et al.* (2003), and is related to the increase in abundance of nannolith genera *Faviconus, Conusphaera* and *Polycostella*, gaining lithogenetic abundances in the middle Lower Tithonian (CM21-CM20). NCE I is mainly determined by the increase in number and size of *C.mexicana mexicana*, which contributes to most of biogenic calcite *paleo*-flux. The second event, NCE II, was not identified by Bornemann *et al.* (2003) and is mainly related to the exponential increase in diversification, abundance and dimensions of nannoconids, gaining lithogenetic abundance in the uppermost Tithonian – lower Berriasian (CM19n-CM18). NCE II is also characterized by high abundances of the genus *Conusphaera* and by the appearance of calcified calpionellids (genera *Crassicollaria* and *Calpionella*). Within NCE II, two additional intervals were distinguished, namely NCE IIA and NCE IIB, characterized by an increase in nannoconid abundance and diversity and by an "explosion" of large nannoconids (*N.steinmannii* subsp. *minor, N.kamptneri* subsp. *minor, N.steinmannii* subsp. *steinmannii, N.kamptneri* subsp. *kamptneri)*, respectively.

6.3.2. Impact of NCEs on western Tethys Ocean sedimentation.

NCEs have important implications on the pelagic sedimentation, particularly in the western Tethys Ocean (Fig. 2.2.1). The nannofossil cumulative *paleo*-flux curve plotted against the carbonate content curve and the lithostratigraphic framework permit an interpretation of the transition from predominantly siliceous sediments (Radiolariti) through an interval of siliceous marlstones and limestones (Rosso ad Aptici) to mostly calcareous ones (Maiolica). The Torre de Busi section is taken as a representative of the pelagic sedimentation (relatively expanded) in the Southern Alps. The link between nannoplankton evolution, diversification and abundance, its calcite *paleo*-fluxes, carbonate content are interpreted to understand the role (if any) of coccoliths/nannolith production of pelagic sediments. In the Late Jurassic of the western Tethys three sedimentary intervals are distinguished from bottom to top: a siliceous, a

siliceous-calcareous and a calcareous intervals. Indeed, at Torre de Busi these three intervals correspond to three lithostraigraphic units, namely the Radiolariti, the Rosso ad Aptici and the Maiolica formations. At Torre de Busi is possible to identify five intervals (Fig.6.3.1):

1) A first increase in carbonate content from 20% to 60% correlates with the upper Radiolariti to lowermost Rosso ad Aptici interval, but no change in nannofossil *paleo*-flux was observed.

2) A second increase in carbonate content up to 60% to 80% correlates with the middle-upper Rosso ad Aptici. This increase correlates with the explosion of nannolith genera *Conusphaera* and *Polycostella paleo*-fluxes.

3) A third interval, marked by $CaCO_3$ slightly increasing but still in a 60-80% range, corresponds to the NCE I during the transition from Rosso ad Aptici to Maiolica formations.

4) A fourth interval is characterized by $CaCO_3$ fluctuating between 80 and 90%, and roughly correlates with the lower part of NCE II (NCE IIA).

5) The fifth interval, with $CaCO_3$ between 90 and 100%, corresponds to the Maiolica limestones *sensu strictu* and NCE IIB.

Similar pelagic sedimentation changes occurred in the western Tethys and central Atlantic oceans, and different interpretation has been forwarded, such as:

- A deepening of the calcite compensation depth (CCD) after a major shallowing in the Middle Jurassic (Winterer & Bosellini, 1981);

- a shift of carbonate deposition from the shallow seas and shelf areas to the open-ocean, due to a major increase in calcareous nannofossil carbonate production (*Kuenen Event*, Roth, 1986);

- a tectonic plate drifting initially towards, and subsequently away from, a near-equatorial upwelling zone of high biosiliceous productivity (Muttoni *et al.*, 2005; Channell *et al.*, 2007).

The results presented in Chapter 5 show that the transition from siliceous sediments (Radiolariti) to calcareous limestones (Rosso ad Aptici) are independent from the calcareous nannofossil calcification history, and most probably is related to a tectonic plate drifting history. On the other hand, the middle Rosso ad Aptici to Rosso ad Aptici-Maiolica transition correlates with the increase in abundance of nannoliths *Conusphaera* and *Polycostella,* and

specifically with NCE I. This gradual increase in carbonate content in thus linked to the calcareous nannofossil evolution, which directly affected the oceanic inorganic carbon pool and acted as a driving factor of pelagic sedimentation, at least for the western Tethys and central Atlantic oceans. Finally, the Maiolica is undoubtedly controlled by the diversification and explosion of the nannoconid group, and correlates with NCE II. In this case, the appearance, diversification and production of nannoconids determined almost pure micritic limestones (80-100% $CaCO_3$). The Maiolica (Biancone, Blake-Bahama formation) is essentially a "nannoconites", resulting from proliferation of nannoconids in the Early Cretaceous western Tethys and central Atlantic oceans.

6.3.3. Paleoceanographic and climatic factors controlling NCEs at low latitudes (Tethyan Realm)

Temporal and spatial changes in the distribution and abundance of calcareous nannoplankton are controlled by climatic and oceanographic factors; consequently calcareous nannofossil can be used as proxies of paleoceanographic condition in the past.

Quantitative data show that only few taxa are occurring in lithogenetic proportion during the studied interval. The common genus *Watznaueria* is considered to be a cosmopolitan form, indicating oligotrophic surface water conditions (Premoli-Silva *et al.*, 1989; Pittet & Mattioli, 2002). High abundances of *Watznaueria* coccoliths during the studied interval let to suggest a low to moderate surface water nutrient levels for the Tethys Ocean, as well as Central Atlantic (Bornemann *et al.*, 2003). The Tithonian interval is mainly characterized by high abundances of *incertae sedis* nannolith taxa such as *Faviconus, Conusphaera*, *Polycostella* and *Nannoconus*. *Nannoconus* is interpreted as an inhabitant of the lower photic (Erba, 1994). In this study, *Faviconus* is interpreted as a precursor of *Nannoconus* (see paragraph 6.4), thus is considered as an inhabitant of the same ecological niche. The ecological affinities of the genera *Conusphaera* and *Polycostella* are unknown, but due to some similarities with *Nannoconus* as far as form and/or structure, these groups possibly inhabited a similar ecological niche. It was suggested that the onsets of these four nannolith acmes reflect either a competition between these groups for the ecological niche or/and slight differences in their ecological affinities (Bornemann *et al.*, 2003).

72

The present PhD project pointed out that huge change in size and calcification degree of genera *Faviconus*, *Conusphaera* and *Nannoconus* are at least partly controlled by changes of the paleoenvironment or palaeoceanography. In the Tithonian – lower Berriasian high abundances of strongly calcified nannoliths co-occur with large *Watznaueria*, highly calcified dinoflagellate cysts and calcified calpionellids, thus reflecting a global increase in calcification of planktonic calcifiers. This PhD project results suggest that the Tithonian mass occurrences of strongly calcified nannoplankton and its evolution are coeval with: low oceanic Mg/Ca ratio values, low pCO_2 value and cool climatic conditions (Fig.6.3.2).

pCO_2. A factor which is considered to control the calcification among coccolithophorids is the atmospheric pCO_2 and the resulting seawater pH: in culture studies, lower pCO_2 levels allow an increase in calcification rates of modern coccolithophores, whereas high pCO_2 inhibits calcification. In the Late Jurassic a decrease of atmospheric pCO_2 levels is predicted (Berner & Kothavala, 2001, Berner, 2006). This is in agreement with low spreading rates (Sheridan, 1983), dry climate (Abbink *et al.*, 2001) and cool temperatures at high latitudes (Price, 1999; Price *et al.*, 2002). The synchroneity of predicted low pCO_2 levels and nannofossil calcification events leads to hypothesize that the increase in calcification of calcareous nannofossils during the Tithonian – lower Berriasian NCEs was facilitated by low pCO_2, relatively cold and stable conditions. Nevertheless, due to the absence of reliable pCO_2/pH proxies, the poor knowledge of the buffer capacities of the oceans and the influence of seawater pH on the biogenic calcification on geological timescales, the interpretation of these factors remains speculative.

Mg/Ca ratio. Starting in the Middle Jurassic, the Mg/Ca ratio shows a significant and continuous decrease, associated to a coeval increase of sea water Ca concentration. Mg/Ca secular variations seem to be controlled by the rate of ocean crust formation (Hardie, 1996): in areas of seafloor formation Mg is removed from seawater and Ca is released through hydrothermal activity. Thus, when rates of the sea floor formation rise, the Mg/Ca ratio declines. A minimum in isotopic strontium values (due to high rate of oceanic crust production and/or volcanic activity) was predicted for the Kimmeridgian - early Tithonian (Sheridan, 1983). From a thermodynamic point of view, the decrease in the Mg content could promote a
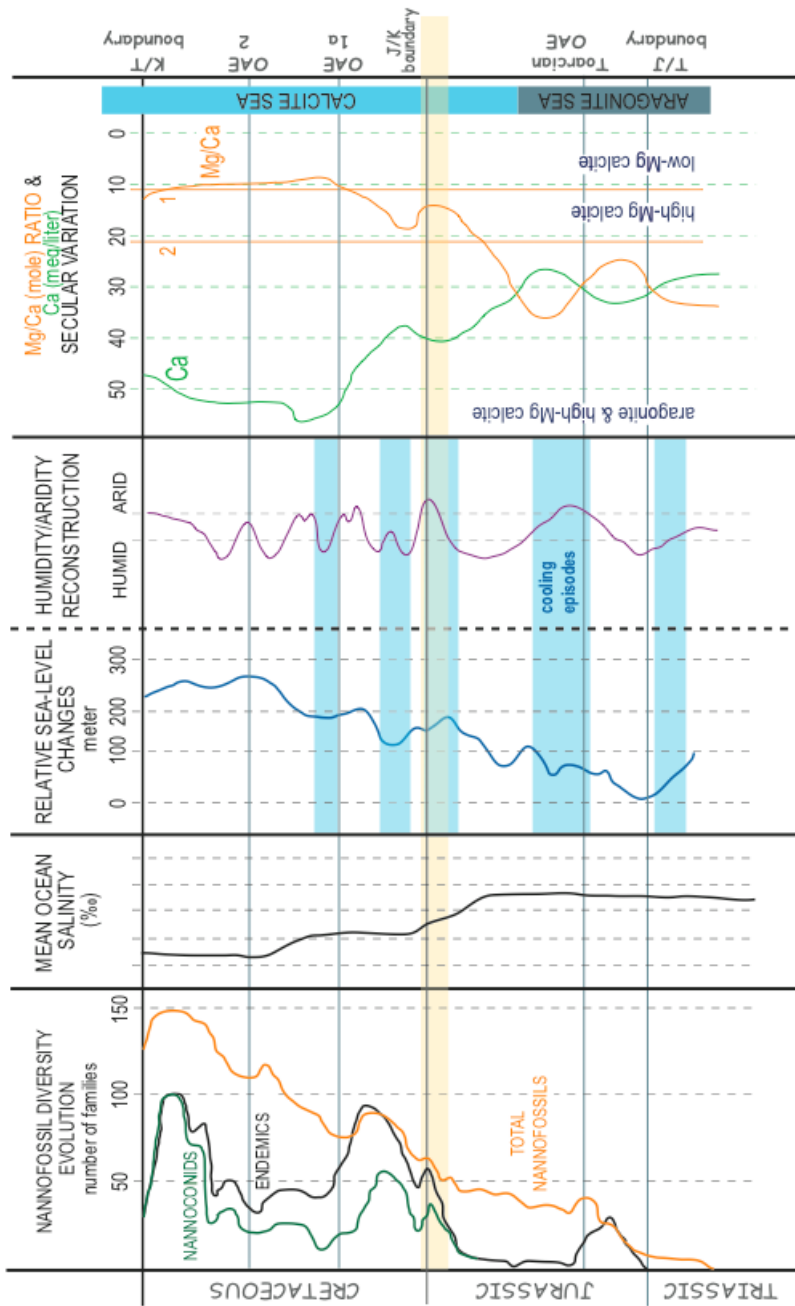
Fig. 6.3.2 – General overview on nannofossil diversity evolution, sea level, humidity/aridity reconstuction and Mg/Ca ratio in the Mesozoic.

shift from a prevalent "aragonite" toward "low-Mg calcite" biocalcification. Such conditions could generally stimulate nannoplankton biocalcification and perhaps favor and/or solicit the highly calcified forms, promoting low Mg-CaCO$_3$ and CaCO$_3$ biomineralization (*nannofossil fertilization* sensu Stanley, 2006).

Cool climatic condition. The relative sea-level change curve (Haq *et al.*, 1987) shows a regressive episode in the middle-upper Tithonian, and was related to a minor global cooling event (Price, 1999), as supported by the occurrence of dropstones and glendonites. Studies on modern coccolithophores in culture reveal that at low water temperatures coccolithophorids experience an enlargement of both chloroplasts and cell dimensions and are stimulated to produce coccoliths, so are stimulated to bio-calcify (Sorrosa *et al.*, 2005). A climatic change with a northward expansion of the dry climate zone (Abbink *et al.*, 2001) accompanied by cooler temperatures (at least at high latitudes) may have stimulated nannofossil biocalcification, and perhaps favoured nannolith production in the late Tithonian.

Stable VS unstable conditions. The Tithonian can be regarded as a "quiet" interval as far as the oceanic environment is concerned. The δ^{13}C curve shows a gradual minor decline after the Oxfordian anomalies and prior to the Valanginian event. No major paleoceanographic episodes have been pointed out and, therefore, the Tithonian may be regarded as a stable interval. The nannofossil changes pointed out in this PhD thesis and specifically the accelerated originations, increase in abundance and calcification degree, thus correlate with stable environmental conditions, without significant perturbations. It is well possible that stable condition favoured diversification and expansion of calcareous nannoplankton, more adapted to oligotrophic oceans, but suffering under high-fertility and upwelling settings. If so, the onset of the massive nannoplankton diversification, abundance and calcification might represent the beginning of a stable environment under low pCO$_2$ and relatively cool climate.
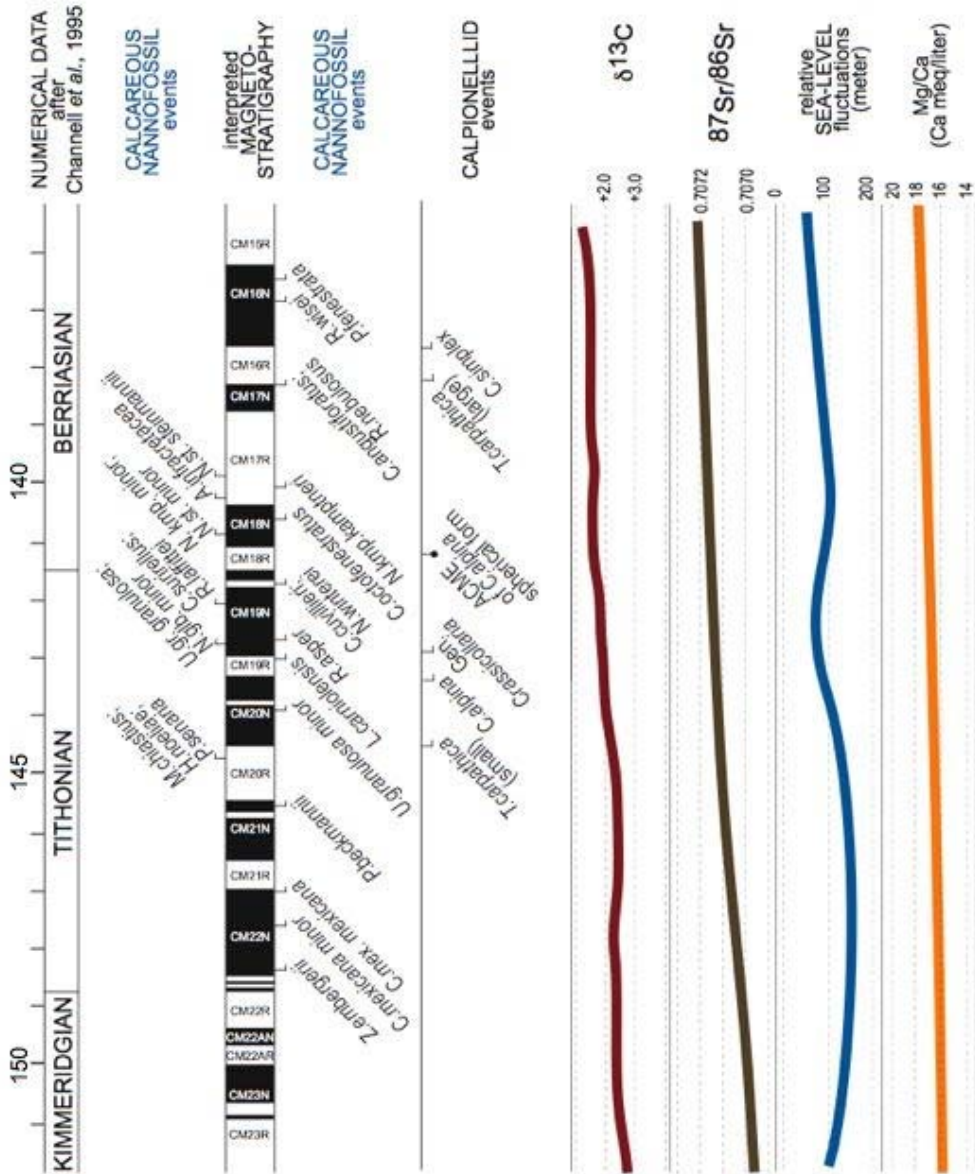
Fig. 6.3.3 – General overview of Tihonian stable interval.

6.4. Calcareous nannofossil evolution: tempo & mode interpretations

Tithonian calcareous nannofossils speciation event provides an excellent opportunity to investigate nannofossil evolutionary modes and their timing, during a period of climatic and environmental stability. This speciation episode, characterized by the first occurrence of several new genera and few new species (figure 5.5.1), has been interpreted in the light of all the speciation modes proposed since Darwin's Evolutionary Theory: Phyletic Gradualism (Darwin, 1859), Punctuated Equilibrium (Gould & Eldredge, 1977) and Punctuated Gradualism (Malmgren et al., 1984). On the basis of magnetostratigraphy each mode duration (kyr) has been evaluated.

Phyletic Gradualism (Darwin, 1859). *New species arise from slow, steady transformation of populations providing gradational fossil series linking separate phylogenetic species.*

A) *U.granulosa minor - U.granulosa granulosa*. Total shield size and central area structure of *Umbria granulosa* change stratigraphically: the maximum diameter increase from 4µm (*U.gr.minor*) to 8-10µm (*U.gr.granulosa*), and the central area is grey and cloudy at all orientations in early specimens (*U.gr.minor*) and become more calcified and birifrangent in later forms (*U.gr.granulosa*). The subspecies are divided based on these changes (Bralower *et al.*, 1989). A fair amount of gradation between the two forms has been observed from the FO of *U.gr.minor* (mid CM20n) to the FO of *U.gr.granulosa* (early CM19n) and interpreted as an example of Phyletic Gradualism (Fig.6.4.1). The transition interval has been evaluated of 1.2 My *circa*.

B) *F.multicolumnatus - N.dolomiticus*. The genus *Faviconus* appears to be a precursor to the genus *Nannoconus* (Bralower *et al.*, 1989). *Faviconus* has a similar general construction to *Nannoconus*. Transitional forms between *Faviconus* and *N.dolomiticus* have been observed in the lowermost Berriasian, suggesting a direct linkage between the two genera. *Faviconus* is here interpreted as a precursor of *N.dolomiticus*. *Faviconus* evolution toward bigger and more calcified specimens, assumed as *N.dolomiticus*, represent an example of Philetic Gradualism (Fig. 6.4.1). The transition interval from the last true *F.multicolumnatus* (CM19n reversal) to the first *N.dolomiticus* (base of CM17r) is estimated as 1.6 My *circa*.
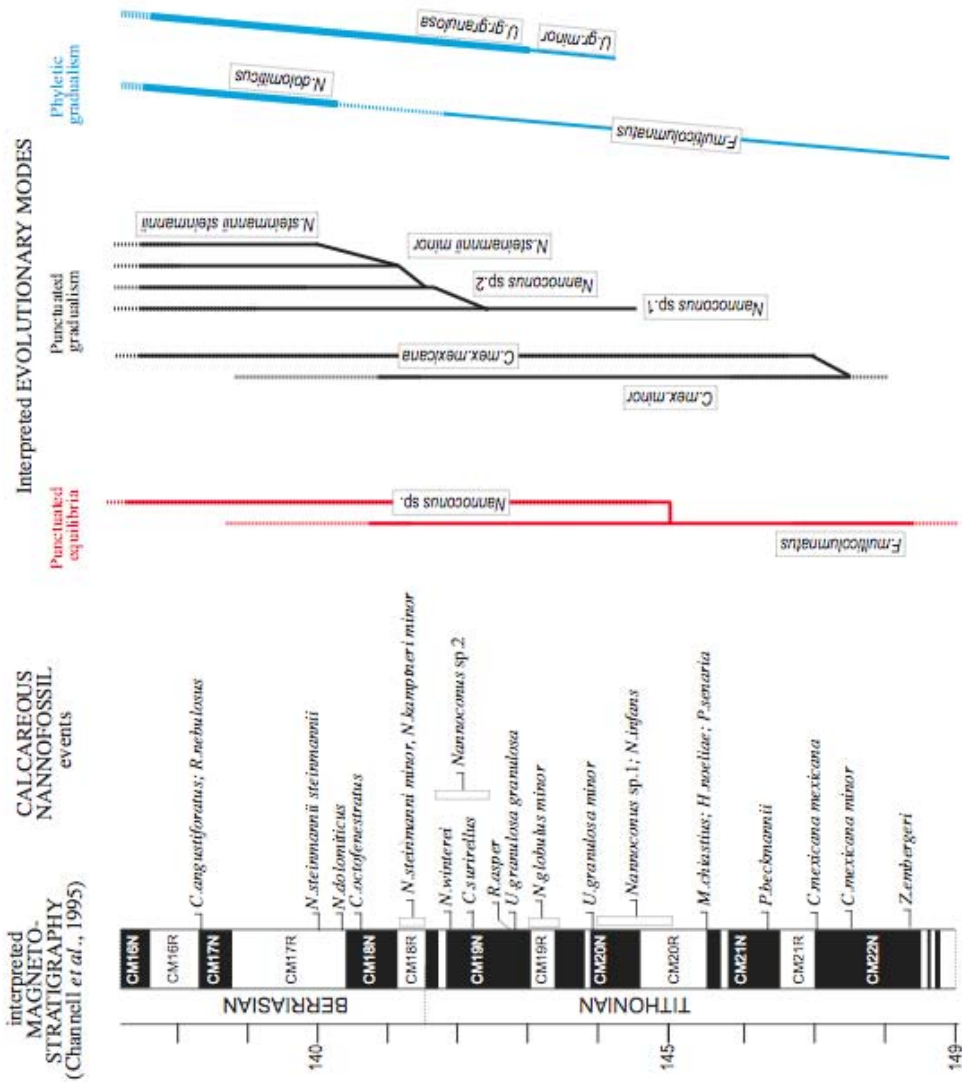
Fig. 6.4.1 – Titonian speciation episode and related examples of phyletic gradualism, punctuated equilibrium and punctuated gradualism.

Punctuated Equilibrium (Gould & Eldredge, 1977). *New species appear by rapid speciation occurring in small isolated populations, followed by migration to other areas where fossil sequence usually shows sharp morphological breaks.*

A) *F.multicolumnatus – Nannoconus. Faviconus* is considered a precursor to *Nannoconus,* which presents a similar general construction (Bralower *et al.*, 1989). *Nannoconus* species such as small and primitive form like *Nannoconus* sp.1 and *N.infans* is thought to derive by *Faviconus.* This evolutionary trend is interpreted as an example of punctuated equilibrium (Fig. 6.4.1).

Punctuated Gradualism (Malmgren et al., 1984). *It implies long-lasting evolutionary stasis interrupted by rapid, but gradual phyletic transformation without lineage splitting.*

A) *Z.erectus - Z.embergeri*. Total shield size and thickness and the central area structure of *Z.erectus* change stratigraphically: shield size and its thickness increase, and the outline of the central bridge changes from lath-shaped to rhomboid/elliptical. Numerous authors adopt the species *Z.salillum* and *Z.noelii* (forms with a thicker cross bar and a wider wall than *Z.erectus)*, while others suggest that these species are intermediate in the evolutionary lineage between *Z.erectus* and *Z.embergeri* (Thierstein, 1976; Wind, 1978; Roth, 1983; Bralower *et al.*, 1989). Indeed, a complete gradation between true *Z.erectus* and true *Z.embergeri* have been observed in this study, but discrimination into separate species is still in progress. Thus, *Z.erectus* evolution toward *Z.embergeri* is interpreted as an example of Punctuated Gradualism.

B) *C.mexicana minor - C.mexicana mexicana*: *C.mexicana minor* clearly represent a precursor to *C.mexicana mexicana* (Bralower *et al.*, 1989). The dimensions of *C.mexicana minor* increase stratigraphically. The earliest *C.mexicana minor* forms are often less than 2µm in length and the later *C.mexicana mexicana* forms are up to 12µm in length. A fair amount of gradation between the two forms has been observed, and interpreted as an example of Punctuated Gradualism (Fig. 6.4.1). The interval characterized by the occurrences of transitional forms lasts 0.6 My *circa*.

C) *M.quadratus - M.chiastius*. The two species are differentiated by the dimension and shape of the central cross. The central cross of *M.chiastius* is small and have a blocky shape, while the central cross of *M.quadratus* is greater, have often a pointy ends and the dimensions of the two arms are often unequal in length. A clear evolutionary transition is observed between *M.quadratus* and *M. chiastius.* There is a complete gradation between

the typical cross structure of the two taxa: for this reason it has been interpreted as an example of Punctuated gradualism.

D) *Nannoconus*. The investigations performed during this PhD project confirm that Berriasian nannoconids might have a precursor of smaller size in the Tithonian, as proposed by Bralower *et al.* (1989). In addition, our results contribute to the interpretation of the evolution lineage of this genus. The size, calcification degree and the central canal dimensions of *Nannoconus* cleary change stratigraphically. Nannoconids characterized by conical outline and narrow canal show an increase of the maximum diameter from less than 4µm (*Nannoconus* sp.1), to 6-8µm (*Nannoconus* sp.2), to 8-10µm (*N.steinmannii minor*) to 10-20µm (*N.steinmannii steinamnnii*). The same trend has been observed for *N.kampneri minor* and *N.kamptneri kamptneri*. These changes provide examples of punctuated gradualism (Fig. 6.4.1). Particularly, the interval between the FO of *Nannoconus* sp.2 and the FO of *N.steinmannii minor* is characterized by the occurrences of transitional forms and lasts 0.7 My *circa*, while the interval between the FO of *N.steinmannii minor* and the FO of *N.steinmannii steinamnniii* lasts 1.6 My *circa.*

As discussed above, the Tithonian mass occurrences of highly calcified nannoplankton and its evolution (NCEs) were possibly controlled by abiotic factors, such as seawater chemistry (Mg/Ca ratio values and pCO_2) and temperature (cool climatic episode). On the other hand Tithonian speciation episode correspond to an interval of environmental stability: stable condition probably favouring diversification and expansion of calcareous nannoplankton, adapted to oligotrophic oceans. If so, the onset of the massive nannoplankton diversification might represent the onset of a stable environment under low pCO_2 and relatively cool climate. Particularly, nannoliths seem to have experienced all three evolutionary modes, while coccoliths provide examples for only two of them. Evolutionary interpretations permit the following considerations: on a specific level both nannoliths and coccoliths seem to prefer evolutionary modes implying a gradual transformation from a ancestor species to a descendant one, during time intervals of more that 1 Ma; while on a generic level a by rapid speciation is preferred.

7. CONCLUSIONS

High-resolution calcareous nannofossil biostratigraphy of several sections from the Southern Alps (Tethys Ocean) was obtained and integrated with magnetostratigraphy and, where available, with calpionellid biostratigraphy, to achieve a high-resolution stratigraphic framework for the Upper Jurassic – lowermost Cretaceous. A revised calcareous nannofossil biostratigraphic scheme is proposed for the Callovian – Tithonian time interval in the Tethyan Realm: three new Zones and two new Subzones are proposed on the base of primary and secondary events, and four Zone, previously defined by Bralower *et al.* (1989), are here revised.

Calcareous nannofossil quantitative analysis were performed on selected sections from the Southern Alps and on DSDP Site 534 A from the Atlantic Ocean, to calculate nannofossil biogenic calcite *paleo*-fluxes and to monitor their impact on pelagic sedimentation during a time interval characterized by a shift from mostly siliceous to mainly calcareous sedimentation.

- Based on *ultra*-thin section analysis, seven nannofacies (Large *Watznaueria; Conusphaera*; *Polycostella; Conusphaera* and *Polycostella; Conusphaera, Polycostella* and small nannoconids; *Nannoconus* nannofacies) are documented and proposed as additional biostratigraphic tools.

- Absolute abundance data show that in the uppermost Tithonian abundances of *F.multicolumnatus*, *C.mexicana* and *P.beckmannii* increase significantly. Nannoconids appear and rapidly develop reaching high abundances in the uppermost Tithonian. On the basis of absolute abundances, four Acme intervals (*F.multicolumnatus, C.mexicana, P.beckmannii* and *Nannoconus* acmes), defined as intervals of specific taxa maximum abundance, are recognized integrated with nannofacies and integrated with nannofossil biozones.

- Based on the obtained *paleo*-fluxes, the Nannofossil Calcification Events (NCEs) are recognized, and interpreted in relation to western Tethys Ocean sedimentation is discussed. Calcareous biogenic *paleo*-fluxes point out a link between the lithologic changes and calcified plankton evolution across the early Tithonian to early Berriasian

interval. During Early Tithonian (Rosso ad Aptici) a first calcification event (NCE I) is characterized by nannolith (*F.multicolumnatus*, *C.mexicana*, *P.beckmannii*) increase in abundance, size and calcification degree, followed by the occurrence of the first calcified calpionellid (*Tintinnopsella*). In the Late Tithonian to Early Berriasian (Rosso ad Aptici – Maiolica transition and Maiolica) a second bigger calcification event (NCE II) is characterized by a dramatic increase in nannoconid abundance and calcification, reaching lithogenetic amounts, concomitant with a moderate abundance increase of calcified calpionellids (genera *Crassicollaria, Calpionella, Remaniella*).

- Paleoceanographic and climatic factors controlling NCEs at low latitudes (Tethyan Realm) are discussed. The Late Jurassic nannoplankton evolution was mostly controlled by the following factors: A) a decrease in pCO_2 due to decreased spreading rates; B) a decrease in oceanic Mg/Ca ratio values promoting low Mg-$CaCO_3$ and $CaCO_3$ biomineralization ("nannofossil fertilization" *sensu* Stanley, 2006); C) cool climatic conditions (Price, 1999; Sorrosa *et al.*, 2005); D) stable environmental conditions, without significant perturbations, favouring diversification and expansion of calcareous nannoplankton.

The calcareous nannofossil speciation episode during the Tithonian was investigated to monitor nannofossil evolutionary behaviour during an interval of inferred paleoceanographic and paleoclimatic stability. This speciation episode provides examples of all the three speciation models: Phyletic Gradualism, Punctuated Equilibrium and Punctuated Gradualism. Evolutionary modes also suggest that at specific level both nannoliths and coccoliths gradually evolve in a time interval of more that 1 Ma, while at generic level a rapid speciation is most common.

8. TAXONOMIC INDEX and NOTES ON SELECTED CALCAREOUS NANNOFOSSIL TAXA

8.1. Taxonomic Index

Calcareous nannofossil species recognized (digital range chart available on the digital support attached), here listed in species alphabetic order.

Anfractus harrisonii Medd, 1979
Ansulasphaera helvetica Grün and Zweili, 1980
Assipetra infracretacea (Thierstein, 1973) Roth, 1973
Axopodorhabdus cylindratus (Noël, 1965) Wind and Wise, 1977
Biscutum constans (Gorkl, 1957) Black ex Black and Barnes, 1959
Biscutum dubium (Noël, 1965) Grün in Grün *et al*., 1974
Braarudosphaera regularis Black, 1973
Conusphaera mexicana (Trejo, 1969) subsp. *mexicana* Bralower and Thierstein, 1989
Conusphaera mexicana (Trejo, 1969) subsp. *minor* Bralower and Thierstein, 1989
Crepidolithus crassus (Deflandre in Deflandre and Fert, 1954) Noël, 1965
Crepidolithus perforata (Medd, 1979) Grün and Zweili, 1980
Cretarhabdus angustiforatus (Black, 1971) Bukry, 1973
Cretarhabdus conicus Bramlette and Martini, 1964
Cretarhabdus octofenestratus Bralower and Thierstein, 1989
Cretarhabdus surirellus (Deflandre, 1954) Reinhardt, 1970
Cruciellipsis cuvillieri (Manivit, 1956) Thierstein, 1971
Cyclagelosphaera argoensis Bown, 1992b
Cyclagelosphaera deflandrei Manivit, 1966
Cyclagelosphaera margerelii Noël, 1965
Cyclagelosphaera sp.1 (Noël, 1965), this study
Cyclagelosphaera riyadhensis Varol, 2006
Cyclagelosphaera tubulata (Grün and Zweili, 1980) Cooper, 1987
Cyclagelosphaera wiedmannii Reale and Monechi, 1994
Diazomatolithus lehmanii Noël,1965
Discorhabdus rotatorius (Bukry, 1969) Thierstein, 1973
Ethmorhabdus gallicus Noël, 1965
Faviconus multicolumnatus (Bralower in Bralower, Monechi and Thierstein, 1989), emended in this study
Hexalithus noeliae (Noël, 1956) Loeblich and Tappan, 1965
Hexalithus sp. 1 (Loeblich and Tappan, 1964), this study
Hexapodorhabdus cuvillieri Noël, 1965
Lithraphidites carniolensis Deflandre, 1963
Lotharingius barozii Noël, 1973
Lotharingius crucicentralis (Medd, 1971) Grün and Zweili, 1980

Lotharingius hauffii Grün and Zweili in Grün *et al.*, 1974

Lotharingius sigillatus (Stradner, 1971) Prins in Grün *et al.*, 1974

Manivitella pemmatoidea (Deflandre ex Manivit, 1965) Thierstein, 1971

Markalius circumradiatus (Stover, 1966) Perch-Nielsen, 1968

Micrantholithus hoschulzii (Reinhardt, 1966) Thierstein, 1971

Micrantholithus obtusus Stradner, 1963

Microstaurus chiastius (Worsley, 1971) Bralower, Monechi and Thierstein, 1989

Microstaurus quadratus Black, 1971

Miravetesina favula Grün In Grün and Allemann, 1975

Nannoconus bermudezii Brönnimann, 1955

Nannoconus boneti Trejo, 1959

Nannoconus bronnimannii Trejo, 1959

Nannoconus colomii (de Lapparent, 1931) Kamptner, 1938

Nannoconus compressus Bralower and Thierstein in Bralower, Monechi and Thierstein, 1989

Nannoconus dolomiticus Cita and Pasquarè, 1959

Nannoconus globulus (Brönnimann, 1955) subsp, *globulus* Bralower and Thierstein in Bralower, Monechi and Thierstein, 1989

Nannoconus globulus (Brönnimann, 1955) subsp, *minor* Bralower and Thierstein in Bralower, Monechi and Thierstein, 1989

Nannoconus infans Bralower in Bralower, Monechi and Thierstein, 1989

Nannoconus kamptneri (Brönnimann, 1955) subsp, *kamptneri* Bralower and Thierstein in Bralower, Monechi and Thierstein, 1989

Nannoconus kamptneri (Brönnimann, 1955) subsp. *minor* Bralower and Thierstein in Bralower, Monechi and Thierstein, 1989

Nannoconus sp.1, this study

Nannoconus sp.2 this study

Nannoconus steinmannii (Kamptner, 1931) subsp, *minor* Dares and Achéritéguy, 1980

Nannoconus steinmannii (Kamptner, 1931) subsp. *steinmannii*

Nannoconus wintereri Bralower and Thierstein in Bralower, Monechi and Thierstein, 1989

Parhabdolithus splendens (Deflandre, 1953) Noël, 1969

Percivalia fenestrata (Worsley 1971) Wise, 1983

Polycostella sp.1, this study

Polycostella beckmannii Thierstein, 1971

Polycostella senaria Thierstein, 1971

Polypodorhabdus escaigii Noël, 1965

Pseudolithraphidites quattruobacillus Keupp, 1976

Rhagodiscus asper (Stradner, 1963) Manivit, 1971

Rhagodiscus nebulosus Bralower and Thierstein in Bralower, Monechi and Thierstein, 1989

Rotellapillus laffittei (Noël, 1956) Noël, 1973

Rucinolithus wisei Thierstein, 1971

Schizosphaerella punctulata Deflandre and Dangeard, 1938

Triscutum beaminsterensis Dockerill, 1987

Triscutum expansus (Medd, 1979) Deckerill, 1987

Umbria granulosa subsp. *granulosa* Bralower and Thierstein in Bralower, Monechi and

Thierstein, 1989

Umbria granulosa subsp. *minor* Bralower and Thierstein in Bralower, Monechi and Thierstein, 1989

Vagalapilla stradneri (Rood, Hay end Bernard, 1971) Thierstein, 1973

Watznaueria sp.3 Cobianchi *et al.*, 1992

Watznaueria barnesiae (Black, 1959) Perch-Nielsen, 1968

Watznaueria biporta Bukry, 1969

Watznaueria britannica (Stradner, 1963) Reinhardt, 1964

Watznaueria britannica (Stradner, 1963) Reinhardt, 1964, large form, this study

Watznaueria communis (Reinhardt, 1964)

Watznaueria communis (Reinhardt, 1964) large form, this study

Watznaueria contracta (Bown and Cooper, 1989) Cobianchi, Erba and Pirini Radrizzani, 1992

Watznaueria crucicentralis (Medd, 1971) Thierstein, 1976

Watznaueria fossacincta (Black, 1971a) Bown in Bown and Cooper, 1989a

Watznaueria manivitiae (Bukry, 1973) Moshkovitz and Ehrlich, 1987

Watznaueria manivitiae (Bukry, 1973) Moshkovitz and Ehrlich, 1987, large form, this study

Watznaueria rawsonii Crux, 1987

Watznaueria sp.3 Cobianchi, Erba and Pirini Radrizzani, 1992

Zeugrhabdotus cooperi Bown, 1992b

Zeugrhabdotus embergeri (Noël,1959) Bralower, Monechi and Thierstein, 1989

Zeugrhabdotus erectus (Deflandre, 1954) Bralower, Monechi and Thierstein, 1989

8.2. Notes on selected calcareous nannofossil taxa

8.2.1. Genus *Cyclagelosphaera* (Noël, 1965)
    Cyclagelosphaera sp.1
    (Plate VIII, Fig. 4-11)

Description: Circular coccolith with a distal shield composed by 19-25 elements and a proximal one slightly smaller than the former, the two shields are connected by a central circular tube, which determine a central hole.

Remarks: This form is distinguished form *C.margerelii* by its bigger diameter, from *C.deflandrei* by its smaller diameter and from *C.wiedmannii* by its smaller diameter and white colours.

Dimension: *C.margerelii* and *C.deflandrei*, show maximum diameter of 6 µm and a minimum diameter 9 µm, respectively. The form observed both in smear slide and thin section from several sections have a diameter between 6 µm and 9 µm; overgrowth of *C.margerelii* has been excluded.

Distribution: Lower Tithonian (Nannofossil Zone NJT-15, CM21) to Berriasian (Nannofossil Zone NK-2).

8.2.2. Genus *Faviconus* Bralower in Bralower, Monechi and Thierstein, 1989
 Faviconus multicolumnatus Bralower in Bralower, Monechi and Thierstein, 1989
 (Plate I)

> 1978 ?*Nannoconus* sp. aff. *N.bermudezi* Brönnimann, 1955 in Wind, pl. 1, figs. 14, 20.
> 1978 ?*Nannoconus* sp. Wind, pl. 1, figs. 18, 19.
> 1989 *Faviconus multicolumnatus* Bralower in Bralower, Monechi and Thierstein, 1989

Description: Numerous stacked wedges are separated by thin axial canals.
Remarks: This species is often seen as broken pieces in smear slides, while in thin section large aggregate of numerous individuals (up to a maximum of ten) are recognizable. This form is distinguished form *N.dolomiticus* by its smaller dimensions.
Dimension: The forms previously described (Bralower, Monechi and Thierstein, 1989) consist of a maximum length of 6-12 µm and a maximum width of 4-6 µm. The forms observed in thin section from Torre de Busi and Monte Pernice and DSDP Site 534 A are bigger both in length and width; overgrowth bias is excluded.
Length: 6-20 µm; Width: 4-10 µm.
Distribution: Upper Oxfordian (Nannofossil Zone NJT-14) - Upper Tithonian (top of chron CM19n; Nannofossil Zone NJT-17).
Known range: uppermost Oxfordian (*Bimmammatum* Tethyan Ammonite Zone and *Rosenkrantzi* Boreal Ammonite Zone, De Kaenel *et al.*, 1996) to Upper Tithonian (top in chron CM19n, Bralower, Monechi and Thierstein, 1989).

8.2.3. Genus *Hexalithus* Gardet, 1955
 Hexalithus sp. 1
 (Plate IV, Fig. 9)

> 1956 *Hexalithus hexalithus* Noël, 1956, p.329, pl.5, figs. 39, 40 a-c
> 1965 *Hexalithus noeliae* Loeblich and Tappan, 1965

Description: hexagonal nannolith composed of six triangular elements adjacent one to the other. Every single element has a straight rim, no flare is present at the end of petals.
Remarks: This form is distinguished form *H. noeliae* by its always linear outer margin, and its bigger dimension.
Dimension: Diameter 4-8 µm
Distribution: Upper Tithonian (CM19n; upper Nannofossil Zone NJT-17) - Lower Berriasian? (CM17r; Nannofossil Zone NK-1)

8.2.4. Genus *Nannoconus* Kamptner, 1931
 Nannoconus sp.1
 (Plate II, fig.1)

Description: very small and primitive nannoconid with a variable shape: square or sausage-shape. This form has a large canal and narrow apical and basal apertures.

Individual wedges outline are very difficult to be seen in the light microscope.

Remarks: It is distinguished from *Nannoconus infans* by its larger axial canal, and from *Nannoconus globulus minor* by its smaller size. This species is rare in smear slides since it is very small and delicate, but is easily observed in thin-section, as it is one of the first (primitive) nannoconids to appear.

Dimension: Length: 1-4.5 µm; Width: 2-4.5 µm.

Distribution: rare individuals are reported from Lower Tithonian to Upper Tithonian (Nannofossil Zone NJT-16; CM20).

8.2.5. Genus *Nannoconus* Kamptner, 1931
Nannoconus sp.2
(Plate II, figs. 5-6)

Description: rectangular to elongate oval outline toward slightly conical. This form has narrow axial canal and wedges from adjacent walls are closely juxtaposed, also apical and basal apertures are narrow.

Remarks: This form is considered to represent a intermediate form between *N.compressus* and *N. steinmannii minor* since a complete gradation in shape and size was observed. It is distinguished from *Nannoconus compressus* by its slightly conical outline, from *Nannoconus steinmannii minor* by its less conical outline and from *Nannoconus wintereri* by its very narrow axial canal.

Dimension: Length: 6-8 µm; Width: 4-6 µm.

Distribution: rare individuals are reported from Upper Tithonian to Lower Berriasian (Nannofossil Zone NJT-17; CM19n).

8.2.6. Genus *Watznaueria* Reinhardt, 1964
Watznaueria britannica large form
(Plate VII, fig. 12)

Remarks: In the studied sections along with normal size *W.britannica*, several large morphotypes were observed. These specimens are identical for ultrastructure to *W.britannica* holotype, but their size is always greater.

Dimension: Length > 9 µm; Width > 7 µm.

Distribution: Oxfordian (Nannofossil Zone NJT-14) to Lower Tithonian (Nannofossil Zone NJT-16).

8.2.7. Genus *Watznaueria* Reinhardt, 1964
Watznaueria communis large form
(Plate VIII, fig. 3)

Remarks: In the studied sections along with normal size *W.communis*, several large morphotypes were observed. These specimens are identical for ultrastructure to *W.communis* holotype, but their size is always greater.

Dimension: Length > 9 µm; Width > 7 µm.

Distribution: Oxfordian (Nannofossil Zone NJT-14) to Berriasian (Nannofossil Zone NK-2).

8.2.8. Genus *Watznaueria* Reinhardt, 1964

Watznaueria manivitiae large form

(Plate VII, fig. 8-9)

Remarks: In the studied sections along with normal size *W.manivitiae*, several large morphotypes were observed. These specimens are identical for ultrastructure to *W.manivitiae* holotype, but their size is always greater.

Dimension: Length > 12 µm; Width > 10 µm.

Distribution: Upper Callovian (Nannofossil Zone NJT-12) to Lower Tithonian (Nannofossil Subzone NJT-14b).

9. CALCAREOUS NANNOFOSSIL PLATES

PLATE I

1-4. *Faviconus multicolumnatus* (Bralower and Thierstein, 1989) subsp. sp.1

    1- cross-polarized light, DSDP site 534 A 101-04; 98-99, ultra-thin section.
    2- cross-polarized light, DSDP site 534 A 102-01; 111-112, ultra-thin section.
    3- cross-polarized light, Torre de Busi, sample/level TdB 30,15, smear slide.
    4- cross-polarized light, DSDP site 534 A 099-01; 38-39, ultra-thin section.

5-6. *Faviconus multicolumnatus* (Bralower and Thierstein, 1989) subsp. sp.2

    5- cross-polarized light, Torre de Busi, sample/level TdB 7,50, smear slide.
    6- cross-polarized light, DSDP site 534 A 099-01; 38-39, ultra-thin section.

7-8. Spheres of *Faviconus multicolumnatus* (Bralower and Thierstein, 1989) subsp. sp.2

    7- cross-polarized light, DSDP site 534 A 097-01; 43-44, ultra-thin section.
   8- cross-polarized light, Monte Pernice, sample M7, ultra-thin section.
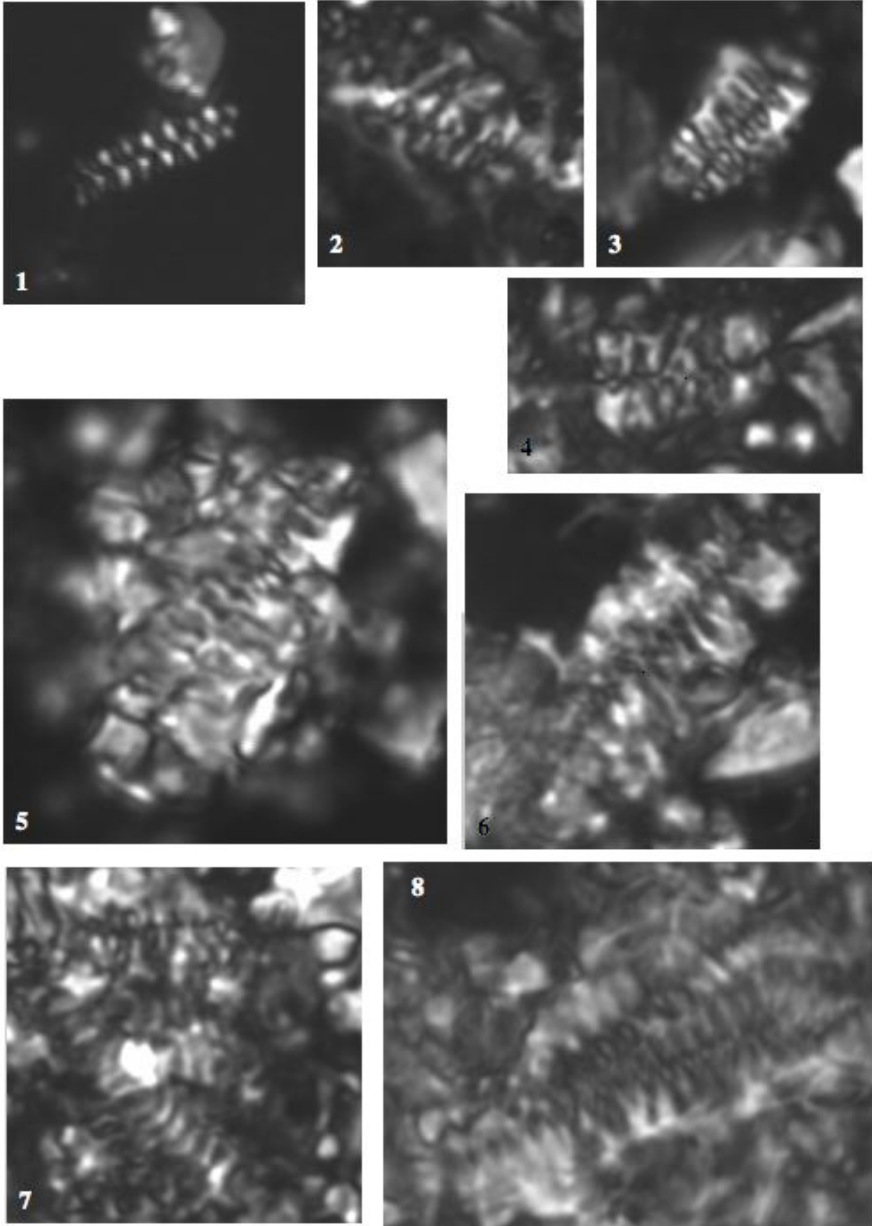
PLATE I

PLATE II

1- *Nannoconus* sp.1, this work
    cross-polarized light, Colma di Vignole, sample/level CdV 8,70, smear slide.

2-3. *Nannoconus infans* Bralower, 1989

    2- cross-polarized light, Monte Pernice, sample/level M3/4,60, ultra-thin section.
    3- cross-polarized light, Foza A, sample/level FZa 12,38, smear slide.

4- *Nannoconus compressus* Bralower and Thierstein, 1989
    cross-polarized light, Foza B, sample/level FZb 53,15, smear slide.

5-6. *Nannoconus* sp.2, this work

    5- cross-polarized light, Bombatierle, sample/level BOM 1,28, smear slide.
    6- cross-polarized light, Colma di Vignole, sample/level CdV 7,04, smear slide.

7. Micrite made by small nannoconids ("nannoconites")
    cross-polarized light, DSDP site 534 A 090-03; 21-22, ultra-thin section.

PLATE II
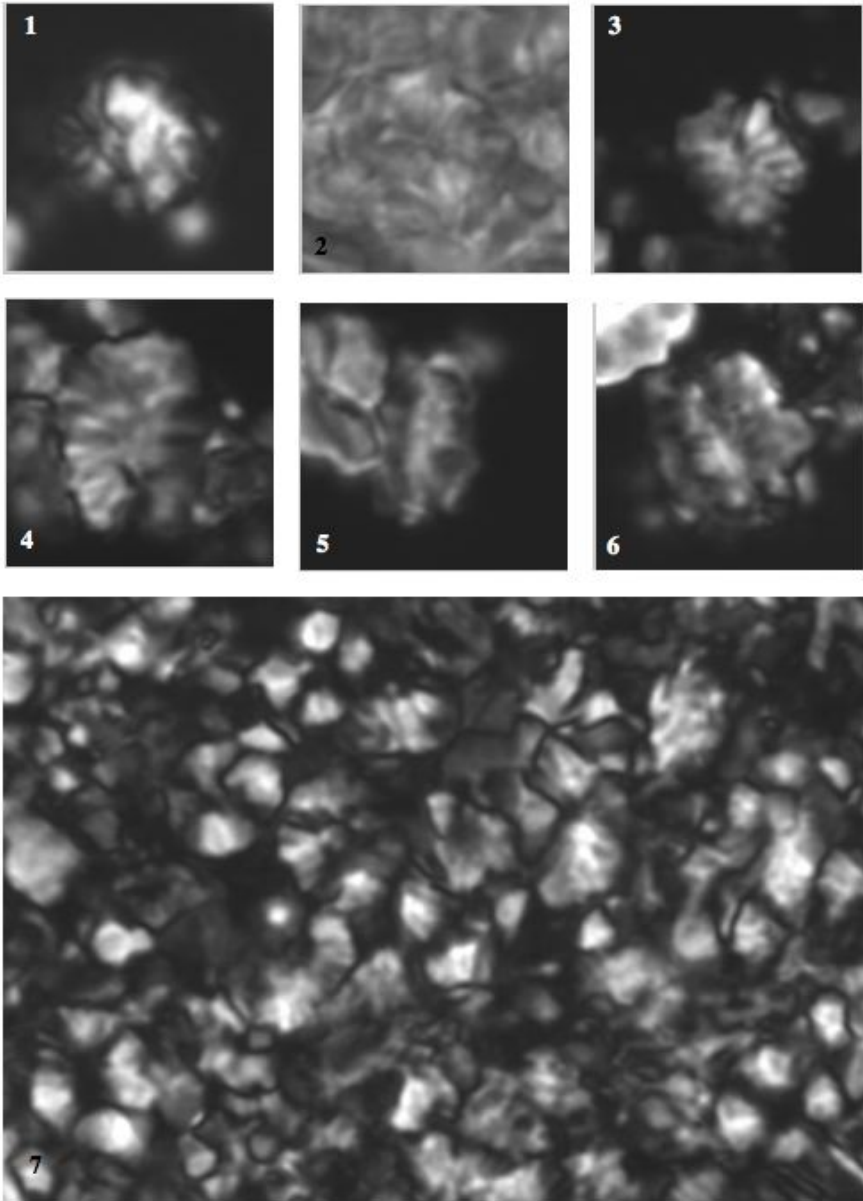
PLATE III

1- *Nannoconus globulus* (Brönnimann, 1955) subsp, *minor* Bralower and Thierstein, 1989
   cross-polarized light, Foza A, sample/level FZa 15,20, smear slide.

2-3. *Nannoconus globulus* (Brönnimann, 1955) subsp, *globulus* Bralower and Thierstein, 1989

   2- cross-polarized light, Foza B, sample/level FZb 63,02, smear slide.
   3- cross-polarized light, Foza B, sample/level FZb 74,95, smear slide.

4-6. *Nannoconus wintereri* Bralower and Thierstein, 1989

   4- cross-polarized light, Torre de Busi, sample/level TdB 4,90, smear slide.
   5- cross-polarized light, Foza B, sample/level FZb 52,33, smear slide.
   6- cross-polarized light, Torre de Busi, sample/level TdB 4,90, smear slide.

7-8. *Nannoconus steinmannii* (Kamptner, 1931) subsp, *minor* Dares and Achéritéguy, 1980

   7- cross-polarized light, Foza B, sample/level FZb 50,50, smear slide.
   8- cross-polarized light, Foza B, sample/level FZb 63,20, smear slide.

9-10. *Nannoconus steinmannii* (Kamptner, 1931) subsp. *steinmannii*

   9- cross-polarized light, Foza A, sample/level FZa 15,20, smear slide.
   10- cross-polarized light, Monte Pernice, sample/level M4/5,40, ultra-thin section.

11- *Nannoconus kamptneri* (Brönnimann, 1955) subsp. *minor* Bralower and Thierstein, 1989
   cross-polarized light, Foza B, sample/level FZb 73,85, smear slide.

12- *Nannoconus kamptneri* (Brönnimann, 1955) subsp, *kamptneri* Bralower and Thierstein, 1989
   fragment, cross-polarized light, Foza B, sample/level FZb 74,95, smear slide.

PLATE III
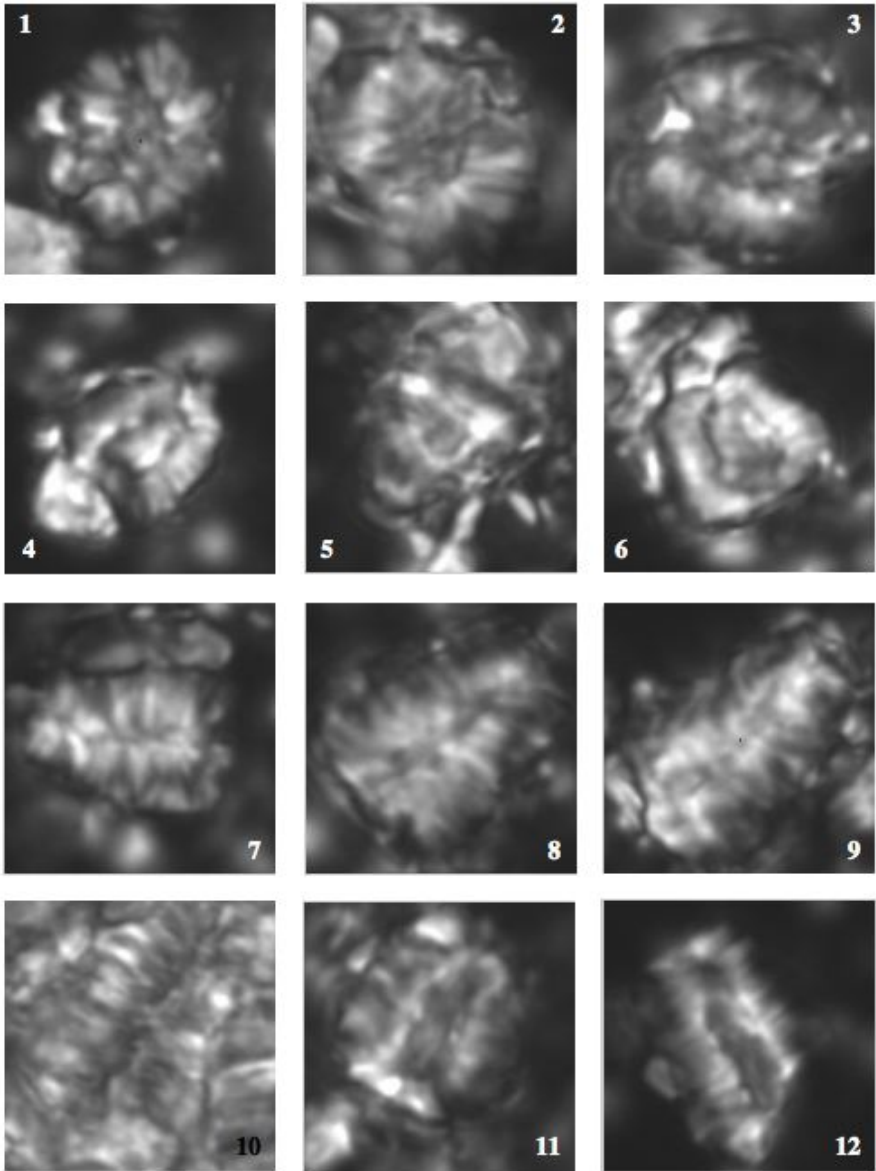
PLATE IV

1-2. *Conusphaera mexicana* (Trejo, 1969) subsp, *mexicana* Bralower and Thierstein, 1989

    1- cross-polarized light, Monte Pernice, sample/level M16/22,00, ultra-thin section.
    2- cross-polarized light, Foza A, sample/level FZa 9,60, smear slide

3-6. *Polycostella beckmannii* Thierstein, 1971

    3- cross-polarized light, Colma di Vignole, sample/level CdV 10,52, smear slide.
    4- cross-polarized light, Colma di Vignole, sample/level CdV 9,28, smear slide.
    5- cross-polarized light, Colma di Vignole, sample/level CdV 10,52, smear slide.
    6- cross-polarized light, Foza A, sample/level FZa 3,40, smear slide.

7-8. *Hexalithus noeliae* (Noël, 1956) Loebllch and Tappan, 1964

    7- cross-polarized light, Torre de Busi, sample/level TdB 15,05, smear slide.
    8- cross-polarized light, Torre de Busi, sample/level TdB 13,30, ultra-thin section.

9. *Hexalithus* sp.1 (Noël, 1956) this work
  cross-polarized light, Torre de Busi, sample/level TdB 3,25, ultra-thin section.

10-12. *Micrantholithus hoschulzii* (Reinhardt, 1966) Thierstein, 1971 transitional to *Micrantholithus obtusus* Stradner, 1963

    10- *M.hoschulzii* cross-polarized light, DSDP site 534 A 091-05; 104-105, ultra-thin section.
    11- transitional form, cross-polarized light, Foza B, sample/level FZb 59,0, smear slide.
   12- *M.obtusus* cross-polarized light, DSDP site 534 A 091-05; 104-105, ultra-thin section.

PLATE IV
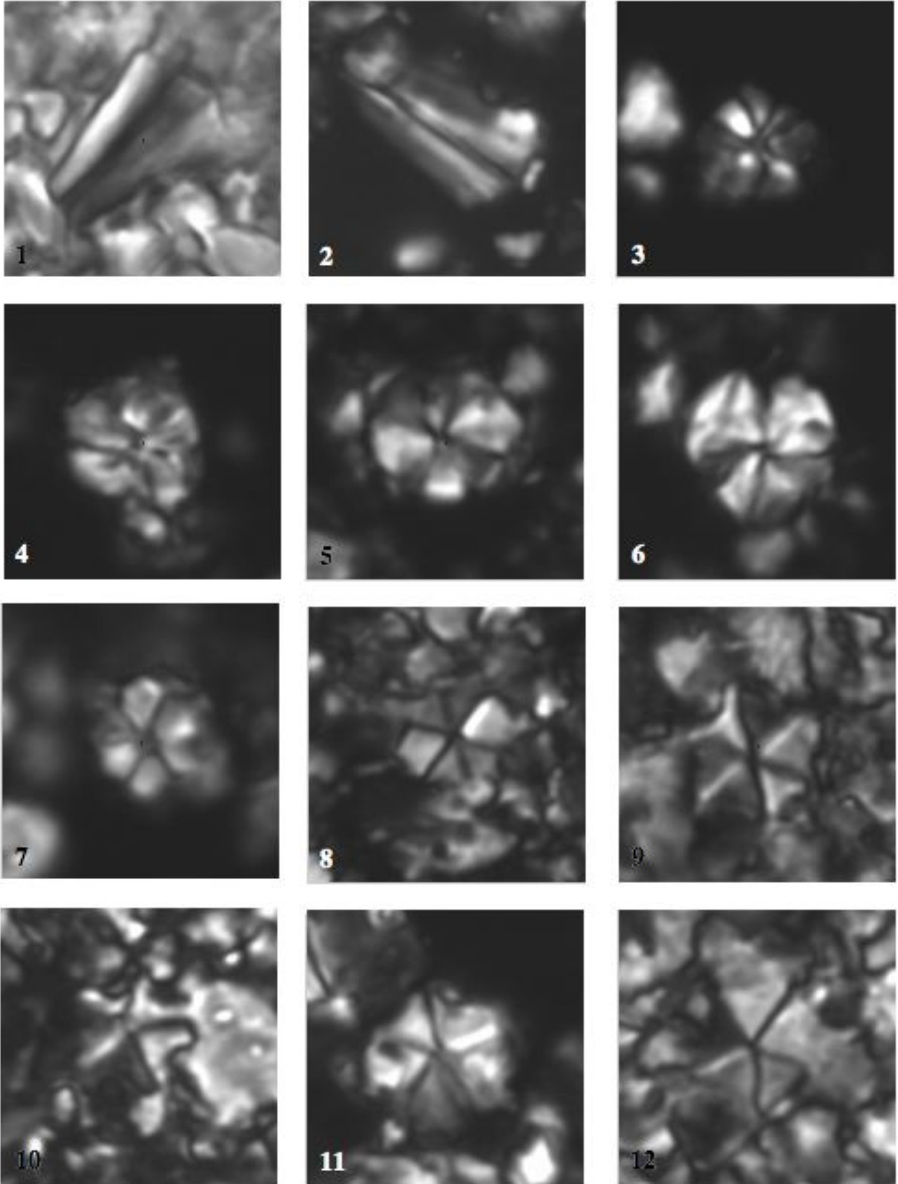
PLATE V

1-3. *Microstaurus quadratus* Black, 1971

    1- cross-polarized light, Torre de Busi, sample/level TdB 14,59, smear slide.
    2- cross-polarized light, Torre de Busi, sample/level TdB 5,22, smear slide.
    3- cross-polarized light, Torre de Busi, sample/level TdB 50,20, smear slide.

4-5. *Microstaurus chiastius* (Worsley, 1971) Bralower et al., 1989

    4- cross-polarized light, Foza A, sample/level FZa 15,20, smear slide.
    5- cross-polarized light, Foza B, sample/level FZb 74,95, smear slide.

6. *Cruciellipsis cuvillieri* (Manivit, 1956) Thierstein, 1971
  cross-polarized light, Foza B, sample/level FZb 62,60, smear slide.

7. *Cretarhabdus surirellus* (Deflandre, 1954) Reinhardt, 1970
cross-polarized light, Torre de Busi, sample/level TdB 6,18, smear slide.

8-9. *Cretarhabdus octofenestratus* Bralower and Thierstein, 1989

    8- cross-polarized light, Foza B, sample/level FZb 59,0, smear slide.
    9- cross-polarized light, Foza A, sample/level FZa 6,55, smear slide.

10-12. *Cretarhabdus angustiforatus* (Black, 1971) Bukry, 1973

    10- cross-polarized light, Foza B, sample/level FZb 68,95, smear slide.
    11- cross-polarized light, Foza B, sample/level FZb 69,90, smear slide.
   12- cross-polarized light, Foza B, sample/level FZb 66,10, smear slide.

PLATE V
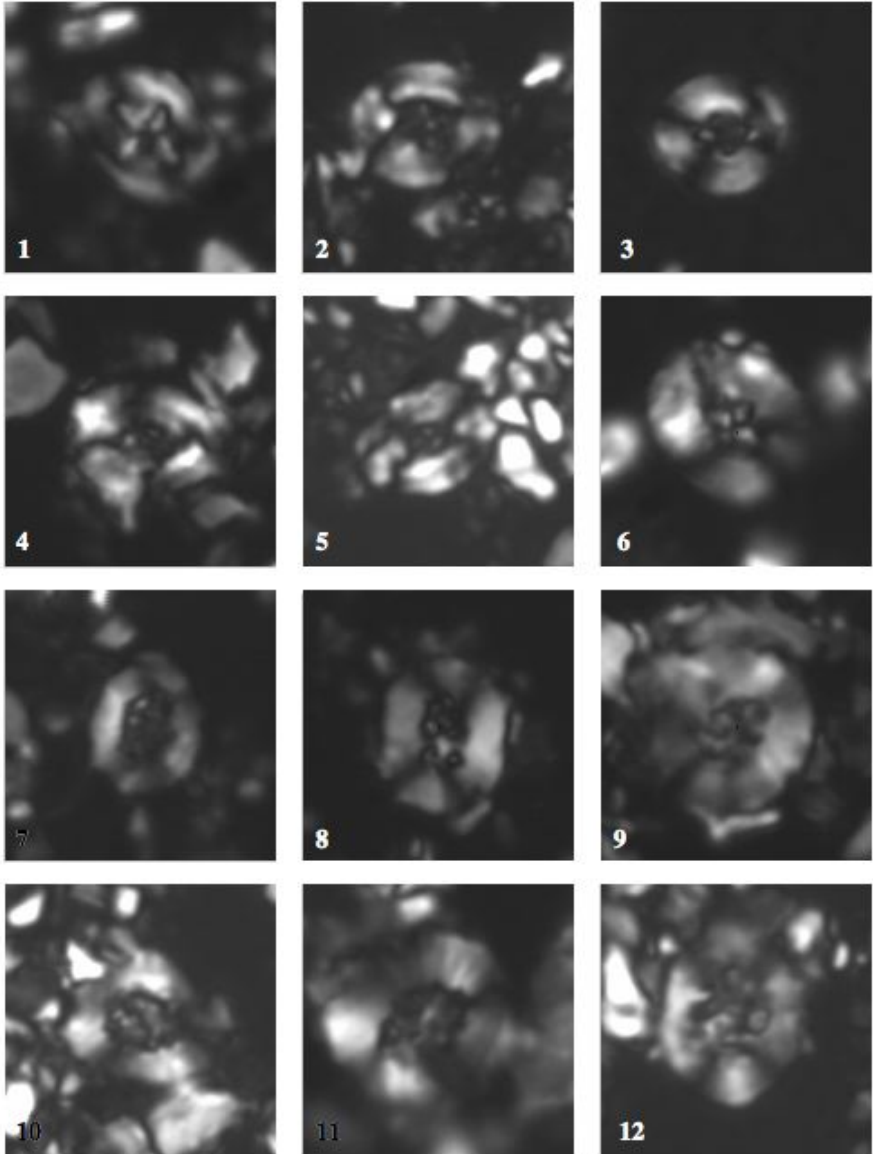
PLATE VI

1-2. *Umbria granulosa* subsp. *granulosa* Bralower and Thierstein, 1989

    1- cross-polarized light, Torre de Busi, sample/level TdB 4,02, smear slide.
    2- cross-polarized light, Torre de Busi, sample/level TdB 15,50, smear slide.

3-4. *Rhagodiscus asper* (Stradner, 1963) Manivit, 1971

    3- cross-polarized light, Foza B, sample/level FZb 66,10, smear slide.
    4- cross-polarized light, Torre de Busi, sample/level TdB 4,28, smear slide.

5. *Rhagodiscus nebulosus* Bralower and Thierstein, 1989
cross-polarized light, Foza B, sample/level FZb 68,95, smear slide.

6-7. *Percivalia fenestrata* (Worsley 1971) Wise, 1983

    6- cross-polarized light, Foza B, sample/level FZb 59,0, smear slide.
    7- cross-polarized light, Foza B, sample/level FZb 63,20, smear slide.

8. *Zeugrhabdotus erectus* (Deflandre, 1954) Bralower et al.,1989
cross-polarized light, DSDP site 534 A 102-02; 93-94, ultra-thin section.

9-10. *Zeugrhabdotus erectus* (Deflandre, 1954) Bralower et al.,1989 transitional to *Zeugrhabdotus embergeri* (Noël,1959) Bralower et al., 1989

    9- cross-polarized light, Torre de Busi, sample/level TdB 2,95, smear slide.
    10- cross-polarized light, Torre de Busi, sample/level TdB 17,54, smear slide.

11. *Zeugrhabdotus embergeri* (Noël,1959) Bralower et al., 1989
cross-polarized light, Foza A, sample/level FZa 9,60, smear slide.

12. *Zeugrhabdotus cooperi* Bown, 1992b
 cross-polarized light, Torre de Busi, sample/level TdB 4,46, smear slide.

PLATE VI
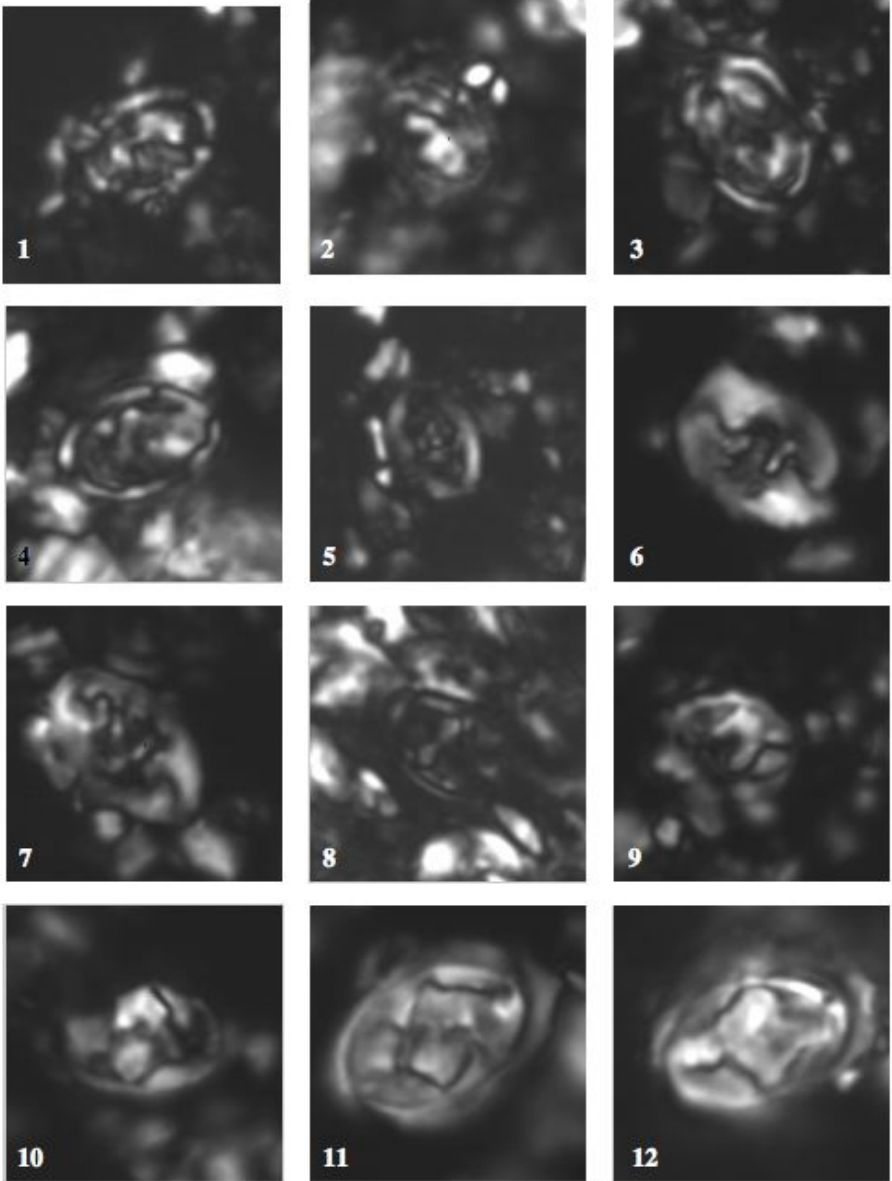
PLATE VII

1-2. *Lotharingius hauffii* Grün and Zweili in Grün *et al.*, 1974

    1- cross-polarized light, Bombatierle, sample/level BOM 8,19, smear slide.
    2- cross-polarized light, Colma di Vignole, sample/level CdV 8,37, smear slide.

3-4. *Watznaueria fossacincta* (Black, 1971a) Bown in Bown and Cooper, 1989a

    3- cross-polarized light, Colma di Vignole, sample/level CdV 8,37, smear slide.
    4- cross-polarized light, Foza A, sample/level FZa 14,15, smear slide.

5-6. *Watznaueria barnesiae* (Black, 1959) Perch-Nielsen, 1968

    5- cross-polarized light, Foza B, sample/level FZb 51,05, smear slide.
    6- cross-polarized light, Monte Pernice, sample/level M13/16,20, smear slide.

7. *Watznaueria* sp.3 (Cobianchi et al., 1992)
cross-polarized light, Colma di Vignole, sample/level CdV 18,00, smear slide.

8-9. *Watznaueria manivitae* (Bukry, 1973) Moshkovitz and Ehrlich, 1987

    8- cross-polarized light, Torre de Busi, sample/level TdB 53,20, smear slide.
    9- large form; cross-polarized light, DSDP site 534 A 100-02; 87-88, ultra-thin section.

10-12. *Watznaueria britannica* (Stradner, 1963) Reinhardt, 1964

    10- cross-polarized light, Foza A, sample/level FZa 9,60, smear slide.
    11- cross-polarized light, Colma di Vignole, sample/level CdV 8,70, smear slide.
    12- large form; cross-polarized light, Foza A, sample/level FZa 2,23, smear slide.

102
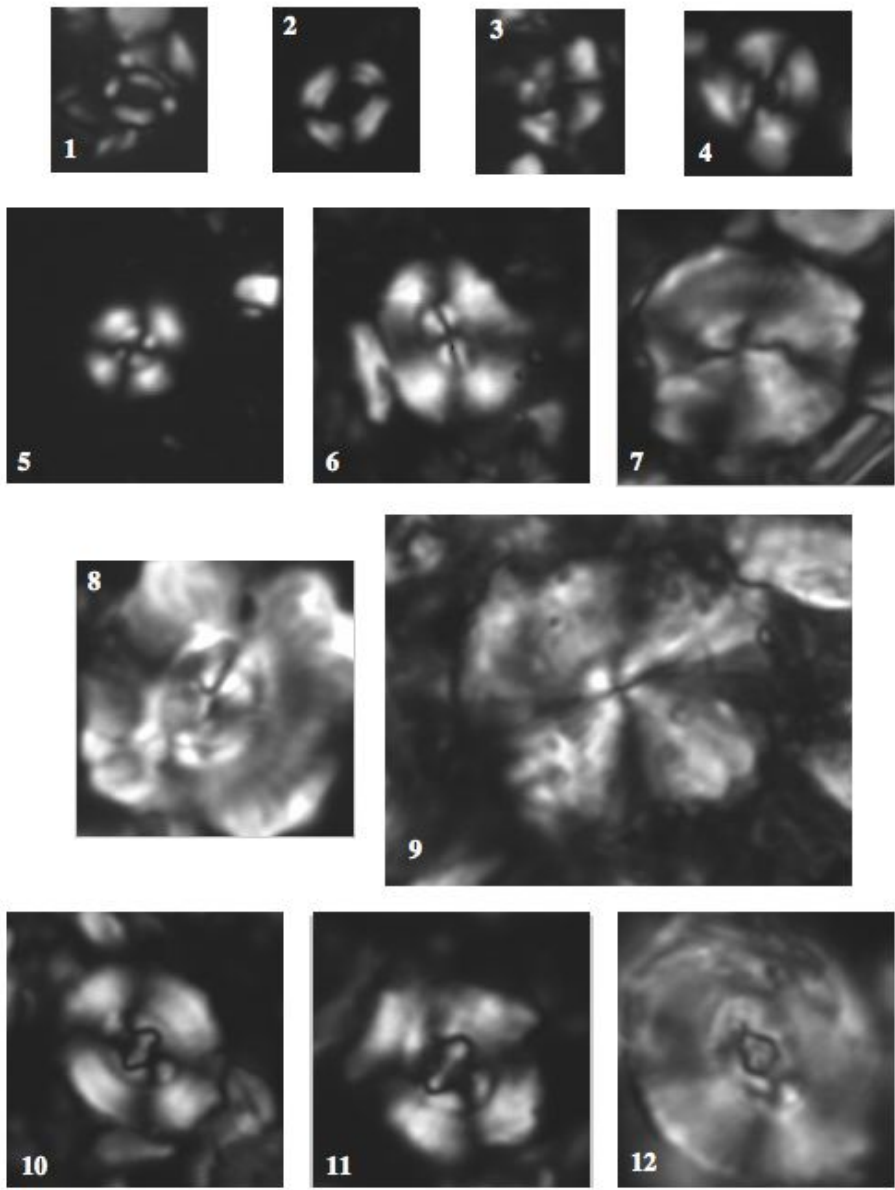
PLATE VII

PLATE VIII

1-3. *Watznaueria communis* (Reinhardt, 1964)

    1- cross-polarized light, Monte Pernice, sample/level M4/5,40, smear slide.
    2- cross-polarized light, Foza A, sample/level FZa 22,00, smear slide.
    3- large form; cross-polarized light, Foza A, sample/level FZa 23,17, smear slide.

4. *Cyclagelosphaera tubulata* (Grün and Zweili, 1980) Cooper, 1987
 cross-polarized light, Foza B, sample/level FZb 82,01, smear slide.

5-7. *Cyclagelosphaera margerelii* Noël, 1965

    5- cross-polarized light, Foza A, DSDP site 534 A 100-02; 87-88, ultra-thin section.
    6- cross-polarized light, Foza A, sample/level FZa 23,17, smear slide.
    7- cross-polarized light, Torre de Busi, sample/level TdB 4,46, smear slide.

8-9. *Cyclagelosphaera argoensis* Bown, 1992b

    8- cross-polarized light, Torre de Busi, sample/level TdB 15,50, smear slide.
    9- cross-polarized light, Torre de Busi, sample/level TdB 4,02, smear slide.

10-11. *Cyclagelosphaera deflandrei* Manivit, 1966

    10- cross-polarized light, DSDP site 534 A 091-05; 104-105, ultra-thin section.
    11- cross-polarized light, DSDP site 534 A 100-02; 87-88, ultra-thin section.

PLATE VIII
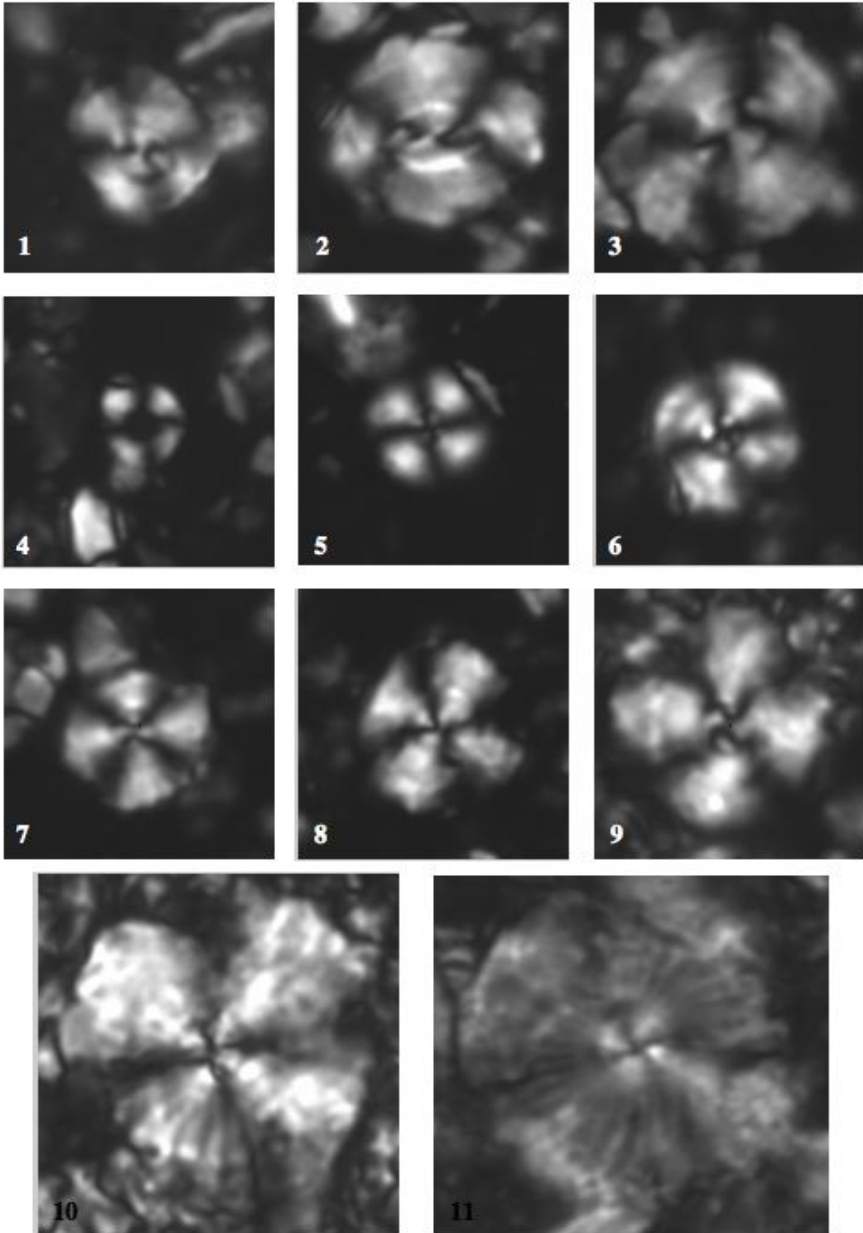
10. REFERENCES

Abbink, O., Targarona, J., Brinkhuis, H. & Visscher, H. (2001). Late Jurassic to earliest Cretaceous paleoclimatic evolution of the southern North Sea. *Global and Planetary Change 30, 231-256.*

Adatte, T., Stinnesbeck, W., Remane, J. & Hubberten, H. (1996). Paleoceanographic changes at the Jurassic-Cretaceous boundary in the Western Tethys, northeastern Mexico. *Cretaceous Research 17, 671-689.*

Andreini, G., Caracuel, J.E. & Parisi, G. (2007). Calpionellid biostratigraphy of the Upper Tithonian-Upper Valanginian interval in western Sicily. *Swiss j. geosci. 100, 179-198.*

Cecca, F., Garin, B.M., Marchand, D., Lathuiliere, B. & Bartolini, A. (2005). Paleoclimatic control of biogeographic and sedimentary events in Tethyan and peri-Tethyan areas during the Oxfordian (Late Jurassic). *Palaeogeo. Palaeoclim. Palaeoeco. 222: 10-32.*

Barberis, A., Fossati, S., Bersezio, R. & Erba, E. (1990). Lithostratigraphy and biostratgraphy of the Maiolica formation from the Lombardy Basin (Souther Alps). *Memorie della Società Geologica Italiana 45, 111-117.*

Bartolini, A., Baumgartner, P.O. & Guex, J. (1999). Middle and Late Jurassic radiolarian paleoecology versus carbon-isotope stratigraphy. *Palaeogeo. Palaeoclim. Palaeoeco. 145, 43-60.*

Bartolini, A., Pittet, B., Mattioli, E. & Hunziker, J.C. (2003). Shallow-platform paleoenvironmental conditions recorderd in deep-shelf sediments: C and O stable isotopes in Upper Jurassic sections of Southern Germany (Oxfordian-Kimmeridgian). *Sedimentary Geology 160, 107-130.*

Baumann, K., Andruleit, H., Bockel, B., Geisen, M., & Kinkel, H. (2005). The significance of extant coccolithophores as indicators of ocean water masses, surface water temperatures, and paleoproductivity: a review. *Palaontologische Zeitschrift 79 (1), 93-112.*

Baumgartner, P.O. (1984). Age and genesis of the Tethyan Jurassic Radiolarite. *Eclogae Geologicae Helvetiae 80 (3), 831-879.*

Baumgartner, P.O. (1987). Age and genesis of the Tethyan Jurassic Radiolarite. *Eclogae Geologicae Helvetiae 80(3), 831-879.*

Baumgartner, P.O. , Martire, L., Gorican, S., O'Dogherty, L., Erba, E. & Pillevuit, A. (1995). New Middle and Upper Jurassic radiolarian assemblages co-occurring with ammonites and nannofossil from the Southern Apls (Northen Italy). In: Baumgartner P.O. *et al.* (Eds.) – Middle Jurssic to Lower Cretaceous radiolaria of Tethys; occurrences, systematics, biochronology. *Mem. Geol. Lausanne, 23, 737-750, Lausanne.*

Baumgartner, P.O., Bernoulli, D. & Martire, L. (2001). Mesozoic pelagic facies of the Southern Alps: Paleotectonics and paleoceanography. *IAS 2001 Davos: Excursion A1.*

Berggren, W.A. & Hollister, C.D. (1977). Plate tectonics and Paleocirculation – Commotion in the ocean. *Tectonophysics 38, 11-48*

Berner, R.A & Kothavala, Z. (2001). GEOCARB III: a revised model of atmospheric CO2 over Phanerozoic time. *American Journal of Science 301, 182-204.*

Berner R.A (2006). GEOCARBSULF: a combined model for Phanerozoic atmospheric O2 and CO2. *Geochimica et Cosmichimica acta 70, 5653-5664.*

Bernoulli, D. (1964). Zur Geologie des Monte Generoso (Lombardische alpen). *Beitr. Z. Geol. Karte Schweiz, Neue Folge, Bern, 134p.*

Bernoulli, D. & Peters, T. (1970). Traces of rhyolitic-trachytic volcanism in the Upper Jurassic of the Southern Alps. *Ecl. Geol. Helv. 63, 609-621.*

Bernoulli, D. & Peters, T. (1974). Traces of rhyolitic-trachytic volcanism in the Upper Jurassic of the Southern Alps: reply. *Ecl. Geol. Helv. 67, 209-213.*

Bernoulli, D. & Jenkyns, H.C. (1974). Alpine, Mediterranean, and central Atlantic Mesozoic facies in relation to the early evolution of the Tethys. *Spec. Publ. Soc. Econ. Paleont. Mineral., 19, 129-160.*

Bernoulli, D., Caron, C., Homewood, P., Kälin, O. & Stuijvenberg, J.V. (1979). Evolution of continental margin in the Alps. *Schweizerische Mineralogische Petrographische Mitteilungen 59, 165-170.*

Bersezio, R., Erba, E., Gorza, M. & Riva, A. (2002). Berriasian-Aptian black shales of the Maiolica formation (Lombardian Basin, Southern Alps, Northen Italy): local to global events. *Palaeogeo. Palaeoclim. Palaeoeco. 180, 253-275.*

Bornemann, A., Aschwer, U & Mutterlose, J. (2003). The impact of calcareous Nannofossils on the pelagic carbonate accumulation across the Jurassic-Cretaceous Boundary. *Palaeogeo. Palaeoclim. Palaeoeco. 199, 187-228.*

Bosellini, A., Lobitzer, H., Brandner, R., Resch, W. & Castellarin, A. (1980). The complex basin of the Calcareous Alps and Paleomargins. *Abh. Geol. B-A. 34, 287-325.*

Bown, P.R, Cooper M.K.E. & Lord A.R. (1988). A Calcareous nannofossil biozonation scheme for early to mid Mesozoic. *Newsletters Staratigraphy 20(2), 91-114.*

Bown, P.R. & Cooper, M.K.E. (1989b). Conical calcareous nannofossils in the Mesozoic. In: *Crux, J.A. & Van Heck, S.E. (Eds.) - Nannofossils and their applications.* Proc. of the International Nannofossil Association Conference, London 1987, *98-106*

Bown, P.R. (1992). New calcareous nannofossil taxa from the Jurassic/Cretaceous boundary interval of site 765 and 261, Argo Abissal Plain. *Proc. ODP, scientific results 123, 369-379*

Bown, P.R. & Cooper M.K.E. (1998). Jurassic. In: *Bown P.R. (ed.), Calcareous nannofossil biostratigraphy. Kluwer Academic Publishers, London, UK, 34-85.*

Bown, P.R. and Young J.R. (1998). Techniques. In: *Bown P.R. (ed.), Calcareous nannofossil biostratigraphy. Kluwer Academic Publishers, London, UK, 16-28.*

Bown, P.R. and Young J.R. (1998). Introduction. In: *Bown P.R. (ed.), Calcareous nannofossil biostratigraphy. Kluwer Academic Publishers, London, UK, 1-15.*

Bown, P.R., Cooper, M.K.E. & Lord, A.R. (1988). A Calcareous nannofossil biozonation scheme for early to mid Mesozoic. *Newsletters Staratigraphy 20 (2), 91-114*

Bown, P.R., Lees, J.A. & Young, J.R. (2004). Calcareous nannoplankton evolution and diversity through time. In: *Thierstein H.R. & Young J.R. (Eds.) - Coccolithophores from molecular processes to global impact, 481-508.*

Bralower, T.J., Monechi, S. & Thierstein, H.R. (1989). Calcareous Nannofossils Zonation of the Jurassic-Cretaceous Boundary Interval and Correlation with the Geomagnetic Polarity Timescale. *Mar. Micropal. 14, 153-235*

Busson, G. & Noel, D. (1991). Les nannoconides indicateurs environnementaux des oceans et mers epicontinentales du Jurassique terminal et du Cretace Inferieur. *Oceanologica Acta 14 (4), 333-356*

Carroll, L. D. (1865). Alice's adventures in Wonderland.

Cecca, F., Garin, B.M., Marchand, D., Lathuiliere, B. & Bartolini, A. (2005). Paleoclimatic control of biogeographic and sedimentary events in Tethyan nd peri-Tethyan areas during the Oxfordian (Late Jurassic). *Palaeogeo. Palaeoclim. Palaeoeco. 222; 10-32*

Cecca, F., Savary, B., Bartolini, A., Remane, J. & Cordey, F. (2001). The Middle Jurassic - Lower Cretaceous Rosso Ammonitico successon of Monte Inici (Trapanese domain, western Sicily): sedimentology, biostratigraphy and isotope stratigraphy. *Bull. Soc. geol. France 172 (5), 647-660*

Channell, J.E.T. & Grandesso, P. (1987). A revised correlation of Mesozoic polarity chrons and calpionellid zones. *Earth and Planetary Science Letters 85, 222-240*

Channell, J.E.T., Bralower, T.J. & Grandesso, P. (1987). Biostratigraphic correlation of Mesozoic polarity chrons CM1 to CM23 at Capriolo and Xausa (Southern Alps, Italy). *Earth and Planetary Science Letters 85, 203-221*

Channell, J.E.T., Massari, F. & Benedetti, A. (1990). Magnetostratigraphy and biostratigraphy of Callovian-Oxfordian limestones fron Trento plateau (Monte Lessini, Northen Italy). *Paleogeogr. Paleoclimatol.Paleoecol. 79(3-4): 289-303.*

Channel, J.E.T., Erba, E., Nakanishm, I. & Tamaki, K. (1995). Late Jurassic – Early Cretaceous time scales and oceanic magnetic anomaly block models. In: *Geocronology Time Scales and Global Stratigraphic Correlation, SEPM special publication 54*

Channell, J.E.T., Muttoni, G., Casellato, C.E. & Erba, E. (2007). Polarity and polar wander at the Jurassic-Cretaceous boundary in the Southern Alps, Italy, *AGU 2007*

Charlson, R.J., Lovelock, J.E., Andreae, M.O. & Warren, S.G. (1987). Oceanic phytoplankton, atmospheric sulphur, cloud albedo and climate. *Nature 326; 655-661*

Chiari, M., Cobianchi, M. & Picotti V. (2007). Integrated stratigraphy (radiorarians and calcareous nannofossils) of the Middle to Upper Jurassic alpine Radiolarites Lombardian basin, Ialy): constrains to their genetic interpretation. *Paleogeogr. Paleoclimatol.Paleoecol. 249, 233-270.*

Clari, P.A., Marini, P., Pastorini, M. & Pavia, G. (1984). Il Rosso Ammonitico Inferiore (Bajociano-Calloviano) nei Monti Lessini Settentrionali (Verona). *Rivista Italiana di Paleontologia e Stratigrafia 90(1), 15-86.*

Cobianchi, M., Erba, E. & Pirini Radrzzani, C. (1992). Evolutionary trends of calcareous nannofossil genera *Lotharingius* and *Watznaueria* during the Early and Middle Jurassic. *Memorie di Scienze Geologiche XLIII; 19-25*

Danelian, T. & Johnson, K.G. (2001). Patterns of biotic changes in Middle Jurassic to Early Cretaceous Tethyan radiolaria. *Marine Micropaleontology 43, 239-260.*

Darwin, C. (1859). L'Origine delle specie. In: *L'Evoluzione. Newton, 1994*

De Kaenel, E., Bergen, J.A. and Perch-Nielsen, K. (1996). Jurassic calcareous nannofossil biostratigraphy of Western Europe. Compilation of recent studies and calibration of bioevents. *Bull. Soc. geol. France 167(1), 15-28.*

De Wever, P. & Baudin, F. (1996). Paleogeography of radiolarite and organic-rich deposits in Mesozoic Tethys. *Geol. Rundsch. 85, 310-326.*

Dromart, G., Garcia, J.P., Gaumet, F., Picard, S., Rousseau, M., Atrops, F., Lecuyer, C. & Sheppard, S.M.F. (2003). Perturbation of the carbon cycle at the Middle/Late Jurassic transition: geological and geochemical evidences. *American Journal of Science 303, 667-707.*

Dromart, G., Garcia, J.P., Picard, S., Atrops, F., Lecuyer, C. & Sheppard, S.M.F. (2003). Ice age at the Middle-Late Jurassic transition? *Earth and Planetary Science Letters 213, 205-220.*

Erba, E. & Quadrio, B. (1987). Biostratigrafia a Nannofossili calcarei, Calpionellidi e Foraminiferi planctonici della Maiolica (Titoniano sup-Aptiano) nella Prealpi Bergamasche (Italia settentrionale). *Riv. It. Paleont. Strat. 93(1), 3-108*

Erba, E. (1989). Upper Jurassic to Lower Cretaceous Nannoconus distribution in some sections from northern and central Italy. *Mem. Sci. Geol. 41, 255 – 261.*

Erba, E. (1994). Nannofossil and superplumes: the Early Aptian "nannoconid crisis". *Paleoceanography 9(3), 483-501.*

Erba, E. (2004). Calcareous nannofossils and Mesozoic ocean anoxic events. *Mar. Micropal. 52, 85-106*

Erba, E. (2006). The first 150 million years history of calcareous nannoplankton: Biosphere - Geosphere interaction. *Paleogeogr. Paleoclimatol.Paleoecol. 232, 237-250.*

Gould, S.J. & Eldredge, N. (1977). Punctuated equilibria: the tempo and mode of evolution reconsidered. *Paleobiology 3:115-151.*

Grabowski, J. & Pszczòlkowski, A. (2006). Magneto- and biostratigraphy of the Tithonian-Berriasian pelagic sediments in the Tatra Mountains (central Western Carpathians, Poland): sedimentary and rock magnetic changes at the Jurassic/Cretaceous boundary. *Cretaceous research 27, 398-417.*

Gradstein, F.M. & Sheridan, R.E. (1983). Introduction to initial reports of DSDP Leg.76. *Init. Rep. DSDP 76, 5-18.*

Gröcke, D.R., Price, G.D., Ruffell, A.H., Mutterlose, J. & Baraboshkin, E. (2003). Isotopic evidence for Late Jurassic – Early Creaceous climate change. *Palaeogeo. Palaeoclim. Palaeoeco. 202, 97-118*

Grün, B. & Blau, J. (1997). New aspects of calpionellid biochronology: proposal for a revised calpionellid zonal and subzonal division. *Revue de Paléobiologie16, 197–214.*

Hallam, A. (1985). A review of Mesozoic climates. *J. Geol. Soc. London, vol.142, 433-445*

Hallam, A. (1988). A re-evaluation of Jurassic eustasy in the light of new data and the revised Exxon curve. *SEMP Spec. Publ. 42, 261-273.*

Hallam, A. (2001). A review of the broad pattern of Jurassic sea-level changes and their possible causes in the light of current knowledge. *Palaeogeo. Palaeoclim. Palaeoeco. 167, 23-37*

Haq, B.U., Hardenbol, J. & Vail, P.R. (1988). Mesozoic and Cenozoic chronostratigraphy and cycles of sea-level change. *In:* Wilgus Cheryl, K. *et al.* (Editors), Sea level changes: an integrated approach. *Soc. Econ. Paleonto. Mineralo., SEMP Spec. Publ. 72-108.*

Hardie, L.A. (1996). Secular variation in seawater chemistry: an explanation for the coupled secular variation in the mineralogies of marine limestones and potash evaporites over the past 600 m.y. *Geology 24, 279–283.*

Hay, W.W. (2004). Carbonate fluxes and calcareous nannoplankton. In: *Thierstein, H.R., Young, J.R. (Eds.), Coccolithophores. From Molecular Processes to Global Impact. Springer-Verlag, Berlin, pp. 509 – 528.*

Hotinski, M.R. & Toggweiler, J.R. (2003). Impact of a Tethyan circumglobal passage on ocean heat transport and "equable" climates. *Paleoceanography **18**(1), 1007, doi:10.1029/2001PA000730.*

Housa, V., Krs, M., Krsova, M., Man, O., Pruner, P. & Venhodova, D. (1999). High-resolution magnetostratigraphy and micropaleontology across the J/K boundary stata at Brodno near Zilina, western Slovakia: summary results. *Cretaceous research 20, 699-717.*

Housa, V., Krs, M., Man, O., Pruner, P., Venhodova, D., Cecca, F., Nardi, G. & Piscitello, M. (2004). Combined magnetostratigraphic, paleomagnetic and calpionellid investigations across Jurassic/Cretaceous boundary strata in the Bosso Valley, Umbria, central Italy. *Cretaceous research 25, 771-185.*

Jones, C.E., Jenkyns, H.C., Coe, A.L. & Hesselbo, S.P. (1994). Strontium isotopic variations in Jurassic and Cretaceous seawater. *Geochim. Cosmochi. Acta, 58(14), 3061-3074.*

Lohmann, H. (1902). Die Coccolithophoridae, eine Monographie der coccolithen bildenden Flagellaten, zugleich ein Beitrat zur Kenntnis des Mittelmeerauftriebs. *Archiv für Protistenkunde. 1, 89-165*

Lohmann, H. (1909). Die Gehause und Gallertblasen der Appendicularien ind ihre Bedeutung fur die Erforschung des Lebens im Meer. *Verhandlungen Deutsche Zoologische Geselleschaft. 19, 200-239.*

Lowrie, W. & Channell, J.E.T. (1983). Magnetostratigraphy of the Jurassic/Cretaceous boundary in the Maiolica limestone (Umbria, Italy). *Geology 12, 44-47.*

Malmgren, B.A., Berggren, W.A. & Lohmann, G.P. (1984). Species formation through Punctuated Gradualism in Planktonic Foraminifera. *Science 225, 317-319*

Martire, L, Clari, P.A. & Pavia, G. (1991). Il significato stratigrafico della sezione di Cima Campo di Luserna (Giurassico delle Alpi meridionali, Italia nord-orientale). *Paleopelagos 1, 57-65.*

Martire, L. (1996). Stratigraphy, facies and synsedimentary tectonics in the Jurassic Rosso Ammonitico Veronese (Altopiano di Asiago, NE Italy). *Facies 35, 209-236.*

Martire, L. (2003). Sequence stratigraphy and condensed pelagic sediments. An example from the Rosso Ammonitico Veronese, northeastern Italy. *Palaeogeo. Palaeoclim. Palaeoeco.* 94, 169-191.

Martire, L., Clari, P., Lozar, F. and Pavia, G. (2006). The Rosso Ammonitico Veronese (Middle-Upper Jurassic of Trento Plateau): a proposal of lithostratigrafic ordering and formalization. *Rivista Italiana di Paleontologia e Stratigrafia 112(2), 227-250.*

Mattioli, E. & Erba, E. (1999). Synthesis of Calcareous Nannofossil events in Tethyan Lower and Middle Jurassic successions. *Rivista Italiana di Paleontologia e Stratigrafia 105(3), 343-376.*

Mc Arthur, J.M., Howarth, R.J. & Bailey, T.R. (2001). Strontium isotope stratigraphy; LOWESS Version 3; best fit to the marine Sr-isotope curve for 0-509 Ma and accompanying look-up table for deriving numerical age. *J. Geol. 109(2), 155-170.*

Moore, G.T., Hayashida, D.N., Ross, C.A. & Jacobson, S.R. (1992a). Palaeoclimatic of the Kimmeridgian-Tithonian (Late Jurassic) world: I. Result using a general cicurlation model. *Palaeogeo. Palaeoclim. Palaeoeco. 93, 113-150*

Moore, G.T., Hayashida, D.N., Ross, C.A. & Jacobson, S.R. (1992b). Palaeoclimatic of the Kimmeridgian-Tithonian (Late Jurassic) world: II. Sensivity tests comparing three different palaeotopographic settings. *Palaeogeo. Palaeoclim. Palaeoeco. 95, 229-252*

Moshkovitz, S. & Ehrlich, A. (1987). *Watznaueria manivitae,* Bukry – Taxonomic problems and distribution in the Jurassic – Lower Cretaceous sediments of Israel and other Tethian areas. *Geo. Surv. Isr. Jerusalem, 9, 110-114*

Mutterlose, J. & Kessels, K. (2000). Early Cretaceous calcareous nannofossils from High latitudes: implications for paleobiogeography and paleoclimate. *Palaeogeo. Palaeoclim. Palaeoeco. 160(2), 347-372.*

Muttoni, G., Erba, E., Kent, V.D. & Bachtadse, V. (2005). Mesozoic Alpine facies deposition as a result of past latitudinal palte motion. *Nature 434, 59-63.*

Ogg, J.G. (1981). Sedimentology and paleomagnetism of Jurassic pelagic limestones: "Ammonitico Rosso" facies. *Ph.D. thesis, La Jolla, California, Scripss Institution of Oceanography, 212 p.*

Ogg, J.G. & Lowrie, W. (1986). Magnetostratigraphy of the Jurassic/Cretaceous boundary. *Geology 14, 547-550.*

Ogg, J.G., Hasenyager, R.W., Wimbledon, W.A., Channell, J.E.T. & Bralower, T.J. (1991). Magnetostratigraphy of the Jurassic/Cretaceous boundary interval - Tethyan and English fauna realms. *Cretaceous research 12, 455-482.*

Olóriz, F., Caracuel, J.E., Marques, B. &. Rodríguez-Tovar, F.J. (1995). Asociaciones de Tintinnoides en facies Ammonitico Rosso de la Sierra Norte (Mallorca). Revista Española de Paleontología, N° Homenaje al Dr. G. Colom, 77–93.

Pasquarè, G. (1965). Il Giurassico Superiore nelle prealpi Lombarde. *Memorie della Rivista Italiana di Paleontologia e Stratigrafia XI.*

Perch-Nielsen, K. (1985a). Mesozoic calcareous nannofossil. In: *Plankton Stratigraphy* (Eds. Bolli, H.M., Saunders, J.B. & Perch-Nielsen K.), Cambridge University Press. 329-426.

Pittet, B. & Mattioli, E. (2002). The carbonate signal and calcareous nannofossil distribution in an Upper Jurassic section (Balingen-Tieringen, Late Oxfordian, southern Germany). *Palaeogeo. Palaeoclim. Palaeoeco. 179, 71-96.*

Podlaha, O.G., Mutterlose, J. & Veizer, J. (1998). Preservation of delta 18O and delta 13C in belemnite rostra from the Jurassic/Early Cretaceous successions. *American Journal of Science 298, 324-347.*

Pop, G. (1994b) Calpionellid evolutive events and their use in biostratigraphy. *Romanian Journal of Stratigraphy 76, 7–24.*

Premoli-Silva, I., Erba, E. & Tornaghi, M.E. (1989). Paleoenvironmental signals and changes in surface water fertility in mid Cretaceous C_{org}-rich pelagic facies of the Fucoidi Marls (Central Italy). *Geobios Mem. Spec. 11, 225-236.*

Price, G.D. (1999). The evidence and implications of polar ice during the Mesozoic. *Earth-Science Reviews 48, 183-210.*

Price, G.D. & Groecke, D.R. (2002). Strontium-isotope stratigraphy and oxygen- and carbon-isotope variation during the Middle Jurassic-Early Cretaceous of the Falkland Plateau, South Atlantic. *Palaeogeo. Palaeoclim. Palaeoeco. 183, 209-222.*

Rais, P., Louis-Schmid, B., Bernasconi, S.M. & Weissert, H. (2007). Paleoceanographic and paleoclimatic reorganization around the Middle-Late Jurassic transition. *Palaeogeo. Palaeoclim. Palaeoeco. 251, 527-546.*

Reháková, D. & Michalík, J. (1997) Evolution and distribution of calpionellidsthe most characteristic constituents of Lower Cretaceous Tethyan microplankton. *Cretaceous Research 18, 493–504.*

Remane, J. (1971). Les Calpionelles protozoaires planctoniques des mer mesogennes de l'epoque secondaire. *Annales Guebhard Neuchatel 47, 370–393.*

Ross, M. & Scotese, C.R. (1988). A Hierarchical tectonic model of the Gulf of Mexico and Caribbean region. *Tectonophysics 155, 139-168.*

Roth, P.H. (1983). Jurrasic and Lower Cretaceous calcareous nannofossil in the Western North Atlantic (site 534): biostratigraphy, presevation, and some observation on biogeography and paleoceanography. *Init. Rep. DSDP 76, 587-621.*

Sheridan, R.E. (1983). Phenomena of pulsation tectonics related to the breakup of eastern North American contnental margin. *Init. Rep. DSDP 76, 897-909.*

Sheridan, R.E. & Gradstein, F.M., et al. (1983). Site 534: Blake-Bahama Basin (Shipboard Scientific Party). *Init. Rep. DSDP 76,141– 340.*

Smuc, A. (2005). Jurassic and Cretaceous stratigraphy and sedimatary evolution of the Julian Alps, NW Slovenia. / *Andrej Smuc; [jezikovni pregled Glenn S Jaecks]. – Ljubljana: Zalozba ZRC, ZRC SAZU, 2005*

Sorrosa, J.M., Satoh, M. & Shiraiwa, Y. (2005). Low temperature stimulates cell enlargement and intracellular calcification of coccosphere. *Marine Biotechnology 7, 128-133.*

Stampfli, G.M., Mosar, J., Favre, P., Pillevuit, A. & Vannay, J-C. (2001). Permo-Mesozoic evolution of the Western Tethys realm: The Neo-Tethys East Mediterranean Basin connection. In*: Ziegler, P.A., Cavazza, W., Robertson, A.H.F. & Crasquin-Soleau, S. (eds). Peri Tethys Memoir 6: Peri-Tethyan Rift/Wrench Basin and passive Margins. Memoires du Museum national d'historie naturelle 186, 51-108.*

Stanley S.M. (2006). Influence of seawater chemistry on biomineralization throughout Phanerozoic tome: Paleontological and experimental evidence. *Palaeogeo. Palaeoclim. Palaeoeco. 232, 214-236.*

Stenseth, N.C. & Maynard Smith, J. (1984). Coevolution in ecosystems: rred queen evolution or stasis? *Evolution 38, 870-880.*

Street, C. & Bown, P.R. (2000). Paleobiogeography of Early Cretaceous (Berriasian-Barremian) calcareous nannoplankton. *Marine Micropaleontology 39, 265-291.*

Tavera, J.M., Aguado, R., Company, M. & Oloriz, F. (1994). Integrated biostratigraphy of the Durangites and Jacobi zones (J/B boundary) at the Puerto Escano section in Southern Spain (Province of Cordoba). *Geobios 17, 469-476.*

Thierstein H.R. (1971). Tentative Lower Cretaceous Cacareous Nannoplankton zonation. *Eclogae Geologicae Helvetiae. 64(3), 459-488.*

Thierstein, H.R. (1973). Lower Cretaceous calcareous nannoplankton biostratigraphy. *Abhandlungen der Geologischen Bundesanstalt. 29, 1-52.*

Tremolada, F. & Joung, J.R. (2002). Volume calculation of cretaceous calcareous nannofossils. *J. nannoplankton reasearch 24(3), 199-202.*

Van Valen, L. (1973). A new evolutionary law. *Evolutionary Theory 1:1-30.*

Weissert, H. & Channell, J.E.T. (1989). Tethyan carbonate carbon isotope stratigraphy across the Jurassic/Cretaceous boundary: an indicator of decelerated global carbon cycling? *Paleoceanography 4(4), 483-494.*

Weissert, H. & Mohr, H. (1996). Late Jurassic climate and its impact on carbon cycling. *Palaeogeo. Palaeoclim. Palaeoeco. 122, 27-43.*

Weissert, H. & Erba, E. (2004). Volcanism, CO2 and palaeoclimate: a Late Jurassic – Early Cretaceous carbon and oxygen isotope record. *Jour. Geol. Soc., London, 161, 1-8.*

Wignall, P.B. & Ruffell, A.H. (1990). The influence of a sudden climatic change on marine deposition in the Kimmeridgian of northwest Europe. *J. Geol. Soc. London 147, 365-371.*

Winterer, E.L. & Bosellini, A. (1981). Subsidence and sedimentation on Jurassic Passive Continental Margin, Southern Alps, Italy. *AAPG Bulletin 65, 394-421.*

Winterer, E.L. (1991). The Tethyan Pacific during Late Jurassic and Cretaceous time. *Palaeogeo. Palaeoclim. Palaeoeco. 87, 253-267.*

Acknowledgements

First of all I would like to express my thanks to all the ones who have been fundamental to my scientific growth (and more than that) during these years.

I am so much grateful to Elisabetta Erba for the wonderful opportunity she gave me with this PhD project. Thank You for Your teachings and Your willingness, for every advice and continuous encouragement. Thank You for the multiple opportunities I had to travel and attend international congresses, and for being involved in the Jurassic/Cretaceous boundary never ending story.

Many thanks to Isabella Premoli for her constant willingness and for every good suggestion. And for the time spent together in Vienna and in Bristol.

Thanks to Jim Channell and Giovanni Muttoni for the wonderful days spent together in the field collecting samples, for the scientific discussions during dinners, and for the opportunity I received to become (or try to…) a "biostratigrapher" that You gave me with this project.

A sincere thank to Daniele Tiraboschi, who suffered my temper during the last two years! Principally, thank You for the time spent together arguing about *fanta*-science and for every good burst of laughter.

Thanks to Jörg Mutterlose for hospitality, for the time dedicated to me talking about my diagenesis-affected stuff and discussing any differences between low and high latitudes Jurassic worlds.

Thanks to Jens Herrle for the good time spent together, for each chat, and for each good advice.

Thanks to André Bornemann for every useful scientific discussion and confrontation on Late Jurassic calcareous nannofossils.

Thank to Johann Schnyder, for the pleasant trip in Paris, and for every scientific confrontation we had in Tunisia.

Much thanks to Bianca De Bernardi and Maria Teresa Galli for the constant help they gave me during these three years.

Then, heartily thank to…

My Dad and my Ma': without Your help, your presence, your good advices this could not have been possible!

My Andrea, just for having been faithful by my side, trusting me.
(…*gestendo con acume e pacatezza il difficile equilibrio del mio scafo…*)

Emme… just because!

Alice and Mussu for having been present during these ten years, for every good chat and confrontation, for every journey and every glass of wine!